Distribution Agreement In presenting this thesis or dissertation as a partial fulfillment of the requirements for an advanced degree from Emory University, I hereby grant to Emory University and its agents the non-exclusive license to archive, make accessible, and display my thesis or dissertation in whole or in part in all forms of media, now or hereafter known, including display on the world wide web. I understand that I may select some access restrictions as part of the online submission of this thesis or dissertation. I retain all ownership rights to the copyright of the thesis or dissertation. I also retain the right to use in future works (such as articles or books) all or part of this thesis or dissertation.

Signature: _____ _____

Dawn E Barnes Date

Molecular, genetic, and biochemical studies on troponin I and tropomyosin in the regulation of muscle contraction

by

Dawn Elizabeth Barnes
Doctor of Philosophy

Biochemistry, Cell and Developmental Biology
Graduate Division of Biological and Biomedical Sciences

_____
Shoichiro Ono, PhD
Advisor

_____
Gary Bassell, PhD
Committee Member

_____
Guy Benian, MD
Committee Member

_____
Ken Moberg, PhD
Committee Member

_____
Winfield Sale, PhD
Committee Member

Accepted:

_____
Lisa A. Tedesco, Ph.D.
Dean of the James T. Laney School of Graduate Studies

_____
Date

Molecular, Genetic, and Biochemical Studies on Troponin I and Tropomyosin in the Regulation of Muscle Contraction

By

Dawn Elizabeth Barnes

B.S., University of Arizona, 2005

Advisor: Shoichiro Ono, PhD

An abstract of
A dissertation submitted to the Faculty of the
James T. Laney School of Graduate Studies of Emory University
in partial fulfillment of the requirements for the degree of
Doctor of Philosophy
in Biochemistry, Cell and Developmental Biology
2016

Abstract

Molecular, Genetic, and Biochemical Studies on Troponin I and Tropomyosin in the Regulation of Muscle Contraction

By Dawn Elizabeth Barnes

The nematode *Caenorhabditis elegans* uses the striated muscles of its body wall for locomotion. The movement is achieved through the collective shortening of sarcomeres on one side of the body (contraction) and simultaneous lengthening of sarcomeres on the opposite side of the body (relaxation). Muscle contraction results from shortening of sarcomeres achieved by interactions between thin filament containing F-actin and thick filament with bipolar arrangement of myosin motors. The myosin motors are constitutively-active and thus the control between actomyosin interactions is through regulatory component of the thin filaments. Mutations of sarcomere proteins often cause uncoordinated ("*unc"*) phenotypes. However, there was no techniques available to analyze kinetics of worm muscle contraction and relaxation in a quantitative manner. We have utilized optogenetically-induced activation of muscle contraction as a novel technique to study the roles of sarcomere proteins in locomotion and we found functional relationships between proteins within the sarcomere. Among these proteins, tropomyosin is important in regulating actomyosin interactions in cooperation with the troponin complex. We identified a novel high molecular weight tropomyosin isoform (LEV-11O) that is the first LEV-11 protein including alternative Exon 7 (7a). We found that LEV-11O has similar biochemical properties to other tropomyosin isoforms and is the major isoform in the body wall muscles of the head-region. The position of tropomyosin in the thin filament is regulated by the troponin complex. Within the troponin complex, troponin I is sufficient to stabilize tropomyosin in a position to inhibit myosin binding. Through sequence analysis we conclude that the core domains of troponin I are conserved across the bilaterian phyla we examined, however, the N- and C-terminal extensions are variable. The N-terminal extension is present in all protostome troponin I and chordate cardiac troponin I, however this region is absent from chordate skeletal muscle isoforms. Through *in vivo* studies, we observed that the N-terminal extension is important in the coordinated muscle contractility important for the sinusoidal locomotion of *C. elegans*. Our work has contributed to the understanding of how different isoforms of thin filament proteins can be important in regulating the activities of different types of muscle.

Molecular, Genetic, and Biochemical Studies on Troponin I and Tropomyosin in the Regulation of Muscle Contraction

By

Dawn Elizabeth Barnes

B.S., University of Arizona, 2005

Advisor: Shoichiro Ono, PhD

A dissertation submitted to the Faculty of the
James T. Laney School of Graduate Studies of Emory University
in partial fulfillment of the requirements for the degree of
Doctor of Philosophy
in Biochemistry, Cell and Developmental Biology
2016

Acknowledgements

I would like to thank my advisor, Dr. Shoichiro Ono, for guiding me through the scientific process. I am grateful for the conscientious time and thought he dedicated to both my research and professional development. I appreciate his openness in allowing me to shape my doctoral research, whether that meant expanding upon different research avenues or trying out new techniques. Sho taught me how to optimally communicate my research, with a focus on the story as a whole. I am grateful for his patience and kindness during my moments of folly. I have learned a lot during my time in his laboratory.

I am grateful for my committee members: Gary Bassell, Guy Benian, Kenneth Moberg, and Winfield Sale. I always looked forward to our bi-yearly committee meetings, for the opportunity to garner their scientific insight and feedback. I am grateful for their persisting positivity and encouragement, as well as their support to "follow the science." Additionally, I am thankful to Gary for challenging me to focus on the mammalian connections for my invertebrate research. I am thankful to Guy for his *C. elegans* expertise and assistance in laboratory protocols and supplies. He served as a second mentor to me. I am thankful to Ken for his encouragement and support during the unexpected challenges that a graduate school education included. I am thankful to Win for both his collegial respect and challenging me to constantly improve my communication skills, with an emphasis on being clear and succinct.

I would like to thank my family. My mother, Suzanne, for her unwavering support and confidence. I know she would have been proud of my accomplishments. I would like to thank my father, Tim, for the help that he provided long before I even began graduate school. My scientific journey began with great laughs as we rapped about DNA binding

and modified Disney music to include lyrics about biological processes. Foremost, I would like to thank my brother, Kyle. I have no greater supporter. There are not too many non-scientist brothers who read their sister's scientific journal articles. I am so proud when he accurately speaks about biomedical or neuroscience information he heard on the radio or television, especially when telling these stories because they reminded him of something we had discussed about in my own research. When I expressed doubt, he bolstered my confidence.

I would like to thank my coworkers for all of their help during these years. Thank you to Kanako Ono for all of her help with my *in vivo* experiments. Thank you for teaching me how to work with the worms, including how to inject them, produce fluorescent staining, and collect high-resolution images. Beyond teaching me the techniques, she conducted immunofluorescence work in both our troponin project and tropomyosin projects. Additionally, Kanako was a joy in the laboratory. Thank you to Kazumi Nomura, my Japanese sister, who was a constant help in the laboratory. She trained me in almost everything, sharing supplies, and wonderful company.

I would like to acknowledge the help of Hyundoo Hwang and Hang Lu. When I wanted to develop optogenetics analyses to be able to study muscle kinetics *in vivo*, they donated their equipment and time to help run and analyze the experiments. I would also like to acknowledge Hidehito Kuroyanagi and Eichi Watanabe for their help with the *in vivo* fluorescence exon splicing assays. I would like to thank Hidehito Kuroyanagi for developing a technique that allows for the visualization of exons of high sequence similarity. Without this technique, we would not have been able to visualize the alternative splicing of our exon 7.

Figures

Tables

Table of contents

Abbreviations

ADF	Actin depolymerizing factor
AIP1	Actin interacting protein 1
Arp	Actin-related proteins
ATP	Adenosine triphosphate
A	Alanine
C	Charged
C	Cysteine
CCD	Charge-coupled
C. elegans	*Caenorhabditis elegans*
ChR2	Channelrhodopsin 2
CRISPR	Clustered regularly-interspaced short palindromic repeats
cTNI	Cardiac troponin I
DNA	Deoxyribonucleic acid
E	Glutamic acid
E7A	Exon 7b
E7B	Exon 7a
E. coli	*Escherichia coli*
F-actin	Filamentous actin
GFP	Green fluorescent protein
H	Hydrophobic
HMW	High molecular weight
K	Lysine
Kd	Dissociation constant
LMW	Low molecular weight
mRNA	Messenger RNA
ΔN	N-terminal deletion
NCBI	National Center for Biotechnology Information
NGM	Nematode growth medium
N-lobe	N-terminal lobe
NMR	Nuclear magnetic resonance
NpHR	*Natronomonas pharaonic*
NTE	N-terminal extension
P	Polar
PAT	Paralyzed at two-fold
PBS-T	phosphate-buffered saline containing 0.1 % Tween 20
PCR	Polymerase chain reaction
PDMS	Polydimethylsolxane
Pep	Peptide
R	Arginine
RFP	Red fluorescent protein

SDS	Sodium dodecyl sulfate
TM	Tropomyosin
TNC	Troponin C
TNI	Troponin I
TNT	Troponin T
UNC	Uncoordinated
V	Valine
WT	Wild-type

Chapter 1 Introduction

1.1 Overview

In vertebrates, there are three principle types of muscle: skeletal, cardiac, and smooth. Each type of muscle has its own method of regulating contractility. Skeletal and cardiac muscles are both striated muscles, which regulate muscle contraction/ relaxation through changes within actin binding proteins. Within the nematode *Caenorhabditis elegans*, there are also differences in their striated muscles, in particular the body wall muscle of the anterior/ head region and those of the main body. Even though they are all striated muscles, variations within their actin binding proteins are important for their different roles within the body. Our work has analyzed differences between different actin binding protein isoforms, with the goal of understanding the role of their functional domains in that larger process of muscle contractility.

1.2 Striated muscles

Each striated muscle fiber is comprised of many myofibrils. Within myofibrils, sarcomeres run perpendicular to the length of the muscle fiber. Striated muscle has a regularly ordered array of sarcomeres, which appear as bands under a compound light microscope. These sarcomeres are comprised of thin actin filaments and actin binding proteins, as well as thick filament bipolar myosin filaments[1] (Figure 1.1). Both skeletal and cardiac muscles are striated muscles. Skeletal muscle is voluntarily controlled and activated by acetylcholine release at neuromuscular junctions[2]. Activation of these ligand-gated nicotinic acetylcholine receptors causes these cation channels to allow a net

movement of sodium and calcium in to the cell and potassium out of the cell[3]. These ion changes then trigger sarcoplasmic reticulum voltage-sensing dihydropyridine receptors to open their calcium channels and also activate the opening of ryanodine receptor calcium channels on the sarcoplasmic reticulum[4]. The sarcoplasmic reticulum acts as a storage source for calcium. To facilitate relaxation, calcium is removed from the cytoplasm by sarco(endo)plasmic reticulum calcium ATPase pumps, which pump calcium back in to the sarcoplasmic reticulum[5,6]. The increases and decreases in calcium levels in the myofilaments are responsible for initiating muscle contraction and relaxation, respectively. Muscle contraction occurs from the pulling of actin filaments inwards on either side of the sarcomere by the myosin head domains projecting from the surface of thick filaments (Figure 1.1).

1.3 Troponin functions as a calcium sensor

The calcium-based regulation of striated muscle contraction is through the thin filament proteins, namely tropomyosin and the troponin complex. The troponin complex is comprised of three proteins troponin I (TNI: inhibitory), troponin C (TNC: calcium binding), and troponin T (TNT: tropomyosin binding or tethering). TNC is composed of two globular lobes, connected by a linker alpha-helix[7]. The COOH-terminal lobe has two E-F hands (III and IV) that have a high (10^7 M^{-1}) affinity for calcium and also an affinity for magnesium. Consequently, they are constitutively occupied. Structural changes in the TNC C-lobe increase its affinity for TNI and the thin filament[8] and these changes are necessary for troponin calcium sensing as a whole. The N-lobe of skeletal TNC has two calcium binding sites (I and II) with a lower affinity (10^5 M^{-1}) for calcium. Binding of calcium induces large structural changes that expose a hydrophobic helix to the surface of

TNC's N-lobe, where TNI can bind[9]. Alternatively, the N-lobe of cardiac (and slow twitch skeletal) TNC only has one E-F hand for calcium binding[10,11]. The structural changes in this N-lobe only open access to the hydrophobic helix, without moving it to the surface[10,12].

1.4 Troponin I N-terminal extension

Cardiac TNI (cTNI) is comprised of an N-terminal extension (absent from skeletal TNI), N-terminal region, helices 1-4, and C-terminal tail. Structural biology studies have elucidated many intra-troponin interactions, with the exception of the highly-mobile N- and C-terminal most regions of cTNI. The N-terminal region of TNI (C-terminal of the N-terminal extension) binds TNC C-lobe[13]. The C-terminal region of helix 1 binds to the C-lobe of TNC and TNT. Helix 2 forms an alpha-helical coiled-coil with TNT. The TNI inhibitory region is C-terminal of helix 2. Upon calcium binding to TNC N-lobe, helix 3 binds the hydrophobic cleft of the N-lobe of TNC[7], which is why it is named the switch region. Helix 4 may bind TNC (our data, unpublished). Biochemical studies indicate that the TNI C-terminal tail exhibits calcium-regulated interactions with tropomyosin[14]. The highly-mobile TNI N-terminal extension (NTE) has been uncaptured in structural studies; however, NMR data indicate the cTNI NTE binds the N-lobe of TNC (Figure 1.2). Additionally, bisphosphorylation of the NTE weakens its interaction with the TNC N-lobe. This indicates amino acids adjacent to the NTE phosphorylation sites are involved with binding the TNC N-lobe[15]. The NTE also appears to be important in heart muscle because mutations in the NTE of human cTNI can lead to cardiomyopathies- characterized by either a thickening (R21C) or thinning (A2V) of ventricle wall[16,17]. Also, transgenic expression of cardiac TNI (cTNI), with an N-terminal

truncation, in wild-type mice, reduced heart muscle activity[18]. The NTE is absent from skeletal TNI, however it is present in all protostome TNI isoforms. While the NTE is not essential for TNI function, this region evolved and has been conserved across the majority of bilaterian animals[19], which indicates an important functional role. In chapter 3, I discuss the molecular evolution of the TNI NTE and its role in regulating nematode locomotion. Nematode locomotion requires the simultaneous contraction and relaxation of opposite sides of the worm. To isolate muscle function into contraction or relaxation phases, we developed an optogenetic analysis technique (Chapter 2).

1.5 Tropomyosin regulates actomyosin interactions and stabilizes filamentous actin

The troponin complex plays an essential role in regulating sarcomeric actomyosin ATPase cycling; however, its action is through positioning tropomyosin between positions on the actin filament that either permit access to, or sterically-hinder myosin head binding sites[20,21]. According to the current model, tropomyosin inherently lies along the inner groove of actin filaments. Myosin binding sites are on the outer groove of the actin filaments. Calcium binding to troponin induces structural changes that release the inhibitory action of TNI and allow tropomyosin to slide into the inner actin groove[20,22,23]. When tropomyosin is in the inner actin groove[20] myosin can interact with actin[23] to cause muscle contraction[22] (Figure 1.3).

Tropomyosin is a right-handed alpha helical structure with a hydrophobic strip along one side. Amino acids flanking the hydrophobic core provide an ionic interaction, or salt-bridge. The alpha helices then form a left-handed coiled-coil conformation. The

amino acid sequence of tropomyosin forms a heptad repeat: H-P-P-H-C-P-C, where H is hydrophobic, P is polar, and C is charged (Figure 1.4). My biochemical assays have found that mutations in amino acids that form charged interactions have different effects on myosin ATPase activity than mutations in the polar amino acids on the outside of the coiled-coil (Chapter 4).

Tropomyosin is also important in stabilizing filamentous actin by reducing pointed end depolymerization[24]. In striated muscle thin filaments, the tropomyosin-troponin complex, in cooperation with tropomyosin, helps stabilize filament length at the pointed ends by reducing both the rate of actin polymerization and depolymerization[25]. Through competitive binding, tropomyosin purified from *C. elegans* inhibits UNC-60B (ADF/cofilin)-AIP1 severing[26,27]. In the presence of caldesmon, a calcium binding protein, tropomyosin inhibits gelsolin severing of actin filaments by occupying a similar actin-binding site. Only tropomyosins with high actin binding affinity elicited severing inhibition[28]. Near dynamic regions of non-muscle cell, lower molecular weight isoforms on tropomyosin are present and in regions such as the leading edge, tropomyosin isoforms are absent[29].

In addition to its role in actin dynamics, tropomyosin is also important in recruiting actin binding proteins in both muscle and non-muscle cells. The mammalian high molecular weight isoform Tm3 induces the formation of filopodia by recruiting active (unphosphorylated) actin depolymerizing factor (ADF/cofilin), as well as fascin to bundle the filaments. Additionally, Tm3 appears to inhibit filament branching by excluding Arp2/3 interactions[30]. Light-chain phosphorylated (higher activity) non-muscle myosin II motors are recruited to mammalian $Tm5_{NM1}$-containing filaments, to provide

the contractile force to induce stress fiber formation and decreased lamellipodia. The tropomyosin isoform-specific recruitment of different actin binding proteins may not be an active process. Rather, different tropomyosin isoforms may occupy slightly-different spaces within the actin major groove, thereby exposing or blocking the binding sites of different actin binding proteins.

1.6 Alternative splicing leads to functional variability in the eukaryotic proteome

Eukaryotic gene transcription leads to precursor mRNAs that must be processed into protein-coding messenger RNA (mRNA) and exported from the nucleus for the subsequent translation to protein[31]. An important pre-mRNA processing step is the removal of intron (non-coding) sequences and the ligation of exon (coding) sequences, in a step known as splicing. This action is accomplished by the spliceosome protein complex[32]. Alternative splicing is the differential combination of exons that allows for greater proteome diversity from a single gene. In fact, isoforms resultant from alternative splicing can execute opposing functions[33] within cells and can be expressed in different cell types[34]. These alternative splicing events are regulated by splicing factors that regulate the spliceosome binding and activity[35,36]. The exons that are always included in mRNA are called constitutive exons. The exons that are variably included are referred to as alternative exons. Through this differential processing, one gene can produce multiple protein isoforms with functional variability.

1.7 *C. elegans* muscle

C. elegans is a powerful model organism for the study of striated muscle structure and function. Their body-wall muscle is obliquely striated[37]. Vertebrate striated muscle is cross-striated, where striation bands run perpendicular to the filaments. Vertebrate thin filaments are anchored to Z-disks. Similarly, *C. elegans* sarcomeric thin filaments are believed to be anchored to dense bodies, which are cone-shaped and anchored to the plasma membrane and basement membrane[37,1] (Figure 1.5), however recent data suggests this may not be accurate (Ono, data unpublished). The high degree of sequence similarity between eukaryotic organisms has allowed rabbit muscle actin to be utilized across *in vitro* studies of actin binding proteins from different organisms. However, there are a few biochemical differences between rabbit and *C. elegans* actin, including differences in critical concentration values[38,39,40] therefore it is optimal to utilize actin from the same organism when studying polymerization and dynamics. *C. elegans* actin has five known isoforms, expressed from five genes. The four sarcomeric isoforms have 99% sequence identity, which suggests redundant functions. Functional redundancy is also supported by the fact that loss of any single actin gene has no phenotype; however, dominant mutations reveal a phenotype[41].

Similar to vertebrates, *C. elegans* thin filament tropomyosin and troponin also regulate actomyosin interactions and muscle contractility. Troponin is similarly a complex of three proteins: TNC, TNT, TNI. *C. elegans* TNC has two known isoforms from two genes: *tnc-2* and *pat-10*. TNC-2 is expressed exclusively in pharyngeal muscle[42]. PAT-10 is expressed in body wall, vulval, and anal muscles[42]. Loss of this protein results in worms that are paralyzed at the two-fold embryonic developmental stage, a phenotype for a loss of 19 other genes[43,44]. *C. elegans* TNT has four known

isoforms from four genes: *mup-2*, *tnt-2*, *tnt-3*, *tnt-4*. MUP-2 is expressed in *C. elegans* embryonic body wall muscles and its tethering properties are important for reestablishing TNI/TNC binding, after calcium activation[45]. *C. elegans* TNI has four known isoforms from four genes: *tni-1*, *unc-27*, *tni-3*, *tni-4*. TNI-1 is expressed in body wall muscles at low levels. UNC-27 is expressed in body wall muscles at high levels. TNI-3 is expressed in body wall muscles concentrated in the anterior/head region, as well as vulva muscle cells. TNI-4 is expressed in pharyngeal muscle[46]. UNC-27 is important in *C. elegans* locomotion and mutations result in an uncoordinated and hyper-contracted phenotype[47]. Similar to cTNI, UNC-27 also contains a 32 amino acid N-terminal extension. This region is highly conserved across invertebrates and important in coordinating the sinusoidal movement in *C. elegans*[48] (Chapter 3). The function of all troponin isoforms is executed through the movement of tropomyosin proteins.

C. elegans tropomyosin is a single gene (known as either *lev-11* or *tmy-1*) that within this dissertation I have demonstrated to be spliced in to at least five isoforms. The isoform variations are achieved through a combination of alternative promotors and mRNA splicing. Two low-molecular weight isoforms (LEV-11C & LEV-11E) are expressed in pharynx and intestines[49]. Two high-molecular weight isoforms (LEV-11A & LEV-11D) are expressed in body wall muscle, and localize to thin filaments[26,50]. Additionally, we have identified a third high-molecular weight isoform (LEV-11O) that is also expressed in body wall muscles, in a subset of head muscles (Chapter 4). Differences between tropomyosin isoforms are a mechanism to generate functionally-distinct filament populations. With the discovery of this high-molecular weight isoform

with an alternative exon 7, we have developed a tool to analyze the role of exon 7 in regulating filamentous actin function.

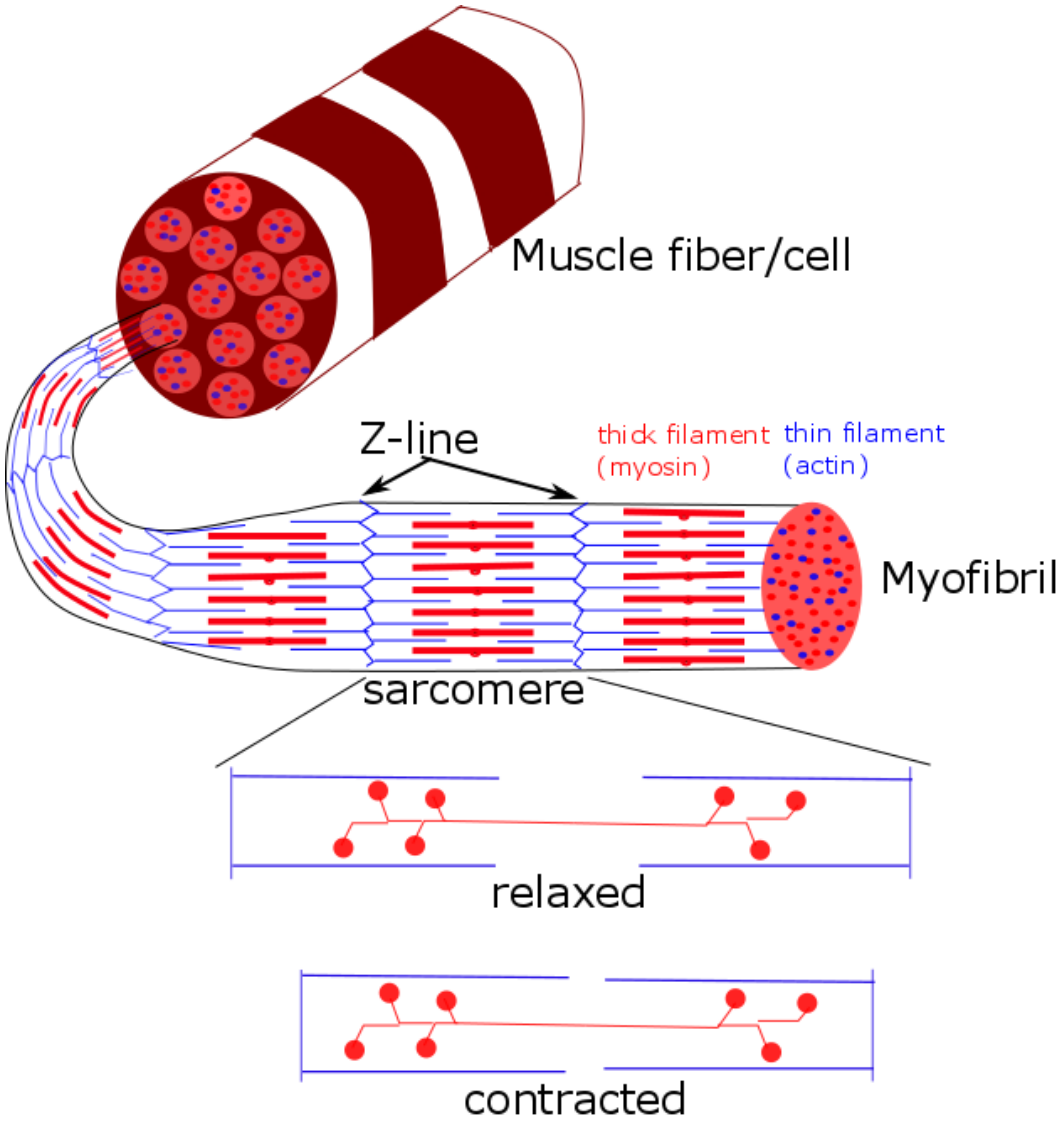

Figure 1.1 Each muscle fiber is comprised of many myofibrils. Within myofibrils, sarcomeres run perpendicular to the length of the muscle fiber. When thick filament myosin motors can bind to thin filament actin, their ratcheting action produces a net translocation of myosin thick filaments with respect to actin thin filaments that pulls Z-lines closer together. This collective shortening of many sarcomeres is the source of striated muscle contraction.

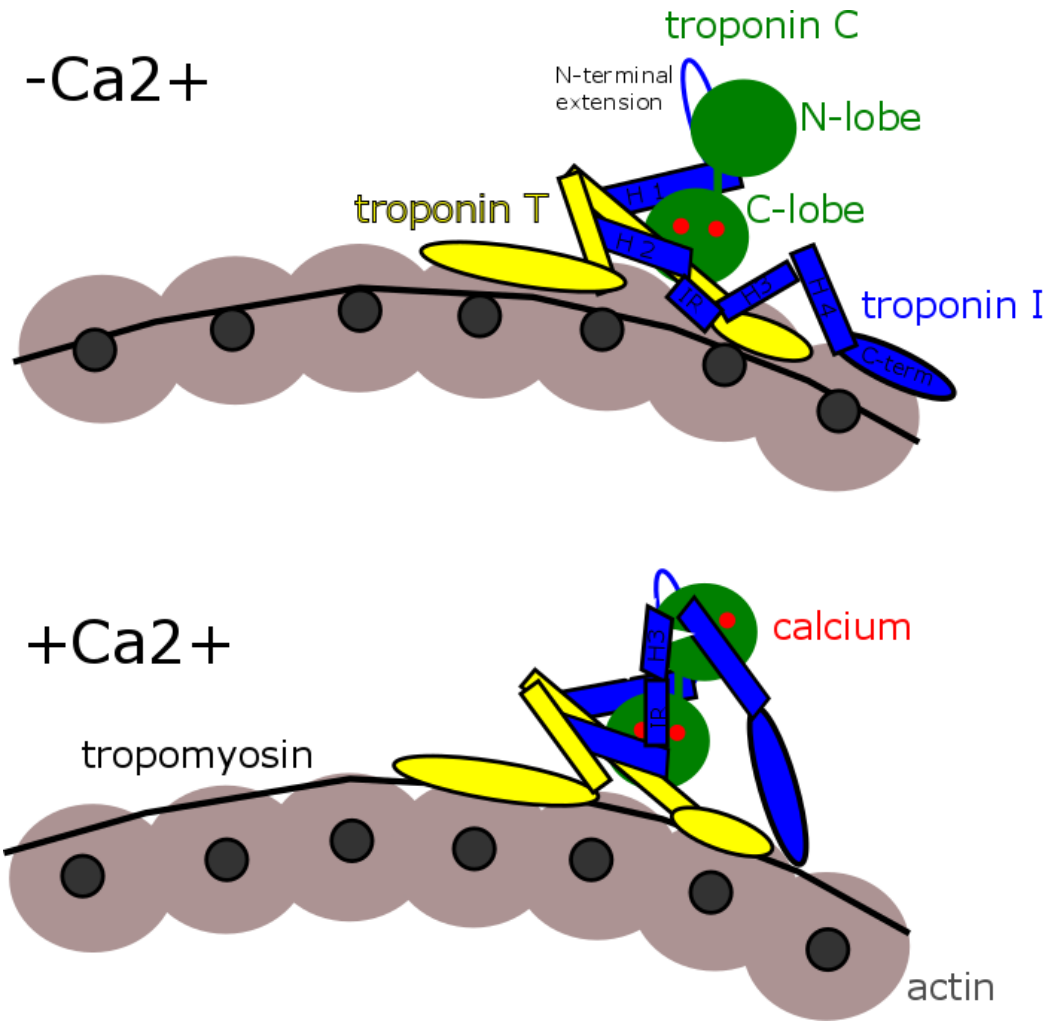

Figure 1.2 Calcium-induced conformational changes in troponin C lead to changes in troponin and tropomyosin movement. Troponin T, pictured in yellow, is named for its tropomyosin binding and tethering properties. It is also important in providing structural support to the complex as a whole. Troponin I, in blue, is named for its inhibitory properties for actomyosin binding. In fact, TNI (a specific inhibitory region) is sufficient to stabilize tropomyosin in a position to sterically block myosin binding sites. Troponin C (TNC), pictured in green, is named for its calcium binding properties (as seen in red). TNC is comprised of two lobes, the C-lobe has high affinity for both calcium and magnesium and is perpetually bound by either ion. In cardiac and invertebrate TNC, the N-lobe has one binding site, which is reversibly-regulated by calcium binding. Calcium binding induces conformational changes in the N-lobe that expose a hydrophobic patch. TNI helix 3 binds the newly exposed hydrophobic region and consequently pulls its neighboring inhibitory region away from tropomyosin/actin.

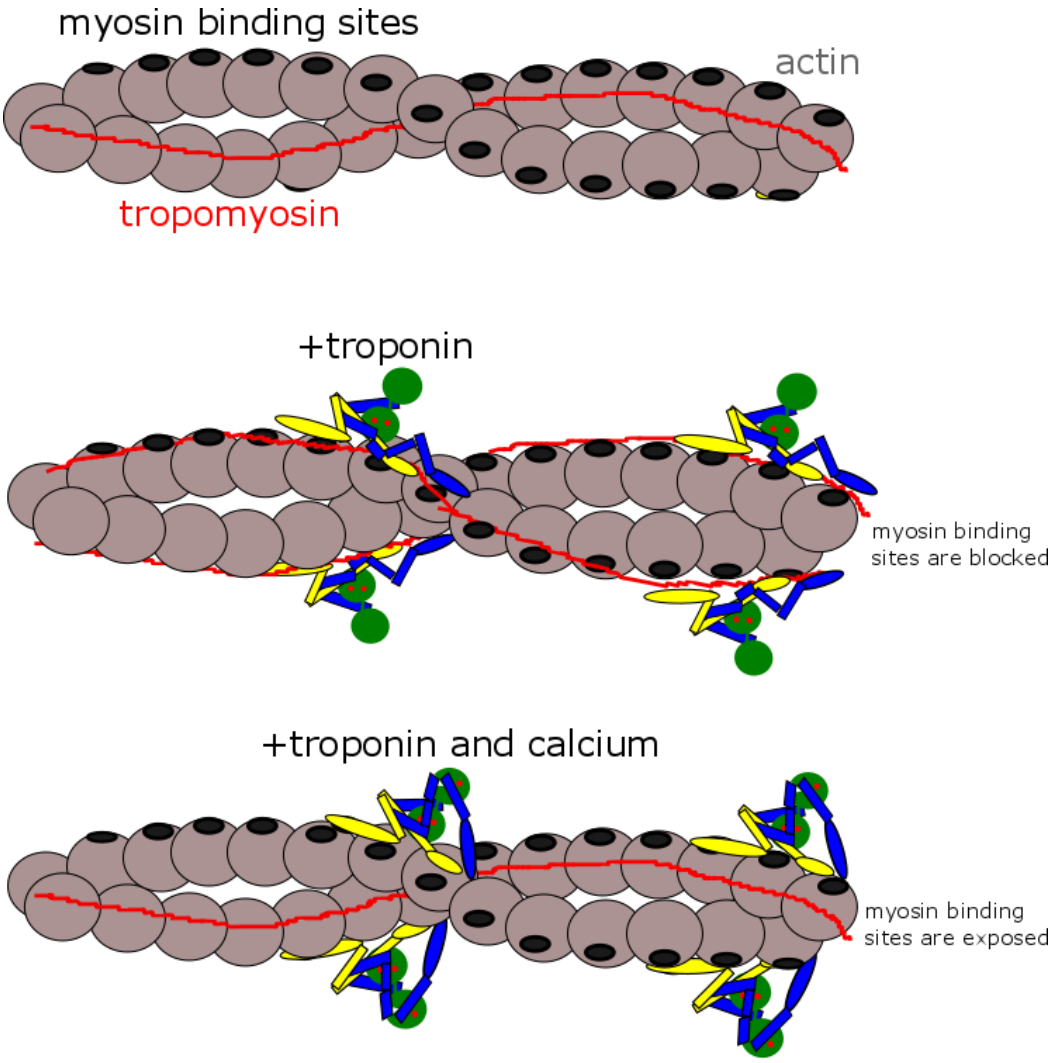

Figure 1.3 Troponin regulates tropomyosin positioning. A) On its own, tropomyosin prefers the inner actin groove. B) In the presence of the troponin complex, tropomyosin is stabilized on the outer groove of actin filaments, sterically blocking myosin binding sites. C) Calcium binding to troponin C induces conformational changes in troponin that release tropomyosin to slide toward the inner actin groove. When tropomyosin is in the inner actin groove myosin can interact with actin to cause muscle contraction.

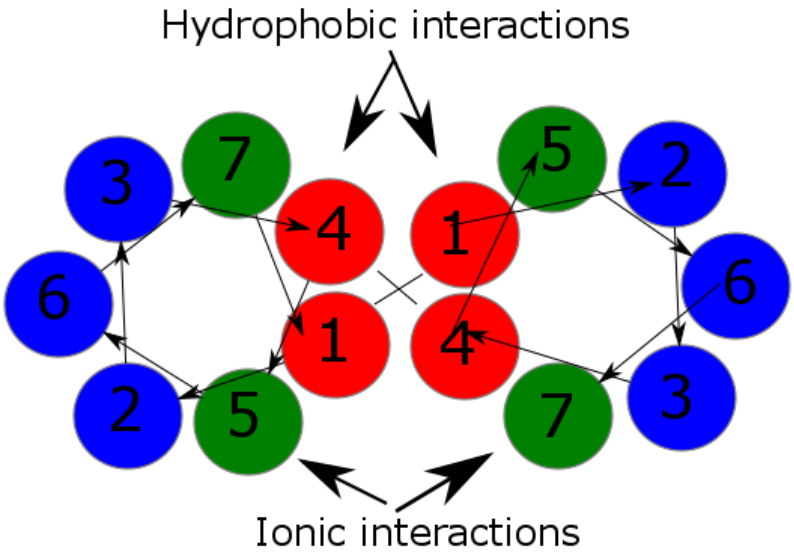

Figure 1.4. Tropomyosin forms an alpha helix with a distinct pattern of amino acid properties. The primary sequence is a heptad repeat of H-P-P-H-C-P-C amino acids, where H= hydrophobic, P= polar, and C= charged. Two alpha helices bind with their hydrophobic strips aligned, as well as complementary ionic interactions on either side of the hydrophobic strip. The polar amino acids along the outside are free to interact with actin and actin binding proteins.

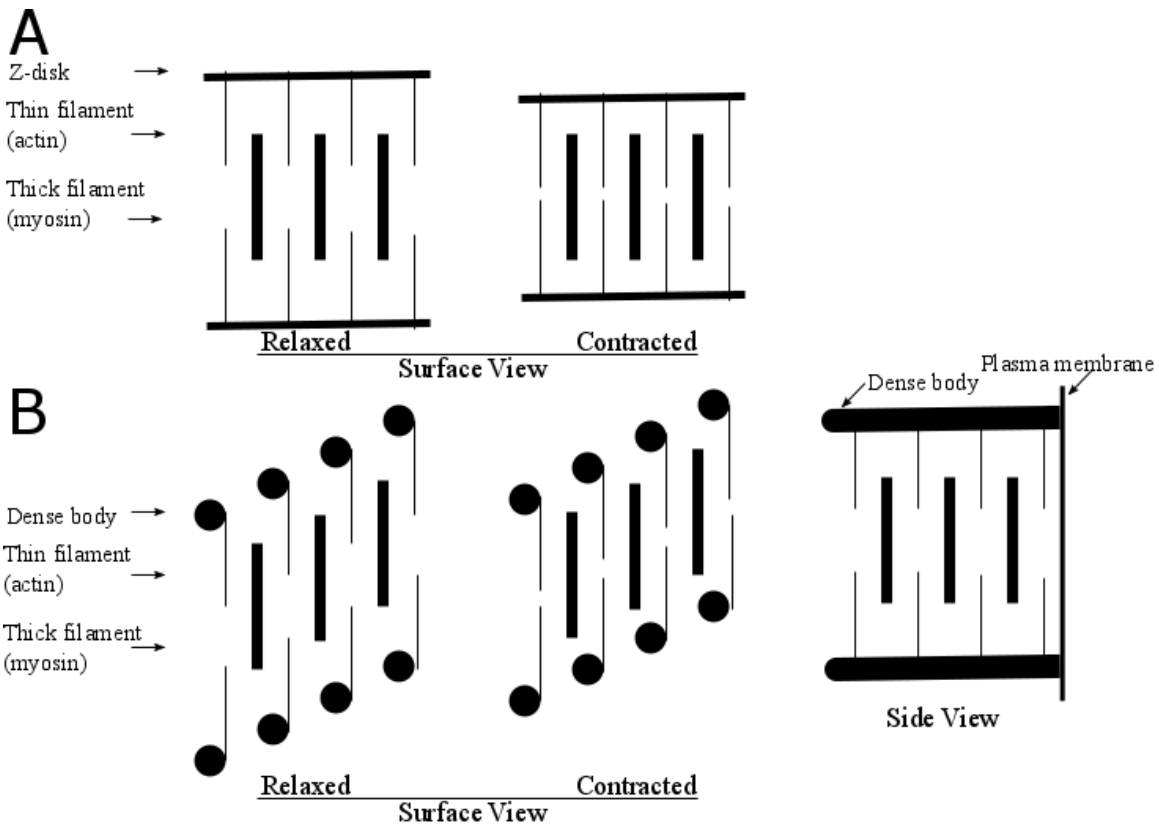

Figure 1.5. Sarcomeres differ between species and contraction state. A) Striated muscles in vertebrates exhibits striations of light and dark bands that run perpendicular to the length of the muscle filament. Thin actin filaments are anchored at Z-lines. They alternate with thick bipolar myosin filaments that make up the M-line. When the muscle is stimulated to contract, bipolar myosins ratchet along the thin filaments, toward the Z-lines, and pull them closer together. B) The thin filaments of obliquely-striated body wall muscles in *C. elegans* are anchored to dense bodies, which are finger-like projections from the plasma membrane. These dense bodies are staggered so the striations are at an angle to the length of the muscle filament.

Chapter 2

Muscle contraction phenotypic analysis enabled by optogenetics reveals functional relationships of sarcomere components in *Caenorhabditis elegans*

2.1 Abstract

The sarcomere, the fundamental unit of muscle contraction, is a highly-ordered complex of hundreds of proteins. Despite decades of genetics work, the functional relationships and the roles of those sarcomeric proteins in animal behaviors remain unclear. In this paper, we demonstrate that optogenetic activation of the motor neurons that induce muscle contraction can facilitate quantitative studies of muscle kinetics in *C. elegans*. To increase the throughput of the study, we trapped multiple worms in parallel in a microfluidic device and illuminated for photoactivation of channelrhodopsin-2 to induce contractions in body wall muscles. Using image processing, the change in body size was quantified over time. A total of five parameters including rate constants for contraction and relaxation were extracted from the optogenetic assay as descriptors of sarcomere functions. To potentially relate the genes encoding the sarcomeric proteins functionally, a hierarchical clustering analysis was conducted on the basis of those parameters. Because it assesses physiological output different from conventional assays, this method provides a complement to the phenotypic analysis of *C. elegans* muscle mutants currently performed in many labs; the clusters may provide new insights and drive new hypotheses for functional relationships among the many sarcomere components.

This chapter is adapted from the following publication:
Hwang H, **Barnes DE**, Matsunaga Y, Benian GM, Ono S, Lu H. Muscle contraction phenotypic analysis enabled by optogenetics reveals functional relationships of sarcomere components in *Caenorhabditis elegans*. *Sci. Rep.* **6**, 19900; doi: 10.1038/srep19900 (2016).

2.1 Introduction

Contractile activity of muscle is required for animal movement. The sarcomere, the fundamental unit of muscle contraction, is composed of hundreds of proteins and highly conserved in most animals. The body wall muscle of the nematode *Caenorhabditis elegans* (*C. elegans*) is a valuable model system to study the assembly, maintenance, and function of the sarcomere in striated muscle. Many genes that are required for organization of sarcomeres and the regulation of muscle contraction have been identified in *C. elegans*. The proteins encoded by these genes have been localized in the sarcomere, and their molecular and/or genetic interactions have been partly identified. For instance,*unc-54* encodes myosin heavy chain B which is a component of the thick filaments[51,52,53]. *unc-22* encodes a large muscle filament protein, twitchin, that is localized to the A-bands, where the thick filaments and the thin filaments are overlapped[54,55]. *unc-89* encodes a homologue of the vertebrate protein, obscurin, a structural component of the M-line, where the thick filaments are anchored[56]. UNC-98 and UNC-96 are also mainly localized to the M-lines and are required for organization of the thick filaments[57,58,59]. *unc-27* and *lev-11* encode troponin I and tropomyosin, respectively, which are parts of the thin-filament associated regulatory system for actin-myosin interactions[60,61]. *unc-60B*and *unc-78* encode a muscle-specific actin depolymerizing factor/cofilin isoform and a homologue of actin-interacting protein 1, respectively, which promote actin dynamics and are required for proper actin filament assembly[62,63]. In 2011, it was conservatively estimated that at least 200 proteins are required for the assembly, maintenance and function of the sarcomere in *C. elegans* body wall striated muscle[64]. We continue to

identify new components of the nematode sarcomere, and the sarcomere in general. However, the biochemical and physiological functions of these proteins are only partly understood. A major challenge is to understand how these proteins work together to build, maintain and regulate the sarcomere.

A very important contribution of the *C. elegans* model system has been, and continues to be, the genetic analysis of sarcomere components – "classical" forward genetics, reverse genetics, transgenesis, and more recently the prospect of gene editing. In fact, classical genetics led to the first identification of many of these conserved sarcomeric proteins in any system; examples include twitchin, UNC-89 (obscurin), UNC-112 (kindlin), UNC-45 (myosin chaperone), and UNC-78 (AIP1). However, phenotypic analysis of these mutants, especially at the physiological level has been limited. This is partially because the phenotyping so far has mainly relied on subjective characterization, and the descriptors have been fairly broad. This is evident in the naming of many muscle-affecting mutants and genes: there are many "unc"s (uncoordinated) and this broad descriptor includes mutants that show a variety of abnormal body movements. An often-used technique is to simply count the number of times a worm bends in C-shaped fashion in liquid over a specified time, usually one minute[65]. However, the locomotion of nematodes in liquid or on semi-solid surfaces like agar is different, and it is likely that a worm uses different gait and different energy expenditure during swimming and crawling locomotion. Recently there have been a few studies in which the swimming or crawling locomotion of *C. elegans* was investigated through computer vision-based image analysis. For instance, Nahabedian *et al.* quantitatively measured the maximum bending amplitude of

crawling worms which have defects in genes encoding muscle focal adhesion components[66]. Krajacic *et al.*quantified various biomechanical properties such as bending frequency and amplitude of swimming in synaptic mutants[67]. These methods allow more nuanced phenotyping, low user bias, and therefore potentially can extract more information; furthermore, it is possible that assays that measure other attributes of muscle contraction and relaxation may expand the repertoire of descriptors of sarcomere functions.

The ability to mechanically analyze individual muscle cells (aka fibers) from vertebrate skeletal muscle, has a long history and has yielded many insights into muscle physiology[68]. It is even possible to conduct these types of experiments using various muscle cells (e.g. thoracic, indirect flight and jump muscles) from *Drosophila melanogaster*[69], in which the influence of mutations in various sarcomeric proteins can be determined. Unfortunately, due to the small size of *C. elegans* and its mono-nucleated muscle cells, these single muscle fiber experiments cannot be done. Therefore, we have taken an alternative approach to measuring the kinetics of muscle contraction/relaxation. To control the contractile activity of *C. elegans* muscle, we utilized optogenetics, a technique that permits control of the electrical activities of neurons with visible light. *C. elegans* moves by the alternating contraction and relaxation of dorsal and ventral body wall striated muscle cells. We employed a worm strain carrying *unc-17p::ChR2*(*H134R*)*::YFP*, which expresses the light-induced channelrhodopsin-2 (ChR2) in its cholinergic motor neurons, to control the contractile activity of the body wall muscle cells and hence the locomotion of the whole nematode, as first described by Liewald *et al.*[70]. When exposed to a blue light (450–

490 nm), channel rhodopsin promotes the uptake of cations, consequently activating the motor neurons and inducing muscle contraction and shrinkage of the entire nematode body. When the light is turned off, motor neurons are no longer activated, muscle relaxes, and the nematode body relaxes to its normal size. Quantitative parameters, including rate constants for contraction and relaxation, could be extracted from these optogenetic experiments. This was performed on wild type nematodes and loss of function mutants for 15 genes that encode proteins of the sarcomere. In this work, we also use clustering analysis based on those parameters to look for information on the functional relationships of the sarcomere components. Our approach should provide a complement to existing behavioral assays for the analysis of *C. elegans* muscle mutants.

2.3 Results

Quantitative study of muscle contraction and relaxation kinetics in *C. elegans* was enabled by optogenetically-induced activation of motor neurons that induce muscle contraction. To investigate roles of sarcomeric proteins in the behavior of nematodes, mutants in 15 sarcomeric proteins were examined (Table 2.1). This set of mutants sample mutations in genes encoding proteins localized to all major structures of the sarcomere (A-bands, I-bands, thick filaments, thin filaments, M-lines and dense bodies (Z-disk analogs in nematode muscle)). To minimize the influence of gross defects in sarcomere structure, our collection of mutants were biased towards those genes whose null phenotypes have mild to no defects in sarcomere structure (*mak-1*, *atn-1*, *scpl-1*, *lim-9*, *unc-27*, *unc-78*), or alleles were chosen that exhibit mild or the mildest

defects among existing alleles (*unc-22*(*e105*),*unc-54*(*s74*), *unc-60B* (*r398*), *lev-11*(*x12*)). Many of our mutants were chosen that have minimal known defects on nematode locomotion (*unc-22*(*e105*), *mak-1*, *atn-1*, *scpl-1*, *dim-1*, *uig-1*, *lim-9*). This criteria was used so that we might determine if optogenetic assays might reveal more subtle defects in muscle function. Finally, our collection includes mutants in several known (UNC-27 (troponin I), LEV-11 (tropomyosin)) or suspected proteins (UNC-22 (twitchin)) that regulate muscle contraction.

To perform the optogenetic muscle contraction experiments, these sarcomere mutants were crossed into *zxIs6* [*unc-17p::ChR2*(*H134R*)*::YFP+ lin-15*(+)] transgenic worms, which express ChR2 molecules in cholinergic motor neurons by the *unc-17* promotor[70,71]. In this study, we refined and applied a microfluidic device where multiple worms can be trapped in multiple channels and illuminated for ChR2 photoactivation simultaneously, previously designed for high-throughput studies of synaptic transmission[72]. The two-layer device has 16 parallel microchannels in the bottom layer, and two pneumatically-controlled valves in the top layer to open or close the channels (Figure 2.1a,b). When the worms were loaded into the device and trapped in the microchannels, a blue light (450–490 nm) was illuminated. With the illumination of blue light, the cholinergic motor neurons in the nematodes were activated and their body muscles were contracted, resulting in decreased body size (Figure 2.1c). Based on image processing for segmentation of worm bodies from the recorded images (Figure 2.1c), we quantitatively tracked the change in the projected body area according to the light-induced muscle contraction (Figure 2.1d). This method allowed us to perform high-throughput non-biased analysis of the kinetics of

body wall muscle contraction and relaxation in *C. elegans*. Here the exposure time was set as 15 s based on preliminary experiments with various exposure times from 5 to 30 s; the contracted body area did not significantly change after 15 s of illumination. When the light was turned off, the relative body area began to increase due to relaxation of the body muscles (Figure 2.1d). Wild type animals showed ~3% decrease in their projected body size and completed the contraction or the relaxation processes within around 5 s after turning on or off the light, respectively (Figure 2.1d).

Some mutant worms exhibit different rates of contraction or relaxation

The optogenetic assays for muscle contraction kinetics were conducted for all of the sarcomere mutant animals we have at hand (Figure 2.7). By fitting the dynamic curves of individual animals with a one-phase decay or association model and calculating rate constants (Figure 2.2a,b), we quantitatively analyzed how fast they contract or relax the body wall muscles. Some muscle mutants including *lim-9*(*gf210*), *mak-1*(*ok2987*), *scpl-1*(*ok1080*), *unc-22*(*e66*), *unc-96*(*sf18*), and *unc-98*(*sf19*) contracted significantly faster than wild type animals, while *unc-54*(*s74*) showed significantly slower contraction compared to the wild type animals ($P < 0.001$; Figure 2.2c). Mutant animals including *atn-1*(*ok84*), *lim-9*(*gf210*), *mak-1*(*ok2987*), *unc-22*(*e105*), *unc-22*(*e66*), *unc-27*(*e155*), *unc-89*(*su75*), *unc-96*(*sf18*), and *unc-98*(*sf19*) relaxed significantly faster than the wild type animals after turning off the illumination ($P < 0.01$; Figure 2.2d). Interestingly, no mutants showed relaxation rates slower than wild type animals.

Although the rate constants for contraction or relaxation provide valuable information, they do not fully describe the range of behaviors observed among the mutants. For instance, *unc-22*(*e66*) showed a unique behavior in that the body size gradually increased due to a slight relaxation of the body muscles, just after the maximum contraction point where the relative body size had a minimum value, even though they were still illuminated (Figure 2.2b). Interestingly, a different allele of the same gene showed very different behavior: the relative body area of *unc-22*(*e105*) at the maximum contraction was similar to that at the steady state, similar to wild type (Figure 2.2a). Such characteristics of the body area change due to the muscle contraction is not captured by the rate constants for contraction and relaxation. Therefore, we extracted two more features from the fitted curves: predicted plateau after contraction, which indicates the relative body area predicted at infinite times after the contraction process ("e" in Figure 2.2a,b); and relative body area at steady state, which is the average relative body area during 5 s before the relaxation process ("f" in Figure 2.2a,b). Some mutant animals including *lim-9*(*gf210*), *mak-1*(*ok2987*), *uig-1*(*ok884*), *unc-22*(*e66*), *unc-89*(*su75*), and*unc-98*(*sf19*) showed significantly smaller predicted plateau after contraction than the wild type animals, while *unc-27*(*e155*), *unc-60B*(*r398*), and *unc-78*(*ok27*) showed significantly higher values ($P < 0.01$;Figure 2.2e). The relative body area of some mutant animals including *lim-9*(*gf210*), *mak-1*(*ok2987*), *scpl-1*(*ok1080*), *uig-1*(*ok884*), *unc-89*(*su75*), and*unc-98*(*sf19*) was significantly smaller than that of the wild type animals at the steady state, while that of *lev-11*(*x12*), *unc-22*(*e66*), *unc-27*(*e155*),*unc-60B*(*r398*), and *unc-78*(*gk27*) was significantly larger than the wild type ($P < 0.01$; Figure 2.2f).

The difference between the plateau after contraction and the relative body area at steady state indicates the ability to maintain the contraction of the muscles. No significant difference between those two values means the muscle contraction is maintained. Amongst all mutants examined, *lev-11*(*x12*) and *unc-22*(*e66*) show smaller or similar plateau after contraction than the wild type animals, while their relative body sizes at the steady state are significantly larger than that of wild type. In these mutants, the muscles relax after the contraction process despite the sustained light illumination. Interestingly, both *lev-11*(*x12*) and *unc-22*(*e66*) also show twitching locomotion while freely moving. This suggests that the inability to maintain the contraction of muscles might be related to the twitching motility observed in free locomotion.

Mutant worms have generally exhibit less bending during contraction

When nematodes carrying ChR2 in their cholinergic motor neurons were illuminated with blue light on an agar surface, they tended to coil up their bodies due to the contraction of their body muscles (Figure 2.3a). We expected that loss of function mutations in sarcomeric proteins might induce distinctive phenotypic defects not only in contraction and relaxation kinetics, but also in this coiling behavior. Thus, we also measured the minimum radius of curvature when their contracted muscles had achieved this coiled body posture. It is likely that the minimum radius of curvature as being inversely proportional to a maximum "ability" of the body to bend. All of the muscle mutants, except *scpl-1*(*ok1080*) and *lim-9*(*gf120*), showed significantly larger minimum radii of curvature ($P < 0.01$; Figure 2.3b).

The difference between the plateau after contraction and the relative body area at steady state indicates the ability to maintain the contraction of the muscles. No significant difference between those two values means the muscle contraction is maintained. Amongst all mutants examined, *lev-11*(*x12*) and *unc-22*(*e66*) show smaller or similar plateau after contraction than the wild type animals, while their relative body sizes at the steady state are significantly larger than that of wild type. In these mutants, the muscles relax after the contraction process despite the sustained light illumination. Interestingly, both *lev-11*(*x12*) and *unc-22*(*e66*) also show twitching locomotion while freely moving. This suggests that the inability to maintain the contraction of muscles might be related to the twitching motility observed in free locomotion.

When nematodes carrying ChR2 in their cholinergic motor neurons were illuminated with blue light on an agar surface, they tended to coil up their bodies due to the contraction of their body muscles (Figure 2.3a). We expected that loss of function mutations in sarcomeric proteins might induce distinctive phenotypic defects not only in contraction and relaxation kinetics, but also in this coiling behavior. Thus, we also measured the minimum radius of curvature when their contracted muscles had achieved this coiled body posture. It is likely that the minimum radius of curvature as being inversely proportional to a maximum "ability" of the body to bend. All of the muscle mutants, except *scpl-1*(*ok1080*) and *lim-9*(*gf120*), showed significantly larger minimum radii of curvature ($P < 0.01$; Figure 2.3b).

Some mutant worms exhibited slower beats and less dorsal or ventral bending

For comparison, we also conducted the conventional assays of swimming and crawling locomotion. For the analysis of swimming behavior, the nematodes including wild type and the muscle mutants were put into a plate containing M9 buffer and their swimming motion was recorded (Figure 2.4a). By post-processing the segmented images, three parameters were measured – beating frequency, dorsal bending amplitude, and ventral bending amplitude. Most of the muscle mutant animals including *atn-1*(*ok84*), *dim-1*(*ra102*), *lim-9*(*gf210*), *mak-1*(*ok2987*),*unc-22*(*e105*), *unc-22*(*e66*), *unc-27*(*e155*), *unc-54*(*s74*), *unc-60B*(*r398*), *unc-89*(*su75*), *unc-96*(*sf18*), and *unc-98*(*sf19*) beat significantly slower than the wild type ($P < 0.01$; Figure 2.4b). Some mutant animals including *atn-1*(*ok84*), *lev-11*(*x12*), *unc-27*(*e155*), *unc-54*(*s74*), *unc-96*(*sf18*), and *unc-98*(*sf19*) bent their bodies less than in dorsal direction than the wild type ($P < 0.01$; Figure 2.4c). Few mutant animals including *uig-1*(*ok884*), *unc-27*(*e155*), *unc-96*(*sf18*), and *unc-98*(*sf19*) showed smaller amplitudes in ventral bending compared to wild type ($P < 0.01$; Figure 2.4d). Interestingly, among those mutant animals, only *unc-22*(*e66*) showed significantly larger bending amplitudes in both dorsal and ventral directions than the wild type ($P < 0.001$; Figure 2.4c,d).

For the analysis of crawling behavior, the nematodes were put on the agar surface of a fresh Nematode Growth Medium (NGM) plate and their head was touched with a platinum wire in a gentle manner, leading to their backward crawling motion (Figure 2.5a)[66]. From the segmented images, we could extract three features for describing the crawling locomotion: frequency, wavelength, and the maximum amplitude of the crawling waves. According to the results, the crawling frequency

of *dim-1*(*ra102*), *lev-11*(*x12*), *mak-1*(*ok2987*), *uig-1*(*ok884*), and*unc-22*(*e105*) was significantly higher than that of the wild type animal, while that of *unc-27*(*e155*), *unc-54*(*s74*), *unc-60B*(*r398*), *unc-78*(*gk27*), and*unc-96*(*sf18*) was significantly lower ($P < 0.01$) (Figure 2.5b). The wavelength in crawling waves of *unc-27*(*e155*), *unc-96*(*sf18*), and *unc-98*(*sf19*) was significantly larger than that of the wild type, while that of *unc-54*(*s74*) was significantly smaller than that of the wild type ($P < 0.01$) (Figure 2.5c). The amplitude of *lev-11*(*x12*), *mak-1*(*ok2987*), *unc-27*(*e155*), *unc-54*(*s74*),*unc-60B*(*r398*), *unc-78*(*gk27*), and *unc-89*(*su75*) was significantly smaller as compared to that of the wild type ($P < 0.01$) (Figure 2.5d).

Optogenetic analysis reveals data clustering that correlate with sarcomere defects

To test whether the features obtained from the optogenetic muscle contraction assays could provide reliable phenotypic profiles to relate to gene function, we conducted a hierarchical clustering analysis based on mean values of the parameters that were extracted from the experiments. From the analysis using the features extracted from the optogenetic muscle assays, the clusters were separated into three groups (Figure 2.6a). The mutants having defects in the proteins localized at thin filaments[73], including *unc-27*(*e155*), *unc-60B*(*r398*), *unc-78*(*gk27*), and *lev-11*(*x12*), were clustered in one group (indicated by blue lines to the right of Figure 2.6a). The mutants having defects in proteins localized at M-lines and dense bodies, such as *dim-1*(*ra102*), *lim-9*(*gk210*), *mak-1*(*ok2987*), *scpl-1*(*ok1080*), *uig-1*(*ok884*), *unc-89*(*su75*), *unc-96*(*sf18*), and*unc-98*(*sf19*), are in one cluster (indicated by red lines to the right of Figure 2.6a). Interestingly, *unc-22*(*e105*) and *unc-54*(*s74*), which have a

normal or nearly normal sarcomere structure[52,74], were clustered in the same group with wild-type animals (indicated by green lines in Figure 2.6a), while the mutants having structural sarcomere defects, such as *dim-1*(*ra102*),*lim-9*(*gk210*), *uig-1*(*ok884*), *unc-89*(*su75*), *unc-96*(*sf18*), and *unc-98*(*sf19*), were included in one cluster. While the clustering analysis based on the parameters from the optogenetic assays showed a result that is consistent with current knowledge, we did not find any reliable clusters from the analysis based on the features extracted from the conventional locomotion assays (Figure 2.6b). Furthermore, combining the results from the optogenetic assays and those from the conventional locomotion assays also did not result in meaningful clusters (Figure 2.6c). This may be due to the ability of the mutant animals to compensate the sarcomere defects during locomotion by changing the kinematics of their locomotion pattern.

Gene	Allele	Type of allele	Protein	Location of protein
unc-22	e66	cannonical	twitchin	A-bands
unc-22	e105	missense, 7th Ig domain, GtoR	twitchin	A-bands
mak-1	ok2987	deletion, null	MAK-1 (MAPKAP kinase 2)	between & around dense bodies
unc-54	s74	missense, myosin head	MHC B (myosin heavy chain B)	thick filaments
unc-89	su75	lacks expression of all large isoforms	UNC-89 (obscurin)	M-lines
unc-98	sf19	splice site, null?	UNC-98 (C2H2 Zn fingers)	M-lines (dense bodies & nuclei)
unc-96	sf18	nonsense, null	UNC-96	M-lines (& dense bodies)
unc-27	e155	null	troponin I	thin filaments
lev-11	x12	missense, E234K	tropomyosin	thin filaments
unc-60	r398	lacking 3 aa at C-term	ADF/cofilin	thin filaments
unc-78	gk27	deletion, null	actin-interacting protein I (AIP1)	thin filaments
atn-1	ok84	deletion, null	α-actinin	dense bodies
scpl-1	ok1080	deletion, null	SCPL-1 (small CTD-phosphatase)	M-lines & I-bands
dim-1	ra102	splice site, null	3 Ig domains	between & around dense bodies
uig-1	ok884	deletion, null	Cdc42 GEF	dense bodies
lim-9	gk210	deletion, null	Four and a half LIM domains (FHL)	M-lines & I-bands

Table 2.1 List of fifteen genes encoding sarcomere proteins examined in this study.

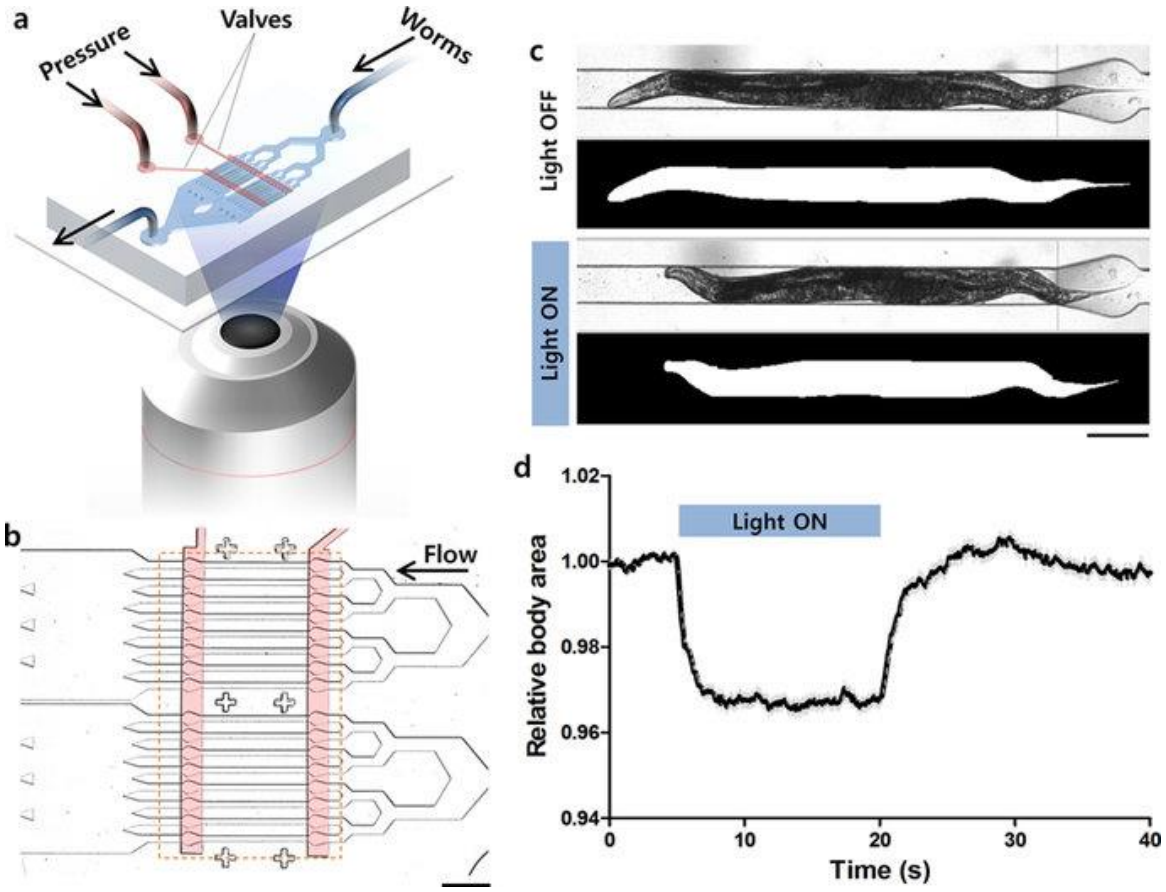

Figure 2.1 Optogenetic analysis of muscle contraction and relaxation kinetics in *C. elegans*.
(a) Schematic diagram for the behavioral phenotypic analysis enabled by optogenetics, microfluidics, and image processing technologies. **(b)** A microfluidic device having sixteen parallel microchannels for simultaneous illumination and analysis of multiple animals trapped by two pneumatically-controlled microvalves (red). Scale bar = 500 μm. **(c)**Microscopic and segmented images of a wild-type animal trapped in the microchannel with (top) and without (bottom) the illumination of blue light. Scale bar = 100 μm. **(d)** Temporal change in the body size of the wild type animals that was calculated from the segmented images and normalized by average value in the first 5 s. The light was turned on for 15 s at the 5-s time point. Data represent mean ± s.e.m. $n = 88$.

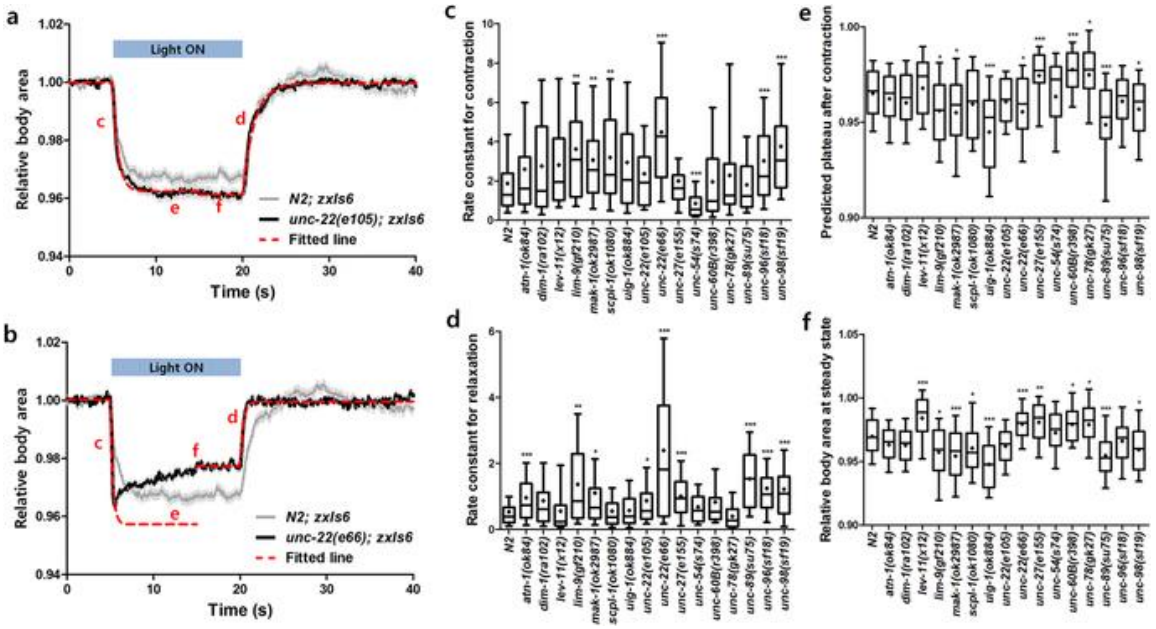

Figure 2.2 Quantitative analysis of the dynamic curves obtained from the optogenetic muscle contraction and relaxation assays in microfluidic devices. Graphs showing the optogenetic muscle contraction and relaxation processes of (**a**) *unc-22*(*e105*) and (**b**) *unc-22*(*e66*) mutants in comparison with that of the wild-type animals. The light was turned on for 15 s at the 5-s time point. Data represent mean ± s.e.m. All the plots obtained from the experiments with sixteen mutant strains were devided into two parts – contraction (0–15 s) and relaxation (15–40 s) processes–and fitted with one-phase decay and association models, respectively, to extract four quantitative parameters to describe the dynamic curves: (**c**) rate constant for contraction; (**d**) rate constant for relaxation; (**e**) plateau after contraction; and (**f**) relative body area at steady state. $n \geq 40$. $^{*}P < 0.01$; $^{**}P < 0.001$; $^{***}P < 0.0001$.

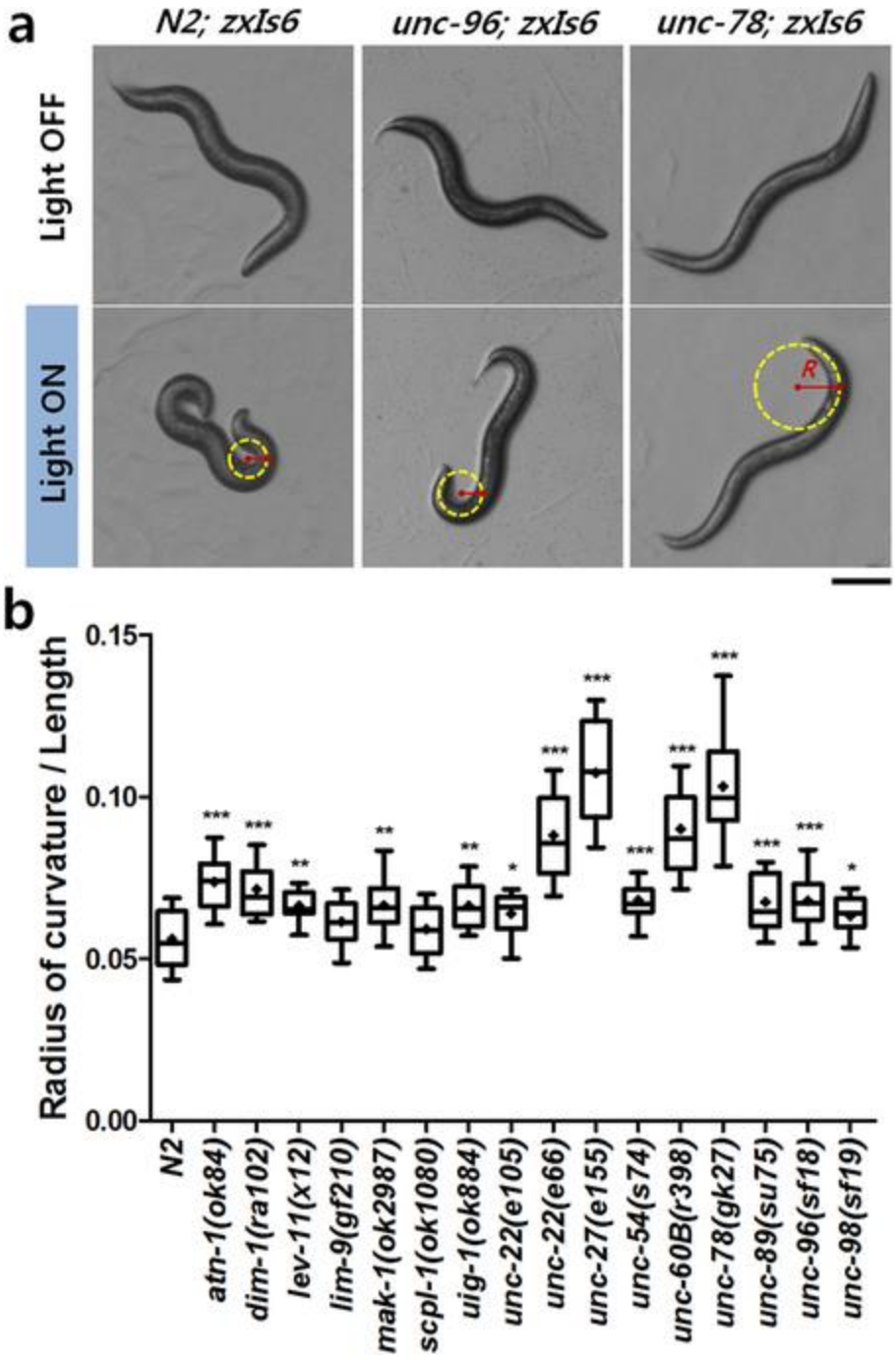

Figure 2.3 Quantitative analysis of the minimum radius of curvature at the full contraction of body wall muscles in *C. elegans*sarcomere mutants on plates.
(**a**) Representative images showing the body postures of the wild-type, *unc-96*(*sf18*), and*unc-78*(*gk27*)) without (top) and with (bottom) the illlumination of blue light to induce the full contraction of their body wall muscles. Scale bar = 100 μm. (**b**) The minimum radius of curvature of the wild-type and sixteen sarcomere mutant strains at full muscle contraction and normalized by the length of the animals. $n \geq 25$. $^{*}P < 0.01$; $^{**}P < 0.001$; $^{***}P < 0.0001$.

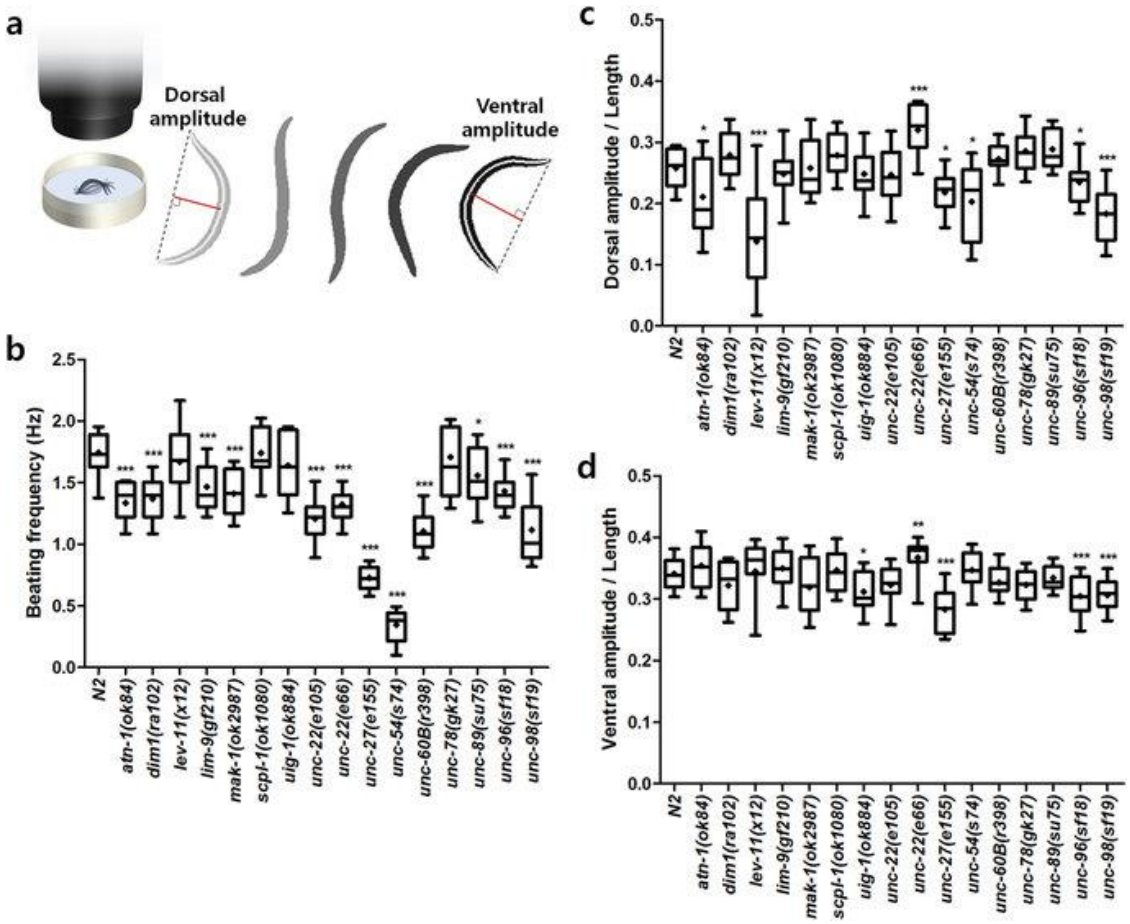

Figure 2.4 Swimming locomotion analysis of *C. elegans* sarcomere mutants.
(a) Schematic diagram of swimming locomotion assays. The nematodes were put into M9 buffer solution and their swimming locomotion was recorded. Three quantitative parameters were extracted from the threshold-segmented images: **(b)** beating frequency, and **(c)** doral and **(d)** ventral bending amplitudes normalized by the length of the animals. $n \geq 20$. $^{*}P < 0.01$; $^{**}P < 0.001$; $^{***}P < 0.0001$.

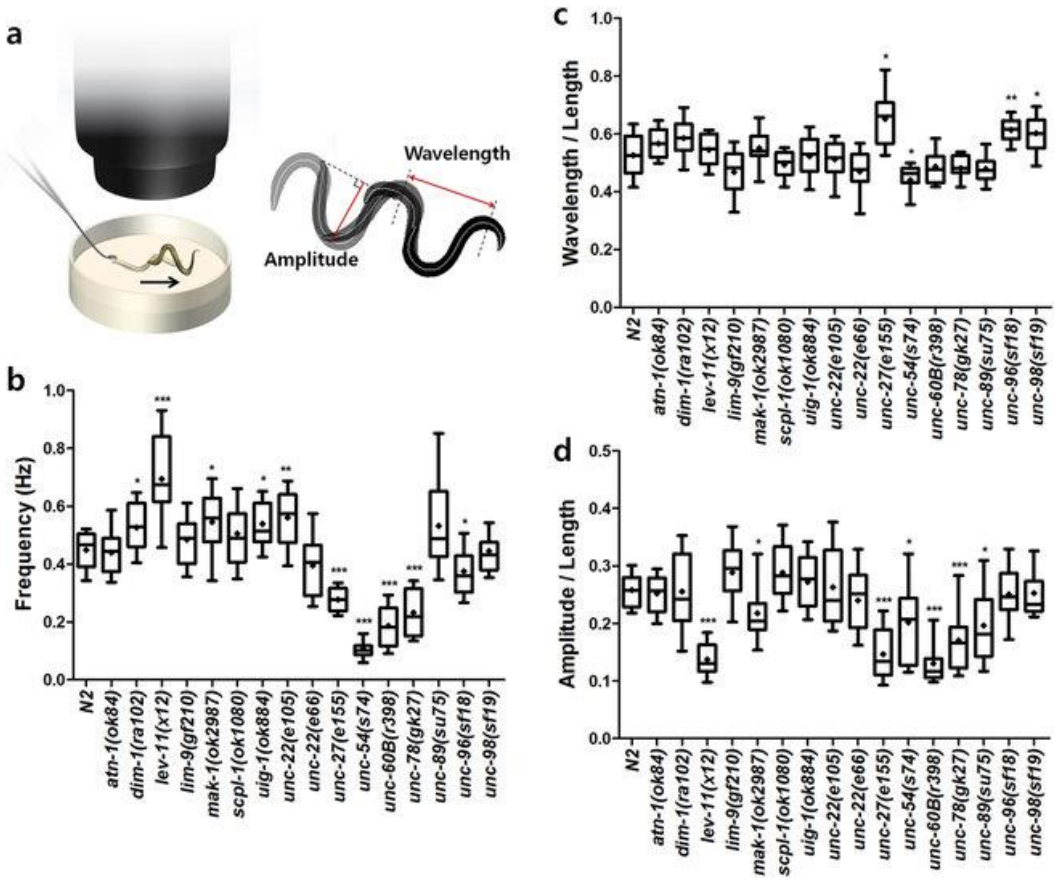

Figure 2.5 Crawling locomotion analysis of *C. elegans* sarcomere mutants. **(a)** Schematic diagram of crawling locomotion assays. The nematodes were put on fresh NGM plates solution and their head was gently touched by a platinum wire to induce the backward crawling locomotion. Three quantitative parameters were extracted from the threshold-segmented images: **(b)** frequency, **(c)** wavelength, and **(d)** amplitude of the crawling waves normalized by the length of the animals. $n \geq 20$. $^{*}P < 0.01$; $^{**}P < 0.001$; $^{***}P < 0.0001$.

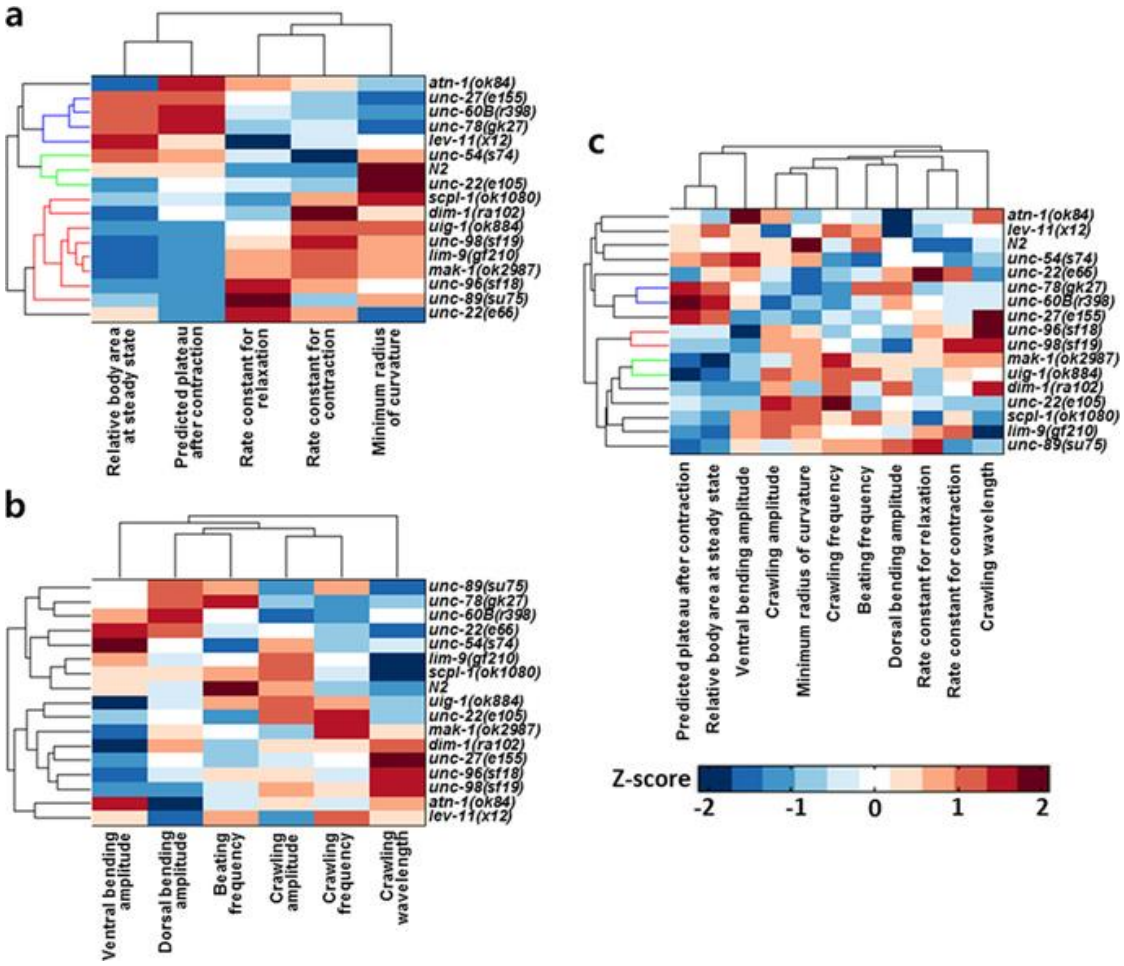

Figure 2.6 Standard hierarchical analysis based on behavioral phenotypes of *C. elegans* sarcomere mutants.
Clustering results of the wild-type and sixteen sarcomere mutant strains based on the Z-score of the mean values of the phenotypic profiles obtained from **(a)** the optogenetic muscle assays, **(b)** the conventional swimming and crawling locomotion assays, and **(c)**both assays. The phenotypic distances between a strain and the average were calculated and the differences were represented as blue (decrease) or red (increase). The mean values were normalized and standard deviations are represented by their Z-score. Based on the distances between strains, they were linked and represented by a cluster tree. Only the phenotypic analysis enabled by the optogenetic muscle assays provides reliable functional relationships among the sarcomere mutants.

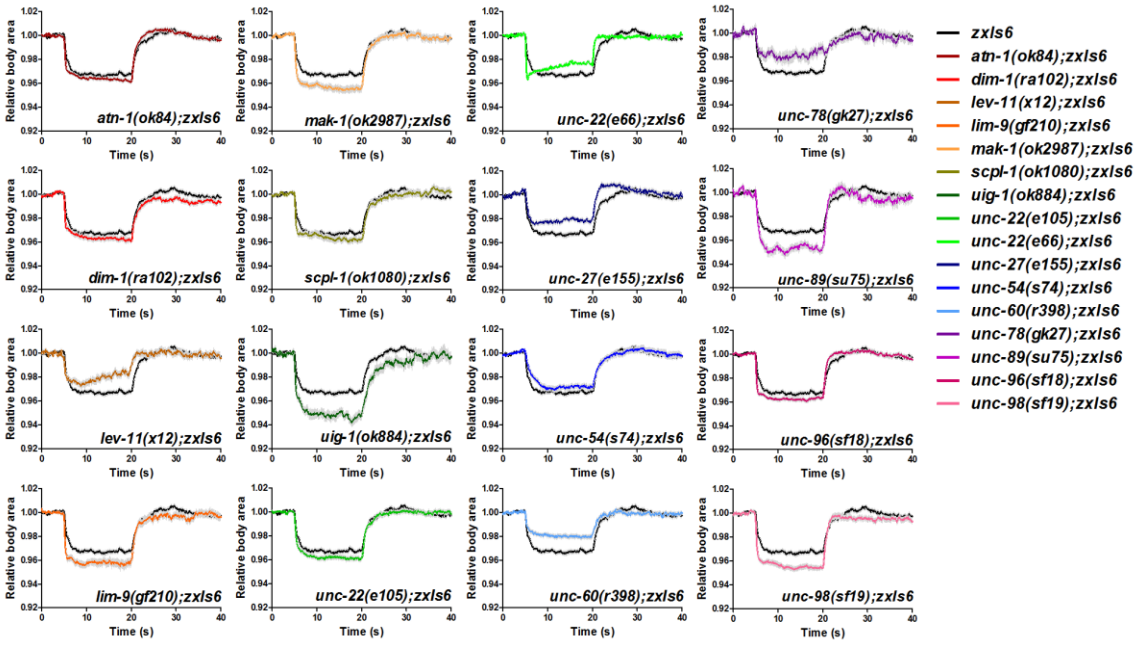

Figure 2.7 Body size changes of the *C. elegans* sarcomere mutant strains due to the optogenetically-induced muscle contraction. All the data are plotted in comparison with the wild-type (black solid line). Blue light was illuminated 5 s after starting the experiments for 15 s, and the body sizes were normalized by the average values of the first 5 s of each measurement. Data represent mean ± s.e.m. $n \geq 40$.

2.4 Discussion

Our results demonstrate the feasibility of a new quantitative assay to study the functions of genes encoding sarcomere proteins in striated body wall muscles of *C. elegans,* both as individual genes, and their relationships to each other. Although there are studies using locomotion phenotypes of *C. elegans* muscle mutants based on their swimming or crawling motion[66,6770,71], it has been difficult to study the kinetics of muscle contraction and relaxation processes in these microscopic freely-moving nematodes due to the lack of appropriate tools. Optogenetics, which enables optical control of neuronal activity, has been applied for analyzing neuromuscular synaptic functions[70,71,72]. Here we applied optogenetics as a tool for studying contraction and relaxation kinetics of the body wall muscles in *C. elegans*: we generated sixteen sarcomere mutant strains carrying ChR2 in their cholinergic motor neurons; a microfluidic device, in which multiple nematodes can be trapped and simultaneously illuminated, and computer vision technology were utilized for high-throughput, non-biased quantification of the body size change due to the light-activated muscle contraction and relaxation processes. It is worth noting that the use of the microfluidic devices greatly enhances the throughput (by reducing the time to locate and identify animals) and the reproducibility (by enhancing the ease of image processing).

We have measured, for the first time, several key parameters of the kinetics of the muscle contraction relaxation cycle, including rate constants for contraction and for relaxation. These data were obtained by studying the contraction/relaxation of the whole animal, the only now practical way such data could be obtained since isolation and manipulation of nematode muscle cells is not currently achievable. We have

surveyed a set of 16 muscle-affecting mutant strains (in 15 genes), and found that many are defective in these and related parameters.*unc-54*(*s74*) was the only mutant that showed a decrease in the rate of contraction. This result is perhaps expected. *unc-54*(*s74*) is a missense mutation (Arg to Cys) in the myosin head domain of the major myosin heavy chain of body wall muscle (MHC B), and results in worms with a slow and stiff locomotion, but normal muscle structure[52,75]. As the affected residue lies near the ATP-binding site, it is likely to affect ATP interactions and result in reduced ATPase and motor velocity, and consequently a slower contraction/relaxation cycle of the muscle. It seems significant that none of the 16 mutants tested showed a decrease in relaxation rate. This may be due to muscle relaxation being a passive, not active process. Although in vertebrate muscle elastic recoil from the giant protein titin is involved, a clear titin homolog in nematode muscle does not exist[76]. Of the 16 mutants assayed, 6 showed an increased contraction rate, and 9 showed an increased relaxation rate. Five (*lim-9*, *mak-1*, *unc-22*(*e66*), *unc-96*, and *unc-98*) showed both increases in contraction and relaxation rates. This suggests that multiple sarcomeric proteins normally inhibit the rates of contraction and relaxation.

Two mutants that showed increased relaxation rates might be explained from what is known or suspected about their roles in muscle activity. *unc-27* encodes one of four troponin I isoforms in *C. elegans*[61], and at least in vertebrate striated muscle is well known to be involved in inhibiting the interaction of myosin heads with thin filaments[77]. Both mutant alleles of *unc-22*, *e105* and *e66*, showed increased relaxation rates. In fact, *unc-22*(*e66*), yielded the greatest increase in relaxation rate among all 9 mutants that increased relaxation rates. *unc-22*encodes the giant polypeptide

twitchin[55]. Both the loss of function "twitching" phenotype, and the presence of a protein kinase domain homologous to the kinase domain of myosin light chain kinase suggested a role for twitchin in regulation of muscle contraction. We suspect that, in fact, *C. elegans* twitchin inhibits the rate of relaxation: (*i*) physiological studies in *Aplysia* suggest that twitchin inhibits the rate of muscle relaxation[78]; (*ii*) in molluscs, some smooth muscles display the "catch" state – a state in which high tension is maintained over long periods with little expenditure of ATP; the release of catch is correlated with protein kinase A phosphorylation of twitchin[79]; and (*iii*) for molluscan muscle, twitchin can be shown to act as a physical linker between thick and thin filaments *in vitro*[80]. It is perhaps significant that the rate constants for relaxation are increased in both alleles of *unc-22,e66* which has disorganized sarcomeres, and *e105* which has normally organized sarcomeres[74]. This suggests that at least one function of twitchin is indeed regulatory rather than structural.

We also conducted a clustering analysis to find functional relationships among the genes encoding the sarcomere proteins. Standard hierarchical clustering based on parameters extracted from the optogenetic assays (relative body area at steady state, plateau after contraction, rate constants for relaxation, rate constants for contraction, minimum radius of curvature) yielded clusters of gene/proteins that corroborate with what is known about the functions of these genes/proteins in the sarcomere. One cluster included all the thin filament proteins in our set of 15 proteins (UNC-27(troponin I), LEV-11(tropomyosin), UNC-60B(ADF/cofilin), UNC-78(AIP1)). Another cluster consisted of 8 of 9 of the proteins that are localized to M-lines and/or dense bodies (MAK-1, UNC-89, UNC-98, UNC-96, SCPL-1, DIM-1, UIG-1 and LIM-

9). Based on this experience, we suggest that when a new sarcomere component is identified, it would be useful to conduct a similar optogenetic and clustering analysis to provide evidence for how such a new component works together with other known components of the sarcomere. A further indication that the optogenetic approach is powerful is that cluster analysis, using parameters extracted from the conventional locomotion assays, did not reveal any statistically significant clusters. In conventional assays, movement relies on the simultaneously-coordinated contraction of some muscles and relaxation of others. With optogenetic regulation of muscle contractility, we were able to isolate the different phases of contraction and relaxation. Optogenetics enabled us to induce the contraction of body wall muscles to maximum capacity directly, thus revealing aspects of the functions of individual sarcomeric proteins that would be too subtle to be detected by conventional locomotion assays.

2.5 Materials and Methods

2.5.1 Strains and maintenance

Nematodes were grown at 20 °C on standard nematode growth medium (NGM) plates seeded with *E.coli* OP50 bacteria as a food source. For optogenetic experiments, all-*trans* retinal (Sigma-Aldrich, St. Louis, MO, USA), as an essential cofactor for ChR2 activation, was added to *E. coli* OP50 cultures to a final concentration of 100 μM and spread onto 5.5-cm NGM plates. The animals were kept in the dark until the assay to avoid unwanted ChR2 photoactivation.

Wild-type nematodes were the N2 strain. Strains used in this study are as follows: N2: wild type (Bristol isolate), ZX460: N2;*zxIs6[punc-17::ChR2*(*H134R*)*::YFP;lin-15*$^{+}$*]V*, GB254: *unc-22*(*e105*)*;zxIs6*, GB255: *unc-22*(*e66*)*;zxIs6*, GB256: *mak-1*(*ok2987*)*;zxIs6*, GB257: *unc-89*(*su75*)*;zxIs6*, GB258: *unc-98*(*sf19*)*;zxIs6*, GB259: *unc-54*(*s74*)*;zxIs6*, GB262: *unc-96*(*sf18*)*;zxIs6*, GB263: *dim-1*(*ra102*)*;zxIs6*, GB261: *atn-1*(*ok84*)*;zxIs6*, GB264: *scpl-1*(*ok1080*)*;zxIs6*, GB265: *uig-1*(*ok884*)*;zxIs6*, GB260: *lim-9*(*ok210*)*;zxIs6*, ON295: *unc-27*(*e155*)*;zxIs6*, ON302: *lev-11*(*x12*)*;zxIs6*, ON303: *unc-60B*(*r398*)*;zxIs6*, and ON304: *unc-78*(*gk27*)*;zxIs6*.

2.5.2 Optogenetic assays

For on-chip optogenetic assays, two-layer microfluidic devices made of polydimethylsolxane (PDMS; Sylgard 184, Dow-Corning Corp., Midland, MI, USA) were fabricated using standard multi-layer soft lithography. The device has 16 parallel microchannels for trapping worms, and their opening and closing are controlled by two valves in the upper layer (Figure 2.1a,b). Each channel is 60 μm wide and has a rectangular cross section, thus fluid flow or small animals are allowed to pass through the channels while the valves are partially closed. The valves were filled with a 58% glycerol solution to match the refractive index of the PDMS resulting in improved image quality. The pressures for the valve actuation and the sample delivery were regulated by off-chip solenoid valves (Series 188, ASCO Valve Inc., Florham Park, NJ, USA).

To trap worms in the microchannels, the valve at the exit of the channels were initially closed. After young adult animals were delivered into the channels by a

loading pressure, the valve at the entrance of the channels was closed and the loading pressure was turned off. The animals were illuminated with blue light (450–490 nm; 0.3 mW/mm^2) for 15 s to induce ChR2 photoactivation. For measurements of projected body area, movies were recorded using a CCD camera (Infinity 3-1, Luminera Corp., Canada). After completing the light illumination and image acquisition, the exit valve was open and the loading pressure was turned on to flush out the worms, followed by another cycle. All the processes including valve actuation, worm injection, and image acquisition were controlled by LabVIEW software.

The movies were post-processed using custom software written in MATLAB. Images of the channels without worms were used for removing background of the captured movies, resulting in high quality segmentation of worm images. The projected body area of the worms in the segmented images was used as a read-out for the light-stimulated muscle contraction and relaxation. The body area measured from the images captured during 5 s before the blue light illumination was used as a baseline, and its change was plotted over time. The curves were fitted with the plateau followed by one phase decay or association equations for the kinetic analyses of the contraction or the relaxation processes, respectively.

For on-plate optogenetic assays looking at maximum body bend, young adult animals were transferred to fresh 5.5-cm NGM plates and images were taken to measure their body length with no illumination. The animals were illuminated with blue light until they fully contract their body, then images were taken to measure the minimum radius of curvature of the worm body at full contraction. The measured values were normalized with the length of each animal.

2.5.3 Locomotion analysis

For swimming or backward locomotion analyses, young adult animals were transferred into 3 cm diameter plates containing 500 μL of M9 buffer or fresh 5.5-cm NGM plates, respectively. After a 2-min acclimation period, the behavior of each animal was observed. To induce backward motion, their head was gently prodded with a platinum wire. For both experiments, movies were acquired on a standard transmitted light stereo microscope.

The movies were post-processed to extract the worm skeleton using custom software written in MATLAB. The average frequencies for swimming or crawling locomotion were measured. The maximum ventral or the dorsal bending amplitudes, or the maximum bending amplitude and the wavelength were measured from the swimming or the crawling locomotion. Those values were normalized by the length of each worm.

2.5.4 Statistical analysis

All curve fitting and statistical analysis were performed using Prism 5 (GraphPad Software, San Diego, CA, USA). Wilcoxon Rank sum test was conducted for comparison of the data when appropriate. *P*-values < 0.01 were considered as statistically significant: $^{*}P < 0.01$; $^{**}P < 0.001$; $^{***}P < 0.0001$.

2.5.5 Clustering analysis

A standard hierarchical clustering analysis was conducted using MATLAB. After normalizing the mean values of the parameters obtained from the experiments into Z-score, the phenotypic distances between the strains were calculated. Based on the

distance information, the strains were linked, and the hierarchical cluster tree was created.

Chapter 3 Molecular evolution of troponin I and a role of its N-terminal extension in nematode locomotion

3.1 Abstract

The troponin complex, composed of troponin T (TnT), troponin I (TnI), and troponin C (TnC), is the major calcium-dependent regulator of muscle contraction, which is present widely in both vertebrates and invertebrates. Little is known about evolutionary aspects of troponin in the animal kingdom. Using a combination of data mining and functional analysis of TnI, we report evidence that an N-terminal extension of TnI is present in most bilaterian animals as a functionally important domain. Troponin components have been reported in species in most representative bilaterian phyla. Comparison of TnI sequences shows that the core domains are conserved in all examined TnIs, and that N- and C-terminal extensions are variable among isoforms and species. In particular, N-terminal extensions are present in all protostome TnIs and chordate cardiac TnIs but lost in a subset of chordate TnIs including vertebrate skeletal-muscle isoforms. Transgenic rescue experiments in *C. elegans* striated muscle show that the N-terminal extension of TnI (UNC-27) is required for coordinated worm locomotion but not in sarcomere assembly and single muscle-contractility kinetics. These results suggest that N-terminal extensions of TnIs are retained from a TnI ancestor as a functional domain.

This chapter is adapted from the following publication:
Dawn E. Barnes, Hyundoo Hwang, Kanako Ono, Hang Lu, S. O. Molecular evolution of troponin I and a role of its N-terminal extension in nematode locomotion. *Cytoskeleton* (2016). doi:10.1002/cm.21281

3.2 Introduction

Across various organisms and muscle types, contraction is regulated by several distinct mechanisms[81]. In vertebrates, striated (skeletal and cardiac) muscle is regulated through a Ca^{2+}-sensitive troponin-tropomyosin system on thin filaments[82]. In contrast, the major regulatory system for vertebrate smooth (or non-striated) muscle is through the phosphorylation of myosin regulatory light chain[83], with additional regulation through actin-binding proteins, such as calponin and caldesmon[84,85]. In comparison to vertebrates, invertebrate muscles are diverged in both morphology and physiology, and these simple correlations cannot be applied[86]. For example, molluscan striated and smooth muscles have both troponin-tropomyosin[87–89] and myosin that is regulated by direct binding of Ca^{2+} to essential light chain[90]. In the nematode *Caenorhabditis elegans*, the troponin-tropomyosin system controls contraction of both striated muscle[42,46,61] and non-striated muscle[47,91,92]. Muscle regulation has been experimentally studied in limited species. Therefore, we currently have a partial view of divergence and conservation of the regulatory mechanisms of muscle contraction across the animal kingdom. Further information on the comparative aspects of the muscle regulatory mechanisms should be important to gain insight in the evolution of various muscle types that have adapted to different functions.

Troponin is a key regulatory component of muscle contraction. It acts as a rapid Ca^{2+}-dependent on-off switch for the actin-myosin interaction[93]. The functional unit of troponin is a complex of three components: troponin T (TnT), troponin I (TnI), and troponin C (TnC). In the vertebrate troponin complex, TnI inhibits actin-myosin interaction at low Ca^{2+} concentrations in cooperation with tropomyosin. At high Ca^{2+}

concentrations, Ca^{2+} binds to TnC and relieves the inhibitory function of TnI. TnT tethers the troponin complex to tropomyosin and promotes the inhibition of actomyosin interaction at low Ca^{2+}[94]. Atomic structures of the core domain of the troponin complex show extensive intra- and inter-molecular interactions among the troponin components[7,95]. Ca^{2+}-dependent dynamic alterations in the troponin conformations are required for its switch function[96,97]. Troponin is present broadly in the animal kingdom, suggesting that molecular evolution of the troponin complex might be a key to understanding the origin of muscle and evolution of its regulatory systems. A recent comparative genomic study has shown that troponin genes emerged in bilaterians (animals with bilateral body plans) but are absent in cnidarians, ctenophores, and porifera[19]. However, how broadly troponin is present in bilaterian species has not been extensively studied.

In this study, we examined databases and literature and report that troponin is present in all representative bilaterian phyla except for the Ambulacrarian clade (Echinodermata and Hemichordata). Comparison of the TnI sequences shows conservation of the core domains and variation in the N- and C-terminal extensions. Particularly, N-terminal extensions are present in all protostome TnIs but absent in a subset of deuterostome TnIs, suggesting an isoform-specific evolutionary loss of the N-terminal extension from TnI. Functional analysis in the nematode *C. elegans* indicates that the N-terminal extension of TnI is important for coordinated locomotive behavior of worms. Thus, the results suggest that the N-terminal extension is retained in most of TnIs as a functionally important domain.

3.3 Results and Discussion

3.3.1 Troponin Evolved Early in the Bilateria

Steinmetz and colleagues analyzed sequences of various muscle proteins from broad species and found that the troponin complex is absent in cnidarians and ctenophores, despite the fact that they have striated muscle[19], suggesting that troponin has evolved in bilaterians. We reexamined this view by analyzing existing literature and sequence data broadly in representative bilaterian species (Figure 3.1). Troponin components have been characterized at genomic and/or mRNA levels in many species. However, in some cases, troponin or troponin-like proteins have been characterized only at protein levels based on their troponin-like biochemical properties with no known sequence information. Therefore, we assessed both molecular and biochemical data in databases and literature and examined whether a component(s) of the troponin complex is present or absent within bilaterian phyla (Figure 3.1).

Troponin components have been identified widely in both protostomes and deuterostomes (Figure 3.1, troponin is present in phyla indicated by red), suggesting that troponin emerged shortly after evolution of bilaterians. Within the Deuterostomia, multiple isoforms of the three troponin components have been extensively characterized in the Chordata including vertebrates (Jin et al. 2008), urochordates (sea squirts) (Obinata and Sato 2012), and cephalochordates (e.g. amphioxus)[98]. Within the Protostomia, in the Arthropoda, all three troponin components have been characterized biochemically or genetically in several crustaceans and insects, including the fruit fly *Drosophila*

melanogaster[99]. In the Nematoda, all three troponin components have been genetically characterized in *Caenorhabditis elegans* (Kagawa et al. 2007) and biochemically in *Ascaris suum*[100] (Kimura et al. 1987). In the Mollusca, the three troponin components from sea scallop have been characterized both molecularly and biochemically[87–89]. However, in other phyla, components of troponin have been reported only based on cDNA or genomic sequences and/or immunoreactivity with antibodies. In the Annelid, a TnT-like protein was detected in the earthworm *Eisenia fortida* by anti-rabbit TnT antibody (Royuela et al. 1996), and a TnI sequence was found in the genome of the polychete worm *Capitella teleta* (Table 3.1). In the Tardigrada, a TnI-like protein was detected by anti-nematode TnI antibody[101], and a TnC cDNA has been cloned from the water bear *Hypsibius*[102]. In the acoel flatworm, which has been recently classified in the new phylum Xenacoelomorpha[103], a TnI cDNA has been cloned from *Symsagittifera roscoffensis*[104]. In addition, TnI-like sequences have been annotated in the genome of the parasitic flatworm *Schistosoma japonicum* (Platyhelminthes) and the bdelloid rotifer *Adineta vaga* (Rotifera) (Table 3.1).

By contrast, within the Deuterostomia, our homology search in the genome of the sea urchin *Strongylocentrotus purpuratus*[105] failed to detect a troponin component. This is consistent with earlier biochemical studies showing the absence of a troponin-like protein in muscles of sea urchin[106], sea cucumber[81], and sea lily[107], suggesting strongly that the phylum Echinodermata lacks troponin (Figure 3.1). Interestingly, a recent biochemical study has demonstrated that the acorn worm *Balanoglissus misakiensis* also lacks troponin in its muscle (Sonobe et al., personal communication), suggesting that the phylum Hemichordata also lacks troponin (Figure 3.1). These observations are indeed

consistent with the current views that the Echinodermata and Hemichordata are related phyla forming the clade Ambulacraria[108,109]. Thus, the widespread presence of troponin in the Bilateria (Figure 3.1) suggests that troponin has emerged in a common ancestor of the Deuterostomia and the Protostomia but was lost in the Ambulacrarian lineage (Figure 3.1).

3.3.2 Phylogenetic Relationships of Troponin I Sequences Suggest That the N-terminal Extension Was Lost in a Subset of Isoforms in the Deuterostomia

Next, we compared molecular phylogenetic relationships among the TnI sequences (Figure 3.2 and Table 3.1). We selected one species from each phylum in which troponin has been detected (Figure 3.1), with the exception of the Chordata, in which we included two species: the vertebrate *Mus musculus* (mouse) and the urochordate *Halocynthia roretzi* (sea squirt). The Tardigrada was not included because a TnI has not been cloned. Alignment of 19 TnI sequences from 9 species using Clustal Omega[110] agreed with the phylogenetic relationship of the organisms (Figure 3.2). TnI sequences in the Protostomia Ecdysozoa, the Protostomia Lophotrochozoa, and the Deutrostomia were grouped (Figure 3.2). The multiple TnI isoforms in the Nematoda, the Arthropoda, and the Chordata branched after each phylum diverged (Figure 3.2), suggesting that the TnI isoforms derive from a single ancestor and evolved after each phylum was established. Likewise, within the Chordata, TnI isoforms in vertebrates and urochordates branched after these groups split, suggesting that these isoforms are derived from a single common ancestor rather than multiple isoform-specific ancestors. Although phylogenetic positioning of the acoel flatworm (Xenacoelomorpha) is still under debate[111,112], our unbiased analysis

suggests that TnI from *Symsagittifera* (acoel flatworms) is an early branch within the Deuterostomia TnI group (Figure 3.2), which agrees with the placement based on extensive molecular phylogenetic analysis[103].

The sequence alignment indicates that the central ~150-amino-acid region of TnI including four helices (H1 – H4) and the inhibitory region (IR) is highly conserved (Fig. 3A and Fig. S1). Ca^{2+}-independent interactions between H1 and the C-lobe of TnC, and H2 with TnT, are important for formation of a stable core[7,95]. H3 functions as a switch region by binding to the N-lobe of TnC in a Ca^{2+}-dependent manner. The inhibitory region (IR) binds to actin and is sufficient to inhibit actomyosin interaction[113–115]. Therefore, the homology suggests that the functions of these regions in the troponin complex formation and Ca^{2+}-dependent regulation of actomyosin interaction are conserved.

In contrast, the N- and C-terminal sequences are variable (Figure 3.3A and Figure 3.8). The C-terminal tails outside of the H4 sequences are highly variable in length and sequence (Figure 3.8). The most extreme TnI is the insect flight-muscle-specific TnI (also known as TnH, not included in the alignment) that has a ~150-residue long proline-alanine-rich extension[99]. The C-terminal sequences among related species are relatively conserved (*e. g.* three mouse isoforms and sea squirt cardiac and skeletal isoforms in Figure 3.8). Among the four TnI isoforms in *C. elegans*, three isoforms (UNC-27, TNI-1, and TNI-3) have similar C-terminal tails, but TNI-4 does not have a tail (Figure 3.8). Likewise, the C-terminal tails are present in *Halocynthia* adult isoforms but absent in all three larval isoforms (Figure 3.3 and Figure 3.8). Interestingly, TnIs from two distant species, *C. elegans* (Nematoda) and *Capitella* (Annelida) have similar C-terminal tails

that are highly enriched in glutamic acids (Figure 3.8), suggesting the presence of a common ancestor. These observations suggest that the C-terminal tail was present in the ancestral TnI and variably truncated or retained during evolution.

The N-terminal extensions (NTEs) of TnIs are also variable but exhibit a different type of evolution than the C-terminal tails. NTEs are present in all examined TnIs in the Protostomia Ecdysozoa and Lophotrochozoa and cardiac isoforms in the Deuterostomia Chordata (Figure 3.2, indicated by red) but absent in non-cardiac TnIs in the Deuterostomia (Figure 3.2, indicated by blue). The lack of an NTE in the acoel flatworm *Symsagittifera* TnI is particularly interesting because truncation of the NTE appears to be a deuterostome-specific event (Figure 3.2). However, in the absence of the genomic sequence of acoel flatworms, we cannot rule out the possibility that another TnI isoform with an NTE exists. Although the length of NTEs range from 30 to 130 amino acids, NTEs commonly contain high percentages of charged amino acids (Figure 3.3B, blue and red indicate acidic and basic residues, respectively). The NTE sequences of TnIs from *C. elegans* and *Drosophila* are strikingly conserved (Figure 3.3B). *Schistosoma* TNI has a longer NTE than *C. elegans* and *Drosophila* TNIs, but it is highly enriched in charged residues, and a part of the *Schistosoma* sequence aligns well with those of *C. elegans* and *Drosophila* (Figure 3.3B). The occurrence of NTEs with a similar feature in broad species strongly suggests that an NTE was present in an ancestral TnI and lost specifically in the Deuterostomia lineage with an exception of cardiac isoforms in the Chordata. In mammals, three TnI isoforms are encoded by three independent genes[116]. However, in sea squirts (urochordates), adult cardiac and body-wall isoforms are produced by alternative splicing of pre-mRNA encoded by a single gene[117,118]. Thus, the

presence or absence of NTE has been accomplished by different strategies in vertebrates and urochordates.

3.3.3 Troponin I N-terminal Extension Is Required for Regulation of Locomotive Behavior in the Nematode *Caenorhabditis elegans*

In addition to the core TnI domains, NTEs are present in all examined protostome TnIs and chordate cardiac TnIs, suggesting that NTEs are important for the function of troponin. The NTE of mammalian cardiac TnI isoform has a modulatory function for Ca^{2+} sensitivity of the thin filaments[119,120]. A biochemical study on molluscan TnI has shown that the NTE is not required for the basic function of TnI but may enhance Ca^{2+}-dependent actomyosin ATPase *in vitro*[89] (Tanaka et al. 2005). However, functional significance of NTEs of invertebrate TnIs has not been studied *in vivo*. Therefore, we examined an *in vivo* role of the NTE in *C. elegans* body wall muscle, which is obliquely striated muscle with highly organized sarcomeres[73], using a transgenic technique.

Among the four *C. elegans* TnI genes, UNC-27 is the major TnI isoform expressed in the body wall muscle[46,61]. In wild-type, actin filaments are regularly organized in a striated pattern in the body wall muscle (Figure 3.4A). In *unc-27*-null mutant [*unc-27(e155)*], sarcomeric actin filaments were disorganized, which is likely due to unregulated actomyosin contraction (Figure 3.4D). When green fluorescent protein (GFP)-tagged UNC-27 [wild-type (WT)] was expressed in the body wall muscle of the *unc-27* mutant using the muscle-specific *myo-3* promoter, striated actin organization was restored nearly to the appearance of wild-type (Figure 4G). GFP-UNC-27(WT) co-localized with actin filaments in a striated pattern (Figure 4H and I). These data indicate that GFP-UNC-27(WT) incorporated into the thin filaments and was functional to

maintain sarcomeric actin organization. Expression of GFP-UNC-27(ΔN), which lacks the NTE (residues 2-29), also restored striated actin organization (Figure 3.4J), and GFP-UNC-27(ΔN) co-localized with sarcomeric actin filaments (Figure 3.4K and L). We isolated three independent transgenic strains for GFP-UNC-27(WT) and GFP-UNC-27(ΔN) and found no significant differences in GFP localization and worm motility among the isolates (our unpublished observations). Expression of GFP-UNC-27(WT) and GFP-UNC-27(ΔN) were confirmed by Western blot with anti-TnI antibody (Figure 3.4M) and anti-GFP antibody (Figure 3.4O). Quantitative analysis of the band intensity of the GFP-fusion proteins (normalized to the relative levels of actin) indicates that the protein levels of GFP-UNC-27(WT) and GFP-UNC-27(ΔN) were not significantly different ($P = 0.66$) (Figure 3.4P). Therefore, we concluded that the NTE of *C. elegans* UNC-27 is not required for incorporation of UNC-27 into sarcomeres and maintenance of sarcomeric actin organization.

Next, we examined roles of UNC-27 in locomotive behavior of worms. *C. elegans* crawl on a flat surface in a sinusoidal motion and swim in liquid in a swinging motion. These locomotive behaviors require coordinated contraction and relaxation of muscle cells in different parts of the body[121]. Worm motility, as determined by beat frequency in liquid, was significantly impaired in the *unc-27* mutant (Figure 3.5). Motility of the *unc-27* mutant worms was considerably restored by expression of GFP-UNC-27(WT) but not by expression of GFP-UNC-27(ΔN) (Figure 3.5). Motility of *unc-27* expressing GFP-UNC-27(WT) was not as fast as wild-type (Figure 3.5). These transgenes were maintained as extrachromosomal arrays, which are sometimes lost in a subset of cells[122]. We manually selected worms that express GFP in most of muscle cells

(roughly >80 %) for analysis, but such mosaicism might have caused the incomplete rescue of the motility. The protein levels of GFP-UNC-27(WT) and GFP-UNC-27(ΔN) were comparable (Figure 3.4P), suggesting that the presence or absence of the NTE in UNC-27 confers the difference in worm motility.

We further quantified amplitude of body bending during touch-induced backward locomotion. This parameter has previously been used to detect locomotive phenotypes in several muscle-affecting mutants[66,123]. Backward locomotion was induced by gently touching the head of a worm (Figure 3.6A), and body bending was observed within two sinusoidal waves with quantification of amplitude (A) normalized by the body length (L) (Figure 3.6B). By comparing wild-type and *unc-27* mutant worms, the bodies of wild-type worms were more curved than those of *unc-27* worms (Compare Figure 3.6B and D). Quantitative analysis shows that bending amplitude of wild-type was nearly twice as much as that of *unc-27* (Figure 3.6I). Expression of GFP-UNC-27(WT) in the *unc-27* mutant restored bending amplitude to the wild-type level (Figure 3.6F and I), whereas expression of GFP-UNC-27(ΔN) did not affect the phenotype (Figure 3.6H and I). These observations strongly suggest that the NTE of UNC-27 is required for efficient sinusoidal locomotive behavior of worms, which involves coordinated regulation of contraction and relaxation of body wall muscle.

Because worm locomotion involves asynchronous muscle contraction and relaxation, we examined synchronous contraction and relaxation events by adapting an optogenetic technique in combination with a microfluidic device and real-time imaging, which had been developed to characterize neuronal circuits and synaptic transmission in *C. elegans*[71,124]. Channelrhodopsin-2, a light-activatable cation channel from

Chlamydomonas, was expressed in cholinergic motorneurons, which allows induction of synchronous whole-body muscle contraction by blue-light illumination[125]. The worms were trapped in microfluidic channels, and temporal changes in their body size after turning the light on (contraction) and off (relaxation) were measured. Then, rates of contraction and relaxation were determined[72]. Expression of channelrhodopsin-2 did not alter sarcomere organization and worm motility (our unpublished data). Recently, we utilized this method to characterize 16 muscle-affecting mutants and verified that this is an excellent non-invasive method for quantitative analysis of muscle contractility[126].

Using this approach, we found that the *unc-27* mutation did not affect the rate of contraction (Figure 3.7A) but significantly increased the rate of relaxation (Figure 3.7B). Enhanced relaxation rate in the *unc-27* mutant was somewhat unexpected. TnI normally inhibits actomyosin contractility at low Ca^{2+}; we therefore expected its absence to decelerate dissociation of actomyosin. However, troponin complexes from ascidian [127,128] and molluscan[89] accelerate actomyosin ATPase in a Ca^{2+}–dependent manner. If UNC-27 is a component of an accelerator-type troponin complex, disruption of such a system might enhance the rate of relaxation. Expression of either GFP-UNC-27(WT) or GFP-UNC-27(ΔN) in the *unc-27* mutant did not affect the rate of contraction (Figure 3.7A) and rescued the faster relaxation rate of the *unc-27* mutant to the wild-type rate (Figure 3.7B). Thus, the results demonstrated that the NTE of UNC-27 is not required for proper control of synchronous muscle contraction or relaxation. Our observations that both GFP-UNC-27(WT) and GFP-UNC-27(ΔN) could rescue sarcomeric disorganization in the *unc-27* mutant at a cellular level (Figure 3.4), suggesting that each muscle cell has functional contractile apparatuses, which are capable of producing maximum outputs

during synchronous muscle contraction.

Previous phenotypic analysis of *unc-27* mutants suggest that they are constitutively contracted under normal culture conditions[61]. In the optogenetic experiments, reduction of the body area upon light stimulation was slightly less in *unc-27* than in wild-type, suggesting that the *unc-27* mutant had been partially pre-contracted before light stimulation[126]. Basal contraction levels can potentially influence the rates of light-induced contraction and relaxation. To minimize the effect of basal contraction, an archeal protein halorhodopsin from *Natronomonas pharaonis* (NpHR), which can be activated by green light to hyperpolarize membranes and silence cells[129], could be used to relax muscle cells before light activation of ChR2.

The discrepancy in the results of synchronous contractility and worm locomotion might indicate that the NTE of UNC-27 is required for fine spatiotemporal tuning of muscle contractility. In the optogenetic synchronous experiments, all cholinergic neurons are simultaneously activated to induce maximum muscle contractile outputs. In contrast, in worm locomotion, muscle cells are regulated by both excitatory and inhibitory neurons in a coordinated manner, such that muscle cells can produce various levels of contractility. In mammalian cardiac TnI, the NTE binds to the N-terminal lobe of TnC and modulates the Ca^{2+} sensitivity of thin filaments[15,130–132]. Phosphorylation of the NTE by protein kinase A weakens its binding to TnC and enhances dissociation of Ca^{2+} from troponin C[133]. Thus, β-adrenergic stimulation induces protein kinase A phosphorylation of cardiac TnI within the NTE and this modification enhances cardiac muscle relaxation[134–136]. Mutations in the NTE of human cardiac TnI (TNNI3) are found in patients with dilated cardiomyopathy[137] and hypertrophic cardiomyopathy[138], indicating

functional significance of the NTE in cardiac muscle. However, proteolytic removal of the NTE from cardiac TnI occurs naturally in tail-suspended rats[139], and transgenic expression of cardiac TnI lacking NTE enhances diastolic function of the mouse heart[140–142], suggesting that removal of the NTE might be an adaptive mechanism in altered cardiac conditions. These effects of NTE-truncation from mammalian cardiac TnI are quite different from those in *C. elegans*, in which muscle relaxation is enhanced by a null mutation of UNC-27 (TnI) and suppressed by full-length or NTE-truncated UNC-27 (this study). Thus, *C. elegans* troponin may have different biochemical properties from vertebrate troponin. Unfortunately, we have not been able to produce recombinant *C. elegans* troponin due to toxicity of UNC-27 in *E. coli* (our unpublished results). Nonetheless, further structure-function analysis of *C. elegans* troponin using both biochemical and genetic approaches should help to understand fundamental mechanisms of the troponin regulation of actomyosin interaction and evolution of troponin in the animal kingdom.

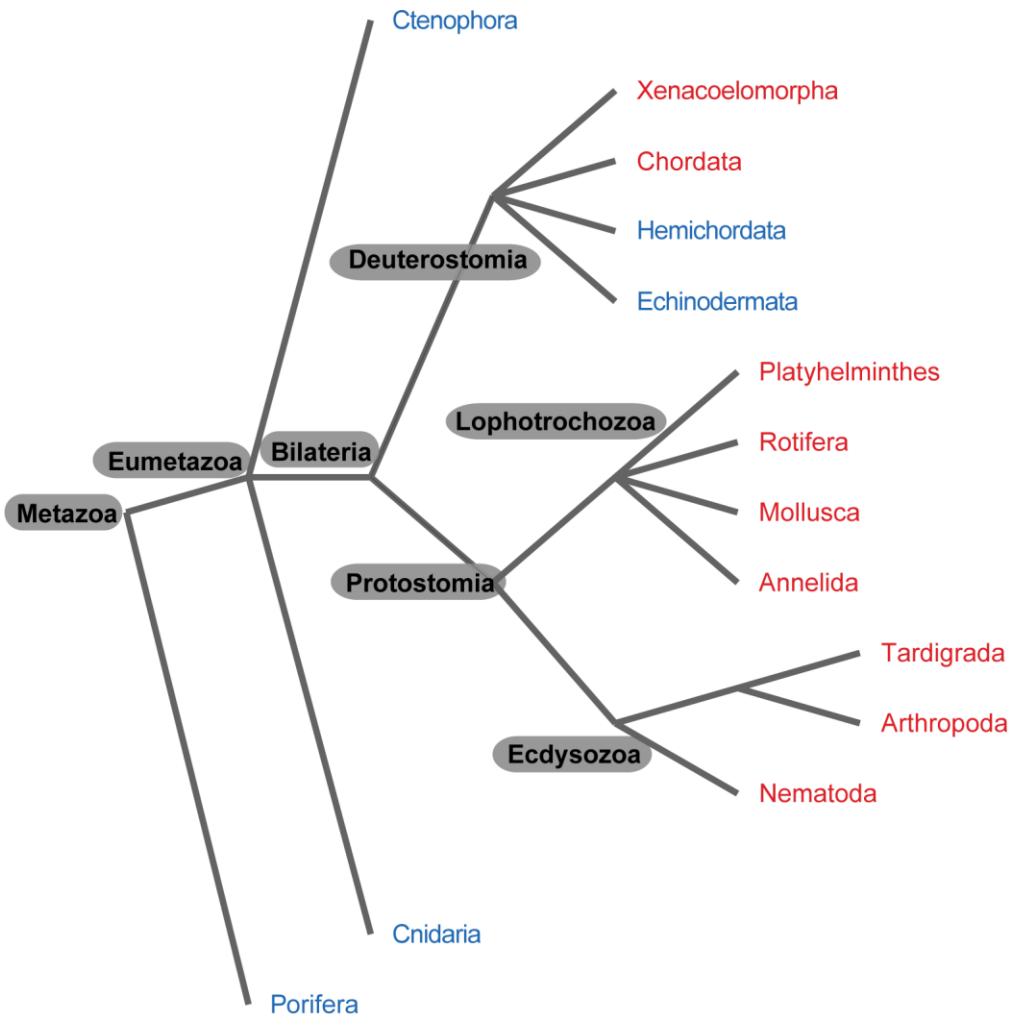

Figure 3.1. Evolution of troponin. Phylogenetic relationships of 14 representative phyla in the animal kingdom are shown. Troponin-positive and –negative phyla are indicated by red and blue, respectively. Major taxonomic groups are indicated at or near branch points.

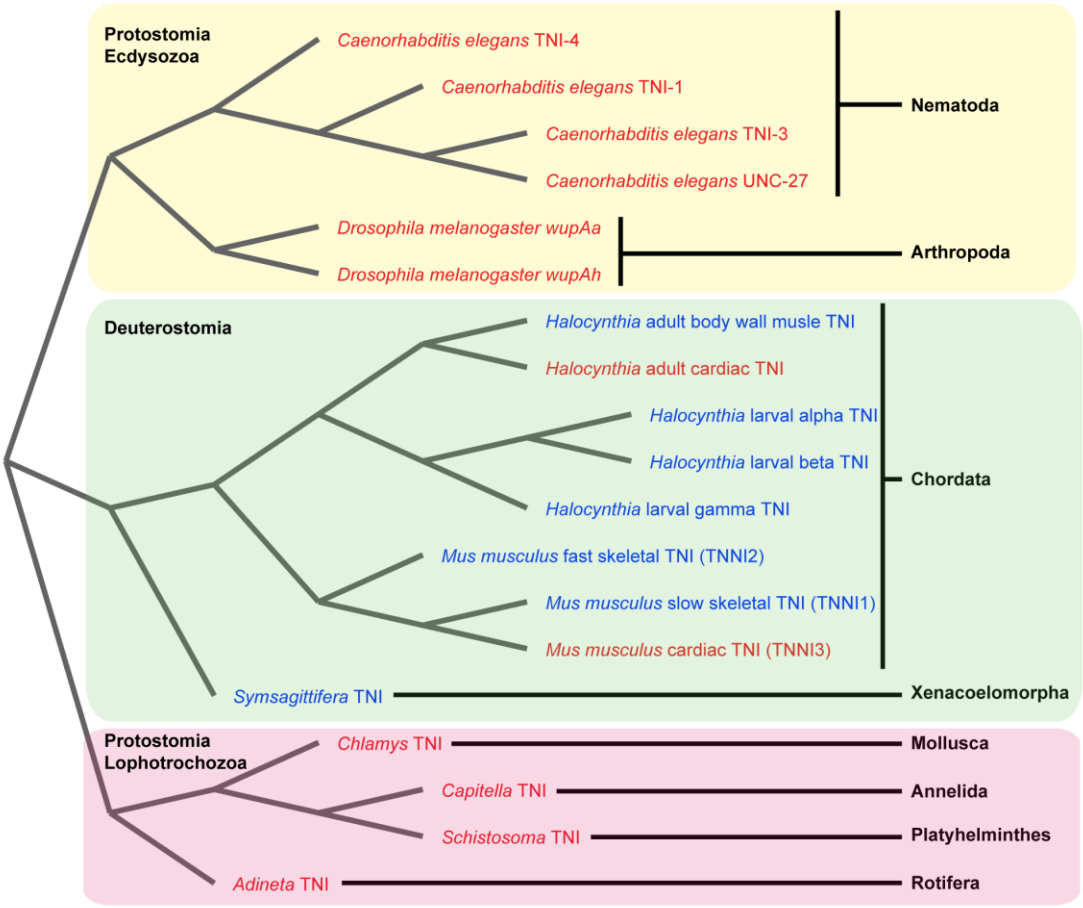

Figure 3.2. Molecular phylogenetic relationships of troponin I. Phylogenetic relationships of 19 TnI sequences from 9 species (8 phyla shown on the right) are shown. Three groups that match with major taxonomic groups are indicated by different colors: yellow (Protostomia, Ecdysozoa), pink (Protostomia, Lophotrochozoa), and green (Deuterostomia). N-terminal extensions are present in TnIs shown in red but absent in TnIs shown in blue. Entire sequence alignment is shown in Figure 3.8.

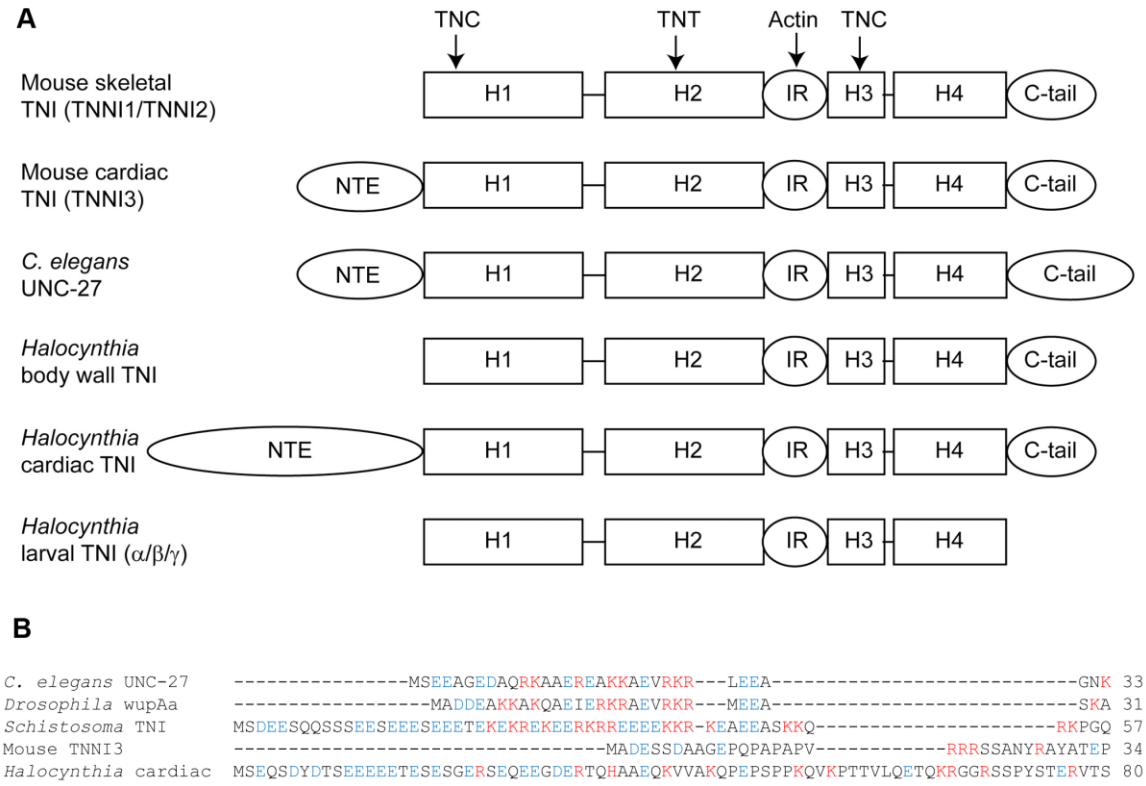

Figure 3.3. Comparison of structures of representative troponin I. (A) Schematic representation of structures of representative TnIs. N-terminal extension (NTE), four helices (H1 – H4), inhibitory region (IR), and C-terminal tail (extension) (C-tail) are shown. Major interaction sites with TnC, TnT, and actin are indicated on the top. (B) Sequence alignment of N-terminal extensions of five TnIs. Basic and acidic amino acids are shown in red and blue, respectively.

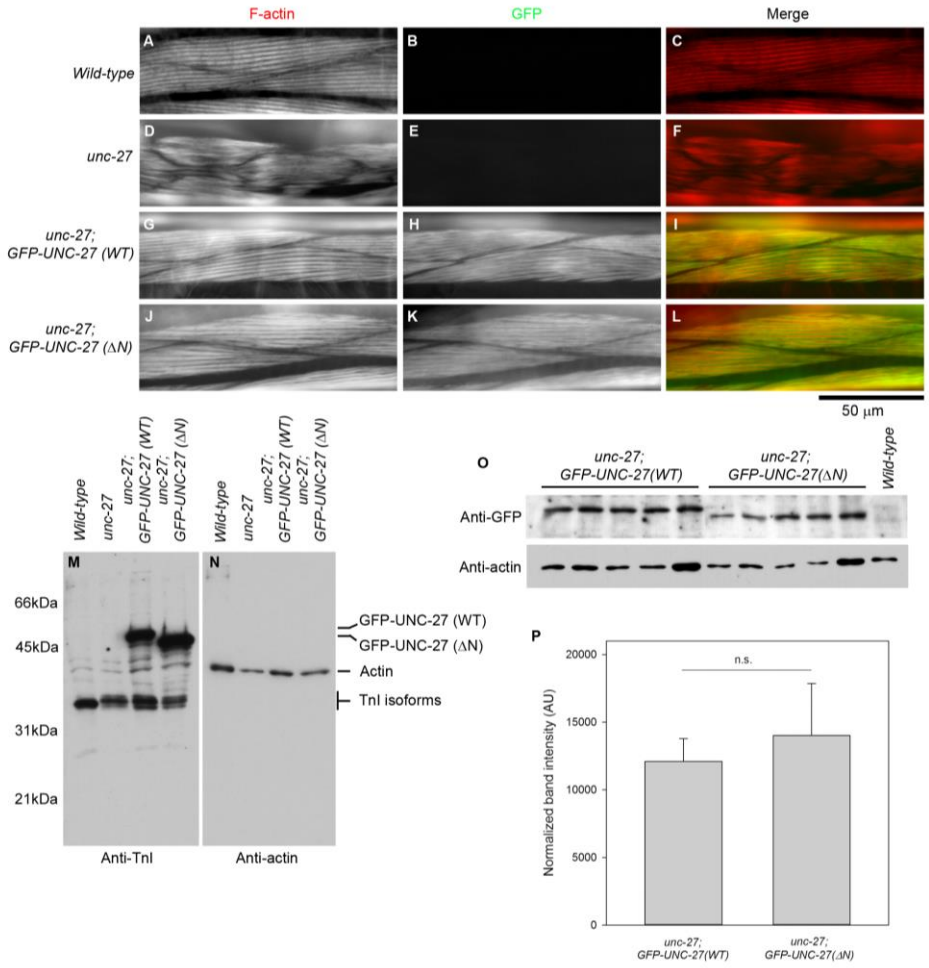

Figure 3.4. Effect of truncation of the N-terminal extension of troponin I on sarcomeric actin organization. (A-L), Micrographs of adult body wall muscle from wild-type (A-C), *unc-27* (D-F), *unc-27; GFP-UNC-27(WT)* (G-I), or *unc-27; GFP-UNC-27(ΔN)* (J-L) are shown for filamentous (F-) actin stained with tetramethylrhodamine-phalloidin (left) and GFP (middle). Merged images are shown on the right column (F-actin in red and GFP in green). Bar, 50 μm. (M, N) Protein levels of TnI (M) and actin (N) were examined by Western blot. Lysates from 15 worms with indicated genotypes were loaded per sample and reacted with anti-*Ascaris* TnI antibody (M). Note that this antibody reacts with all four TnI isoforms, and showed significant reactivity with endogenous TnI with apparently higher molecular weight in the *unc-27* mutant background as described previously (Obinata et al. 2010). (O, P) Quantitative analysis of the protein levels of GFP-UNC-27 (WT) and GFP-UNC-27(ΔN). Worm lysates (10 worms per sample) from *unc-27; GFP-UNC-27(WT)* and *unc-27; GFP-UNC-27(ΔN)* were subjected to Western blot with anti-GFP and anti-actin antibodies (O). Five samples for each strain and one sample for wild-type were examined. Band intensity of the GFP-fusion proteins was normalized to the actin levels and shown in the graph (P). Data are means ± standard errors, n = 5. Transgenically expressed GFP-UNC-27 (WT) and GFP-UNC-27(ΔN) were not at significantly different levels: n. s., not significant ($P > 0.05$).

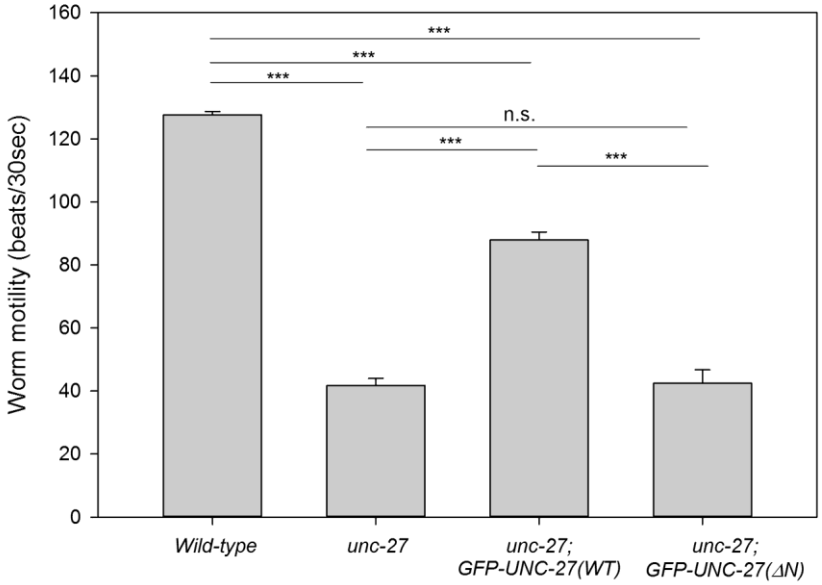

Figure 3.5. Effect of truncation of the N-terminal extension of troponin I on worm motility in liquid. Worm motility of indicated strains was examined in liquid as beat frequency (beating per 30 sec). Data are means ± standard errors, n = 10. n. s., not significant ($P > 0.05$); ***, $P < 0.001$.

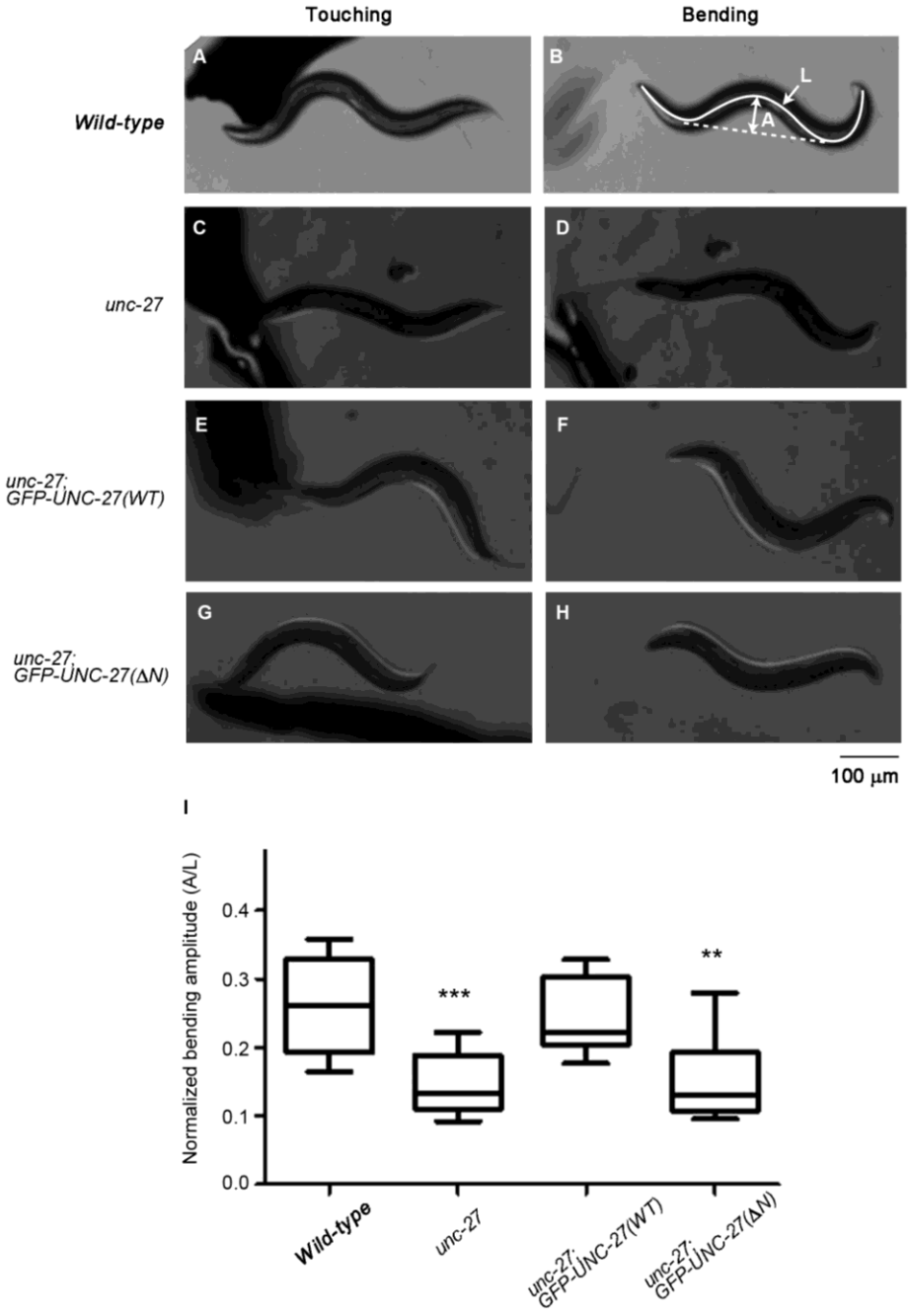

Figure 3.6. Effect of truncation of the N-terminal extension of troponin I on bending amplitude during backward locomotion. Backward locomotion was induced by touching the head (A, C, E, and G). Then, amplitude of body bending (indicated as "A" in B) was measured and normalized by body length (indicated as "L" in B) (B, D, F, and H). Bar, 100 μm. Normalized bending amplitude (A/L) is shown in a box plot (I). Each box represents the 25th and 75th percentiles with a line at the median, and error bars indicate the 10th and 90th percentiles. n = 10. **, $P < 0.001$; ***, $P < 0.0001$.

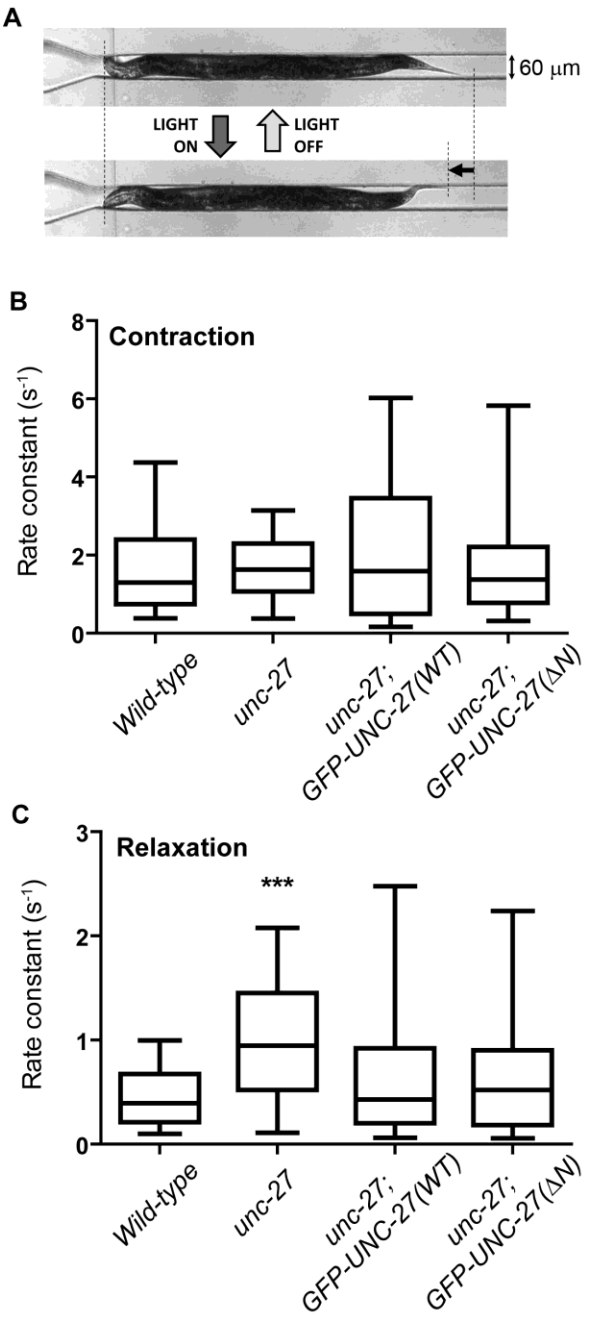

Figure 3.7. Effect of truncation of the N-terminal extension of troponin I on rates of contraction and relaxation examined by optogenetics. (A) Representative images of an optogenetic experiment show that contraction of a worm expressing channelrhodopsin-2 in a microfluidic channel (60 μm wide) is induced by turning blue light on, and relaxation induced by turning blue light off. (B, C) Rate constants (s^{-1}) for contraction (B) and relaxation (C) were measured from changes in the body area and expressed in box plots. n = 30. ***, $P < 0.0001$.

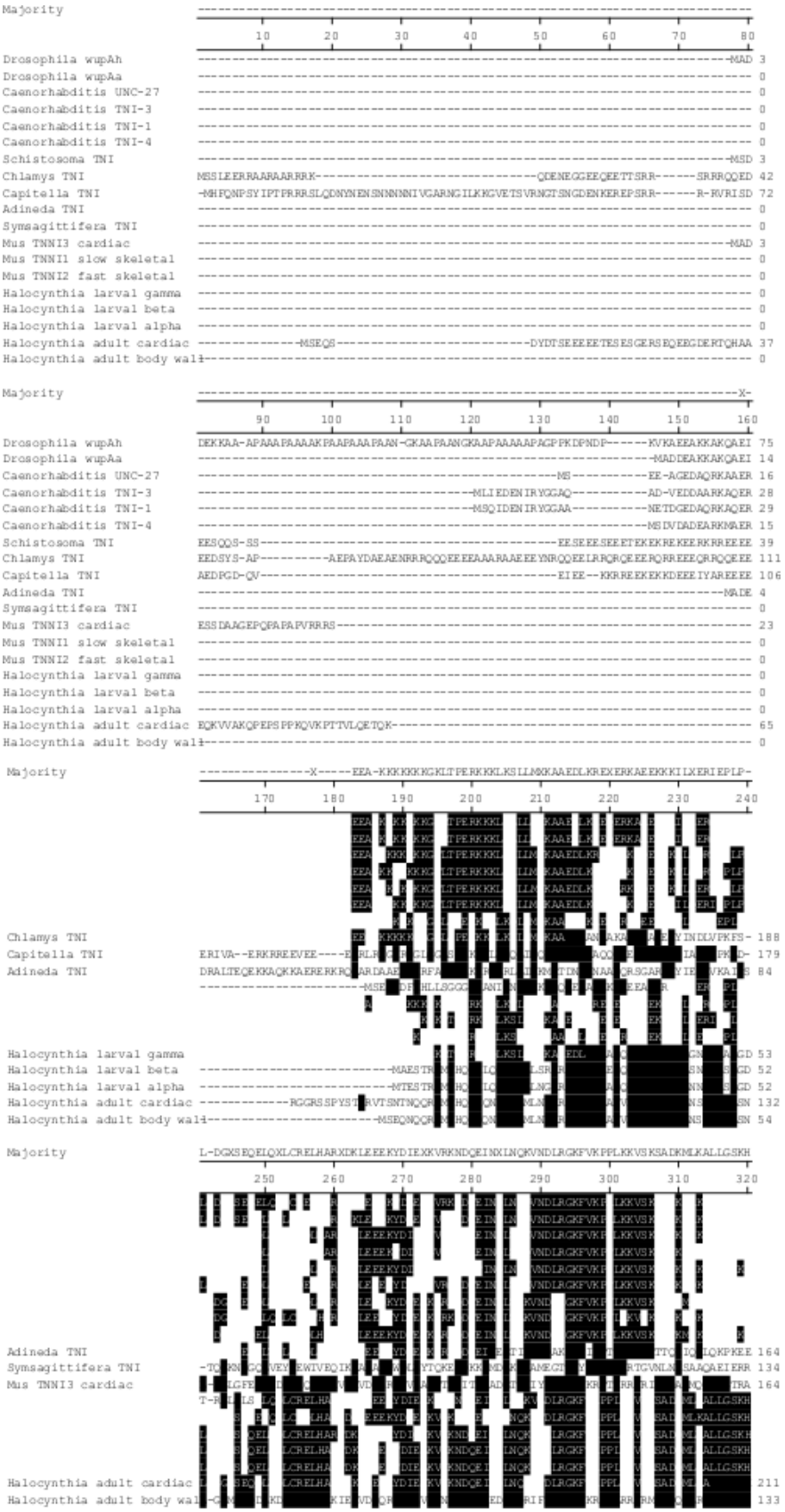
Majority
Drosophila wupAh
Drosophila wupAa
Caenorhabditis UNC-27
Caenorhabditis TNI-3
Caenorhabditis TNI-1
Caenorhabditis TNI-4
Schistosoma TNI
Chlamys TNI
Capitella TNI
Adineda TNI
Symsagittifera TNI
Mus TNNI3 cardiac
Mus TNNI1 slow skeletal
Mus TNNI2 fast skeletal
Halocynthia larval gamma
Halocynthia larval beta
Halocynthia larval alpha
Halocynthia adult cardiac
Halocynthia adult body wall

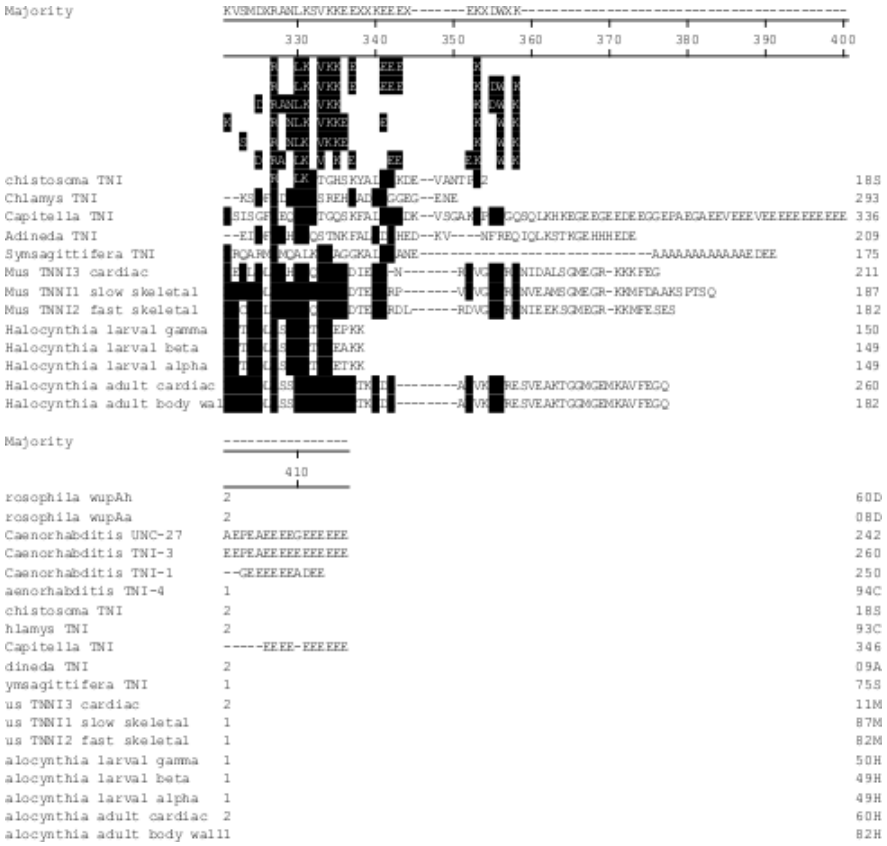

Figure 3.8. Alignment of troponin I sequences. Alignment of 19 TnI sequences from 9 species is shown. Highly conserved residues are shown by white characters with black backgrounds. Positions of N-terminal extension, helix 1 to 4 (H1 to H4), inhibitory region (IR), and C-terminal tail (see Figure 3.2) are indicated on the top. A phylogenetic tree based on this alignment is shown in Figure 3.2.

3.4 Conclusion

Troponin proteins first appear in the evolution of the Bilateria. Our comparison of TnI sequences from representative animals demonstrated conservation of a core region and variations in N- and C-terminal extensions. In particular, the NTE remains in all examined protostome TnIs; however, truncation of NTE appears in a subset of deuterostome TnI isoforms. Functional analysis in the nematodes revealed an important role of the NTE of TnI in coordinated body locomotion but not in single-muscle contractility. This is in contrast to vertebrate TnIs that have diverged to skeletal muscle isoforms with no NTE and a cardiac isoform with an NTE with regulatory properties. From these observations, we hypothesize that an ancestral TnI had an NTE essential for coordination of body movement, and that functions of NTEs have evolved or been eliminated in deuterostomes as their body plans have diverged and increased in complexity. *C. elegans* could be a useful system to test functional conservation of NTE and other domains of TnI from other species by expressing chimeric TnI proteins. Further functional studies on troponin and muscle-regulatory systems in diverse organisms may provide insight in the origin of troponin and fundamental mechanisms of actomyosin regulation.

3.5 Materials and Methods

3.5.1 Phylogenetic Analysis

Phylogenetic relationships of representative metazoan phyla (Figure 3.1) were obtained from the National Center for Biotechnology Information (NCBI) Taxonomy Browser (U.

S. National Library of Medicine), and a tree was drawn by TreeVector[143]. The tree was modified by moving the Platyhelminthes to the Lophotrochozoa according to the recent analysis[144]. Sequences for all TnIs except for *Adineta* TnI were obtained from the NCBI server with accession numbers indicated in Table 1. *Adineta* TnI was searched first by NCBI Basic Local Alignment Serch Tool (BLAST) against the *Adineta* genomic sequence[145] using mouse cardiac TnI sequence, and an annotated protein sequence was obtained from *Adineta vaga* Genome Browser at Genoscope, Centre National de Séquençage (Evry, France). Sequence alignment was performed with Clustal Omega[110] using MegAlign Pro (DNASTAR Inc., Madison, WI), and a tree was drawn by TreeVector.

3.5.2 Nematode Strains

Wild-type strain N2 and CB155 *unc-27(e155)*[146] were obtained from the *Caenorhabditis* Genetics Center (Minneapolis, MN). ZX460 *zxIs6[Punc-17::ChR2(H134R)::YFP + lin-15(+)]* (Liewald et al. 2008) was provided by Alexander Gottschalk (Goethe University, Frankfurt, Germany). Transgenic strains ON239 *unc-27(e155); ktEx170[Pmyo-3::GFP::UNC-27]* and ON242 *unc-27(e155); ktEx173[Pmyo-3::GFP::UNC-27(Δ2-29)]* were constructed as described below. Following strains were generated by crossing the strains described above: ON295 *unc-27(e155); zxIs6*, ON313 *unc-27(e155); zxIs6; ktEx170*, and ON311 *unc-27(e155); zxIs6; ktEx173*. Nematodes were generally grown under standard conditions at 20 °C on Nematode Growth Medium agar plates with *Escherichia coli* OP50 as a food source[147]. For optogenetic experiments, 100 μM all *trans*-retinal was added to the *E. coli* culture as a co-factor for channelrhodopsin-2 activation as described previously[70].

3.5.3 Generation of Transgenic Nematode Strains

A full-length *unc-27* genomic fragment containing all protein coding regions and an N-terminally truncated *unc-27* genomic fragment lacking residues 2 – 29 were PCR-amplified from total genomic DNA from N2 and cloned at the *Eco*RI-*Nhe*I sites of pPD118.20, an expression vector with the *myo-3* promoter[148] and the GFP coding sequence (provided by Andrew Fire, Stanford University, Stanford, CA). The entire coding regions were sequenced to confirm the presence of the inserts and the absence of PCR-induced errors. Transgenic nematodes were generated essentially as described previously[149] except that *unc-27(e155)* was used as the parental strain. Transgenic worms were selected by expression of GFP as observed by fluorescence microscopy, and the transgenes were maintained as extrachromosomal arrays.

3.5.4 Fluorescence Microscopy

Staining of whole worms with tetramethylrhodamine-phalloidin to visualize actin filaments was performed as described[63]. GFP was observed by its own fluorescence. Samples were mounted with ProLong Gold (Life Technologies, Carlsbad, CA) and observed by epifluorescence using a Nikon Eclipse TE2000 inverted microscope with a CFI Plan Fluor ELWD 40x (Dry; NA 0.60) or Plan Apo 60x (oil; NA 1.40) objective (Nikon Instruments, Tokyo, Japan). Images were captured by a SPOT RT monochrome CCD camera (Diagnostic Instruments, Sterling Heights, MI) and processed by IPLab imaging software (BD Biosciences, San Jose, CA) and Adobe Photoshop CS3 (Adobe, San Jose, CA).

3.5.5 Western Blot

Fifteen L4 or young adult worms per sample were picked and lysed in 15 µl of SDS-lysis buffer (2 % SDS, 80 mM Tris-HCl, 5 % β-mercaptoethanol, 15 % glycerol, and 0.05 % bromophenol blue, pH 6.8), heated at 97 °C for 3 min and homogenized by brief sonication. The samples were resolved by SDS-PAGE by using a 12 % acrylamide gel and transferred onto a polyvinylidene difluoride membrane (Immobilon-P; EMD Millipore, Billerica, MA). The membrane was blocked in 5 % nonfat milk in phosphate-buffered saline containing 0.1 % Tween 20 (PBS-T) overnight at 4 °C and incubated for 1 hr with rabbit anti-*Ascaris* TnI antibody (Nakae and Obinata 1993), which was diluted at 1:2000 in Signal Enhancer HIKARI (Nacalai USA, San Diego, CA). After washing with PBS-T, the membrane was reacted with horse radish peroxidase-labeled goat anti-rabbit IgG (1:2000-diluted) (Thermo Fisher Scientific Pierce Protein Biology, Rockford, IL). The reactivity was detected with a SuperSignal West Pico chemiluminescence reagent (Thermo Fisher Scientific Pierce Protein Biology). The membrane was treated with a buffer containing 2 % SDS, 100 mM β-mercaptoethanol, and 62.5 mM Tris-HCl, pH 6.8, at 50 °C for 30 min to remove bound probes and reprobed with mouse monoclonal anti-actin antibody (C4; MP Biomedicals, Irvine, CA) as a loading control.

To quantify protein levels of GFP-UNC-27(WT) and GFP-UNC-27(□N), worm lysates (10 worms per sample) were subjected to Western blot essentially as described above using rabbit anti-GFP antibody (1:2000 dilution) (#600-401-215, Rockland Immunochemicals, Limerick, PA) and mouse monoclonal anti-actin antibody (1:3000 dilution). The reactivity was detected by SuperSignal West Femto (Thermo Fisher Scientific Pierce Protein Biology) for GFP and by SuperSignal West Pico for actin. Band

intensity for the GFP-fusion proteins and actin was quantified using ImageJ. Data for the GFP-fusion proteins were normalized to relative band intensity of actin (actin in wild-type was set to 1.0). Statistical analysis (unpaired t-test) was performed using SigmaPlot 13 (Systat Software, Inc., San Jose, CA).

3.5.6 Locomotion Assays

Worm motility (beat frequency) in liquid was quantified as described previously[65]. Briefly, adult worms were placed in M9 buffer. Then, one beat was counted when a worm swung its head to either right or left. The total number of beats in 30 s was recorded. To measure bending amplitude, young animals were transferred to fresh NGM agar plates with a 2-min acclimation period and prodded at their heads with a platinum wire to induce backward locomotion. Movement of the worms were recorded as movies on a standard stereo microscope with transmitted light. The movies were post-processed to extract the worm skeleton for quantitative measurements using custom software written in Matlab (the Mathworks, Inc., Natick, MA). The maximum bending amplitude was determined and normalized by the length of each worm. Statistical analysis (one-way ANOVA) was performed using SigmaPlot 13 (Systat Software, Inc., San Jose, CA).

3.5.7 Optogenetic Assays

Kinetic analysis of muscle contraction and relaxation was performed using a microfluidic device to trap worms and an optical system for light illumination and imaging as described previously[71,72] with an optimization for analysis of muscle contractility phenotypes as described[126]. Briefly, two-layer microfluidic devices made of polydimethylsiloxane (PDMS; Sylgard 184, Dow-Corning Corp., Midland, MI, USA) with 16 straight microchannels with membrane valves at the entrance and the exit were

used to trap worms. After young adult animals were trapped in the channels, they were illuminated with blue light (λ = 450-490 nm; 0.3 mW/mm^2) for 15 s to induce channelrhodopsin-2 photoactivation. Movies were recorded using a CCD camera (Infinity 3-1, Luminera Corp., Canada) and post-processed using custom software written in Matlab. The projected body area of the worms in the segmented images was used as a read-out for the light-stimulated muscle contraction and relaxation. The body area measured from the images captured during 5 s before the blue light illumination was used as a baseline, and its change was plotted. The curves were fitted with the plateau followed by one phase decay or association equations for the kinetic analyses of the contraction or the relaxation processes, respectively. Curve fitting and statistical analysis were performed using Prism 5 (GraphPad Software, San Diego, CA).

Chapter 4 A novel alternative exon of the *Caenorhabditis elegans lev-11* tropomyosin gene is used to express a head-muscle-specific isoform

4.1 Abstract

Tropomyosin (TM) is a coiled-coil dimer that binds along actin filaments in muscle and non-muscle cells. TM is critically-involved in muscle contractility. Four *Caenorhabditis elegans* TM isoforms have been reported from a single gene, *lev-11*. We identified a novel Exon (7a) that is alternative to 7b (previously 7) and cloned a new isoform containing Exon 7a, termed LEV-11O. 7b was preferentially-included in pharynx and main body body-wall muscles. 7a was alternatively spliced in the head region of body wall muscle. Levamisole induces hyper-contracted muscle paralysis in wild-type nematodes. An amino acid charge reversal mutation within *lev-11* Exon 7b (LEV-11A) prevented levamisole-induced hyper-contraction in the main body but not the head, whereas an Exon 7a (LEV-11O) charge reversal mutation prevented levamisole-induced hyper-contraction in the head but not in the main body. These data indicate that Exons 7a and 7b have non-redundant functions for muscle regulation in the head or main body. LEV-11A and LEV-11O bound actin with similar affinity and mediated inhibition of actomyosin ATPase by a troponin I (TNI) inhibitory peptide. The charge reversal mutant of LEV-11O strongly-inhibited actomyosin ATPase even in the absence of the TNI inhibitory peptide, suggesting that enhanced inhibitory effects on actomyosin ATPase is the basis of levamisole resistance. These results suggest that *C. elegans* utilize muscle-type-specific alternative splicing to produce functionally distinct TM isoforms.

This currently-unpublished research is the product of work by:
Dawn Barnes, Eichi Watanabe, Kanako Ono, Euiyoung Kwak,
Hidehito Kuroyanagi, and Shoichiro Ono.

4.2 INTRODUCTION

Filamentous actin is important in numerous cellular functions. These roles range from providing cell and organelle architecture, adhesion and signaling, motility of the cell itself, as well as intracellular transport, apoptosis, cytokinesis, and muscle contractility. In vertebrates, there are only six known actin isoforms[150,151]; therefore, the functional diversity of filamentous actin is facilitated through association with a myriad of actin-binding proteins, such as tropomyosin (TM)[152,153].

Tropomyosin is an alpha-helical coiled-coil dimer, with intermolecular head-to-tail binding[154]. This polymer lies along the major groove of actin, is integrally involved in processes such as stabilizing actin filaments,[28,26,155] and regulating actin-myosin binding[156]. Tropomyosin is an extensively-spliced gene. In mammals there are four recognized tropomyosin genes that probably arose by gene duplication and the genes are alternatively spliced to produce at least 40 protein isoforms. These numbers are achieved by gene duplication, alternative promotors, and variations within exon splicing. Some of the exons exhibit high degrees of sequence similarity, while other exons exhibit significant differences that may play important roles in functional variability. The roles different tropomyosin isoforms play in regulating actin function are still unclear. A study of the different isoforms may help elucidate the roles they play within the cell.

Within striated muscles, tropomyosin effects actomyosin binding through changes in position, which are regulated through conformational changes within the troponin complex. In the absence of the troponin complex, tropomyosin lies along the inner actin groove. In the presence of the troponin, tropomyosin is stabilized along the outer actin groove, sterically-hindering actomyosin binding. The movement between these two

positions is regulated by calcium-binding to troponin and the switch is important in the transition from muscle contraction to muscle relaxation, respectively. While troponin is a complex of three proteins (troponin I, troponin T, and troponin C), the "inhibitory region" (approximately 11 amino acids in length) of troponin I is sufficient[157] to stabilize Tm on the outer actin groove. *C. elegans* TNI has four known isoforms from four genes: *tni-1*, *unc-27 (tni-2), tni-3,* and *tni-4*. UNC-27 is expressed in body wall muscles at high levels while TNI-3 is expressed in body wall muscles concentrated in the anterior/head region[46]. TNI-1 is also expressed in body wall muscles, however, its concentrations are much lower than UNC-27[46]. TNI-4 is expressed exclusively in pharyngeal muscles[46].

In the nematode *C. elegans*, *lev-11* is the single gene for tropomyosin (*tmy-1*)[50]. The gene was named from mutations correlating with nematodes with resistance to levamisole, an acetylcholine receptor agonist that induces muscle hyper-contraction[158,159]. *lev-11(x12)* was identified by its ability to resist muscle paralysis, as well as a twitching phenotype that was exacerbated by levamisole. *lev-11(x12)* has a mutation in its seventh exon, with a single amino acid conversion from glutamic acid to lysine, which was thought to affect all LEV-11 isoforms[158,60]. Through optogenetic induction of muscle contraction, we demonstrated that *lev-11(x12)* worms were unable to maintain a contracted muscle state[126] and while relaxing, some worms spontaneously contracted (data not pictured). However, the biochemical basis of how this tropomyosin mutation causes the levamisole resistance is unknown.

lev-11 is an extensively-spliced gene[49,50]. It was previously reported that three of its nine exons were conserved across all isoforms[49,50]. Isoforms included two high molecular weight isoforms of 284 amino acids (CeTMI (LEV-11A) & CeTMII (LEV-

11D)) expressed in body wall muscles[50], as well as two low molecular weight isoforms of 256 amino acids (CeTMIII (LEV-11C) & CeTMIV (LEV-11E)) expressed in pharynx and intestines[49]. Express Sequence Tag (EST) analyses, aligned with the sequenced *C. elegans* genome, has proposed 23 theoretical isoforms (WormBase). All four previously-cloned isoforms contain exon 7b (previously Exon 7)[49]. We found that one EST clone (yk78g10) contains a novel exon sequence (designated as Exon 7a) instead of Exon 7 (designated as Exon 7b) (unpublished). RNA-seq analysis confirmed usage of Exon 7a[160]. Quantitative analysis showed five percent total reads for the alternative Exon 7a, while Exon 7b had the remaining 95%[160]. Exon 7a exhibits 71.2% nucleotide sequence identity to Exon 7b (Figure 4.1). By understanding the role the seventh exon plays within LEV-11 isoforms, we can gain insight in increasing functional diversity of actin filaments.

We have cloned a high molecular weight isoform of *lev-11* that is similar to *lev-11a*, with an alternative seventh exon. This isoform is in agreement with a predicted sequence: *lev-11o* (WormBase). We utilized *lev-11(x12)* and *lev-11(gk334531)* worms with mutations within either Exon 7b or 7a, respectively, to analyze the function of LEV-11A and LEV-11O *in vivo*. We analyzed the localization of LEV-11A and LEV-11O within cells, as well as the *C. elegans* body. We hope the confirmation of Exon 7a and identification of the LEV-11O isoform will help in the elucidation of the different functional roles tropomyosin plays within the diverse cellular functions of filamentous actin. We suspect differences within *lev-11* Exon 7a and 7b may be important for functional variability for LEV-11A and LEV-11O in muscle contractility.

4.3 RESULTS

4.3.1 Identification of a novel high molecular weight tropomyosin isoform, *lev-11o*, containing a novel alternative Exon.

Through analysis of Expressed Sequence Tag sequences and reverse transcription-PCR of the *lev-11* gene products, we identified a novel Exon (Exon 7a) that is alternative to the previously reported seventh Exon 7 (Exon 7b). We identified a transcript driven by the upstream promoter containing the Exon 7a sequence and a full-length cDNA encoding a novel HMW tropomyosin isoform (284 amino acid). The presence of a BstYI restriction site in Exon 7b was crucial in our process of isolating 7a containing sequences. We confirmed the sequence is similar to *lev-11a*, with the exception of Exon 7, and is the same as the predicted sequence on WormBase: *lev-11o* (Figure 4.1A). Additional RT-PCR analysis suggests that Exon 7a is also utilized in a transcript driven by the downstream promoter to produce a LMW isoform (data not pictured). Exon 7b and 7a contain 71.2% nucleotide sequence identity and encode peptides that are 78.3% identical. The previously characterized *lev-11(x12)* allele has a mutation in Exon 7b that results in an amino acid conversion from E to K at position 234. Additionally, we found that *lev-11(gk334531)*, which was isolated in the Million Mutation Project[161], has a mutation in Exon 7a that results in an amino acid conversion from E to K at position 196 (Figure 4.1B).

4.3.2 Expression of Exon 7a is restricted to head and neck, while 7b is restricted to neck and main body body-wall muscles.

In order to investigate expression patterns of mutually-exclusive Exons 7a and 7b, we constructed mini-gene cassettes, spanning from Exon 6 to Exon 8, including RFP or GFP

reporters when Exon 7a or 7b were included, respectively (Figure 4.2A and B). When expressed under the ubiquitous *eft-3* promotor (Figure 4.2A), E7A-RFP was expressed in body-wall muscles of the head (anterior to the anterior bulb of the pharynx) and neck (between the anterior and posterior bulbs of the pharynx); E7B-GFP was expressed in body-wall muscles of the neck and main body (posterior to the posterior bulb of the pharynx), as well as the pharynx (Figure 4.2C). There was slight overlap of both E7A-RFP and E7B-GFP in the neck. To determine if E7A-RFP and E7B-RFP were body-wall muscles or alternative cell types, we utilized the body-wall-specific *myo-3* promotor (Figure 4.2B) and observed a similar expression profile, with the loss of pharynx expression (Figure 4.2D).

4.3.3 *lev-11* Exon 7 mutations do not change LEV-11 localization to sarcomere thin filaments

Mutations within Exon 7a or 7b are valuable tools for studying the functions of their encoded protein isoforms within *C. elegans*. *lev-11(x12)* has a mutation with Exon 7b. *lev-11(gk334531)* has a mutation in Exon 7a (Figure 4.1B). To examine if mutations within Exon 7a or 7b affect localization of LEV-11A or LEV-11O proteins, anti-tropomyosin antibody that recognizes all LEV-11 isoforms along with anti-actin antibody (AAN01) were utilized in immunofluorescence microscopy (Figure 4.3). In wild-type worms, LEV-11 proteins (green) co-localized with actin in sarcomeres (red). *lev-11*(gk334531) and *lev-11*(x12) strains exhibited similar localization of LEV-11 and this pattern was not altered depending on if the image was acquired in body wall cells of the worm neck or main body (Figure 4.4). These mutations within alternative Exons 7a and

7b that result in a glutamic acid to lysine amino acid changes do not change the ability of LEV-11 proteins to localize to sarcomeric thin filaments (Figure 4.3).

4.3.4 Levamisole resistance was restricted to regions where the mutated isoform was expressed.

In order to analyze different LEV-11 isoforms functionally, we tested levamisole sensitivity in worms, since the original *lev-11* mutants were isolated by the levamisole-resistant phenotype[158]. Levamisole, an acetylcholine receptor agonist, normally induces muscle hyper-contraction. On agar plates with no levamisole, wild-type worms were relaxed (Figure 4). However, when transferred to agar plates with 500uM levamisole, adult wild-type worms exhibited a contracted body and head within a minute (Figure 4.4). The bodies became shortened and the heads became shorter and rounded (Figure 4.4). *lev-11(x12)* worms were previously identified because of their ability to resist levamisole[60]. In the absence of levamisole, *lev-11(x12)* worms are relaxed but they twitch when attempting to move. Upon closer analysis, on 500uM levamisole plates, we observed that *lev-11(x12)* worms were relaxed in their bodies, though their heads were shortened and rounded suggesting hypercontraction of the head region (Figure 4.4). In the presence of levamisole, *lev-11(gk334531)* bodies become hypercontracted; however, the tip of their heads are still relaxed and moving (Figure 4). *lev-11(x12)* and *lev-11(gk334531)* exhibited different patterns of levamisole resistance, restricted to the body or head respectively. Therefore, Exon 7b has important functions in the body and Exon 7a is prominent in the head.

4.3.5 LEV-11A and LEV-11O with or without Exon 7 mutations bind to actin filaments with similar affinity

To determine biochemical properties of LEV-11 isoforms and effects of Exon 7 mutations *in vitro*, we produced recombinant LEV-11A and LEV-11O with wild-type sequence and with Exon 7 mutations: LEV-11A(E234K) for *lev-11(x12)* and LEV-11O(E196K) for *lev-11(gk334531)*. First, we determined their affinity for actin filaments by actin co-sedimentation assay (Figure 5). In this assay, actin filaments sediment at high gravitational forces and proteins bound to them sediment along with the actin. LEV-11A is a previously identified LEV-11 high molecular weight isoform. This protein bound actin with a Kd of 0.0085 μM (Figure 5). LEV-11A(E234K) had a Kd equal to 0.0157 μM (Figure 4.5). Recombinant LEV-11O had a Kd of 0.0687 μM (Figure 5). LEV-11O(E196K) had a Kd of 0.0136 μM. All free vs precipitated LEV-11 concentrations were included in the same curve so statistical differences could not be compared; however, the highest Kd of LEV-11O is only eight times that of the lowest Kd of LEV-11A (Figure 4.5). We believe this difference is a reasonable binding affinity range affinity to not be significant for functional differences both *in vivo* and *in vitro*.

4.3.6 LEV-11O(E196K) inhibited actomyosin ATPase independent of troponin I (UNC-27) inhibitory peptide

Myosin motors bind to F-actin and hydrolyze ATP to ADP and inorganic phosphate. The actin-activated myosin ATPase activity can be characterized by measuring liberation of inorganic phosphate. This assay simulates one aspect of the interactions necessary for muscle contraction. To quantify actomyosin ATPase in the presence of different LEV-11

isoforms and variants, we combined F-actin with LEV-11 by itself or also in the presence of a peptide from UNC-27 troponin I to reconstitute a minimal TNI-tropomyosin inhibitory complex[157]. In the absence of actin, myosin ATPase activity was low. When actin was added, myosin ATPase activity was greatly enhanced (Figure 4.7). The ATPase activity in the presence of actin was normalized to 1 for all assays and the numbers for other conditions were represented as a fraction in of this number. Through alignment with vertebrate cardiac TNI, we focused on the region within UNC-27 that was similar to the already known inhibitory region sufficient to stabilize tropomyosin on the outer groove of actin and block myosin binding[162] and synthesized overlapping peptides, 20 amino acids in length at intervals of six amino acids, within this region of UNC-27 (Figure 4.6). By testing these peptides in the presence of LEV-11A, we identified a sequence with the strongest inhibitory properties for actomyosin ATPase (Figure 4.7A). The strongest inhibitor was peptide 25 (GKFVKPSLKKVSKYDNKFKK), with ATPase levels close to those in the absence of actin (Figure 4.6 and Figure 4.7A). We subsequently utilized peptide 25 for our comparisons of different LEV-11 isoforms and variants. Actin: LEV-11: peptide 25 ratios ranged from 5:1:10 to 5:1:1 and we found that increasing amounts of peptide 25, produced incremental increases in ATPase inhibition (data not pictured). We chose to utilize a 5 actin: 1 LEV-11: 1 peptide 25 ratio because the partial inhibition could elucidate any finer differences in activity. In the case of LEV-11A, LEV-11A(E234K), or LEV-11O, there were no differences in ATPase activity in the presence of LEV-11A. In all these cases, peptide 25 decreased ATPase activity significantly, $p<.05$. Interestingly, LEV-11O(E196K) inhibited ATPase activity even in the absence of peptide 25, $p<0.05$, and further reduced ATPase activity in the presence of peptide 25 (Figure

4.7B). Despite the inhibitory effect of the *lev-11(x12)* mutation on levamisole-induced hyper-contractility, LEV-11A(E234K) did not exhibit different effects than LEV-11A on myosin ATPase activity. On the other hand, the inhibitory effect of the *lev-11(gk334531)* mutation on levamisole-induced hyper-contractility correlated with LEV-11O(E196K) inhibiting myosin ATPase activity, even in the absence of UNC-27 peptide 25.

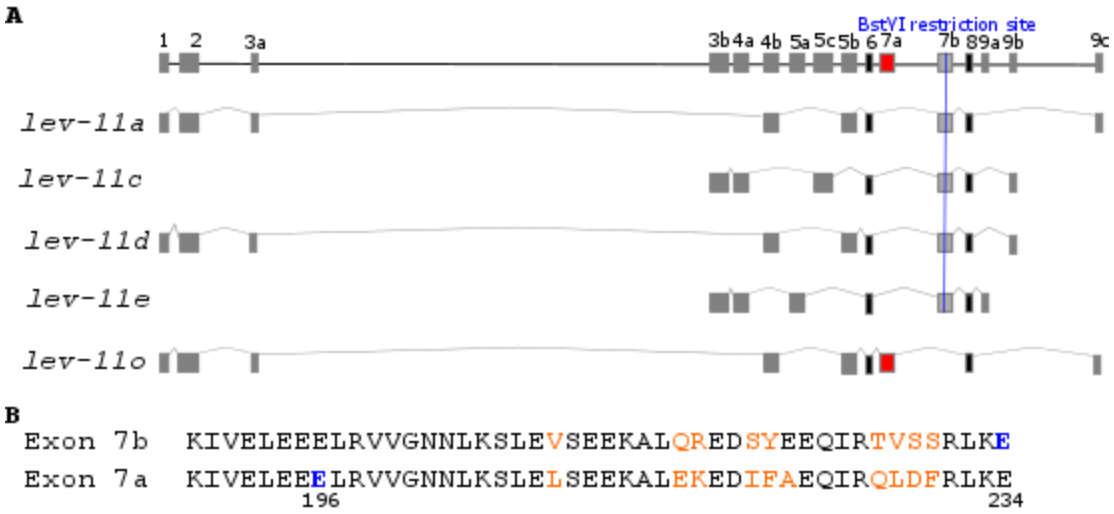

Figure 4.1. Identification of a novel *lev-11* alternative Exon (7a) and cloning of LEV-11O. A) Alternative splicing of *lev-11 a,c,d* and *e* have been confirmed, but *lev-11 o* has not been previously reported. In particular, Exon 7a of *lev-11o* has not been previously observed. Exon 7b has a BstYI restriction digest site; Exon 7a does not have a BstYI restriction site. This difference provided a valuable tool to differentiate between the two Exons. Our clone matched the predicted sequence of *lev-11o* in WormBase. The two constitutive Exons (6 and 8) are highlighted in black. B) Exon 7a and 7b have 71.2% identity in nucleotide sequences and their encoded amino acid sequences have 78.3% identity. Differences in amino acids are highlighted in orange. *C. elegans* mutants in *lev-11* Exon 7a or 7b contain amino acid conversions from glutamic acid (E) to lysine (K), highlighted in blue. *lev-11(x12)* E234K has a mutation in Exon 7b; *lev-11(gk334531)* E196K has a mutation in Exon 7a.

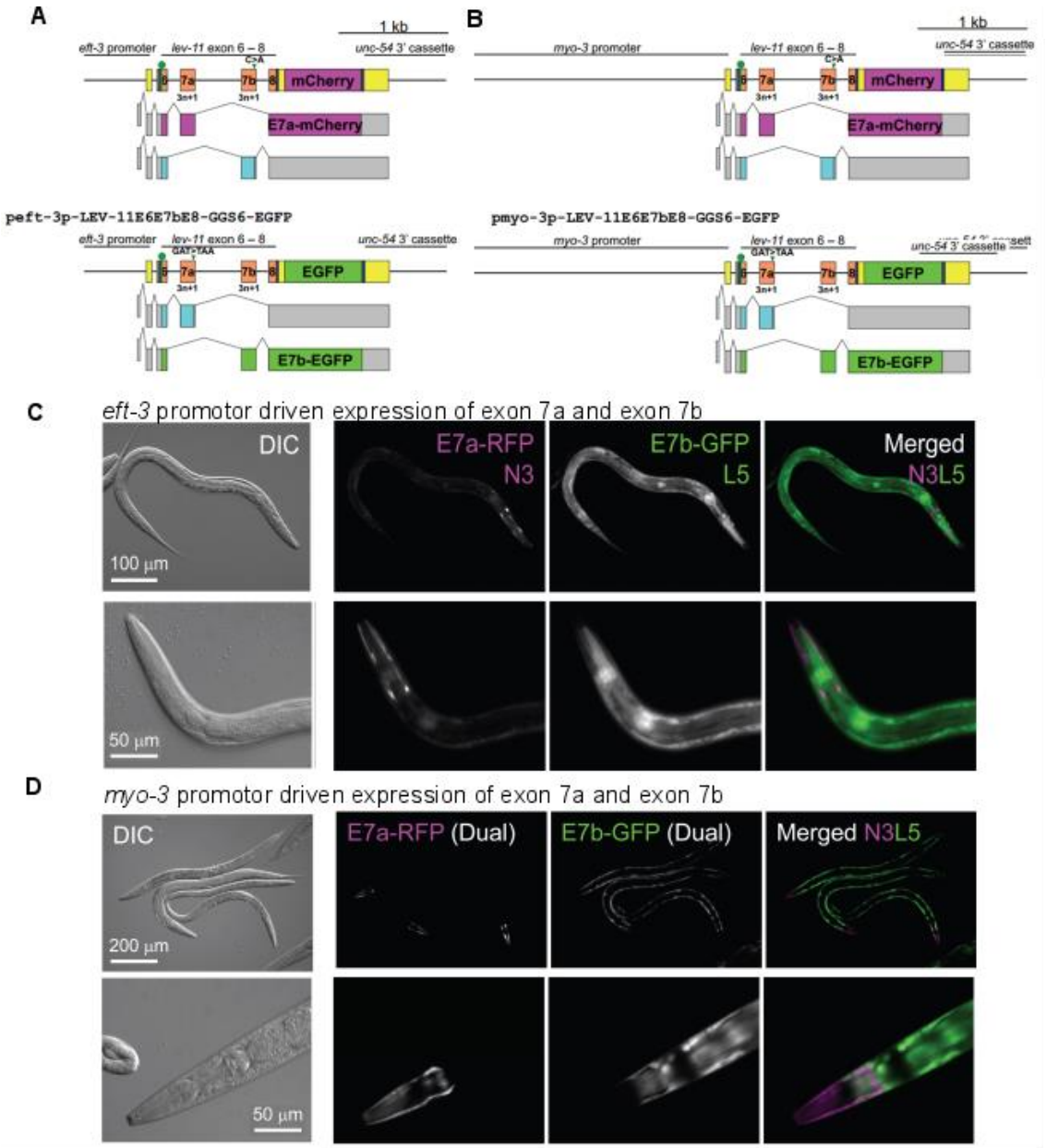

Figure 4.2: LEV-11 Exon 7a was expressed in head body wall muscles and 7b in main-body body wall and pharyngeal muscles. A) A reporter cassette systems were utilized, in extra chromosomal arrays, to be able to detect the inclusion of either Exon 7a or 7b. The partial 3' end of Exon 6 was included with the appropriate introns and Exon 7a, 7b, and 5' portion of Exon 8. Exon 8 was fused to mCherry in cassettes where a translation stop codon was included in Exon 7b. The sequence for EGFP was 5' of Exon 8 in cassettes containing a stop translation codon was included in Exon 7a. From cassettes with the ubiquitous *peft-3* promotor, mCherry was expressed when Exon 7a was expressed. EGFP was expressed with Exon 7b. B) The cassette same system was used with the body-wall specific *pmyo-3*. C) With the *peft-3* system, E7a-RFP (mCherry) was expressed in the nematode head. E7b-EGFP was expressed in the body and pharynx. The two reporters overlap at the base of the head. D) With *pmyo-3*, a similar pattern was found, with loss of pharynx.

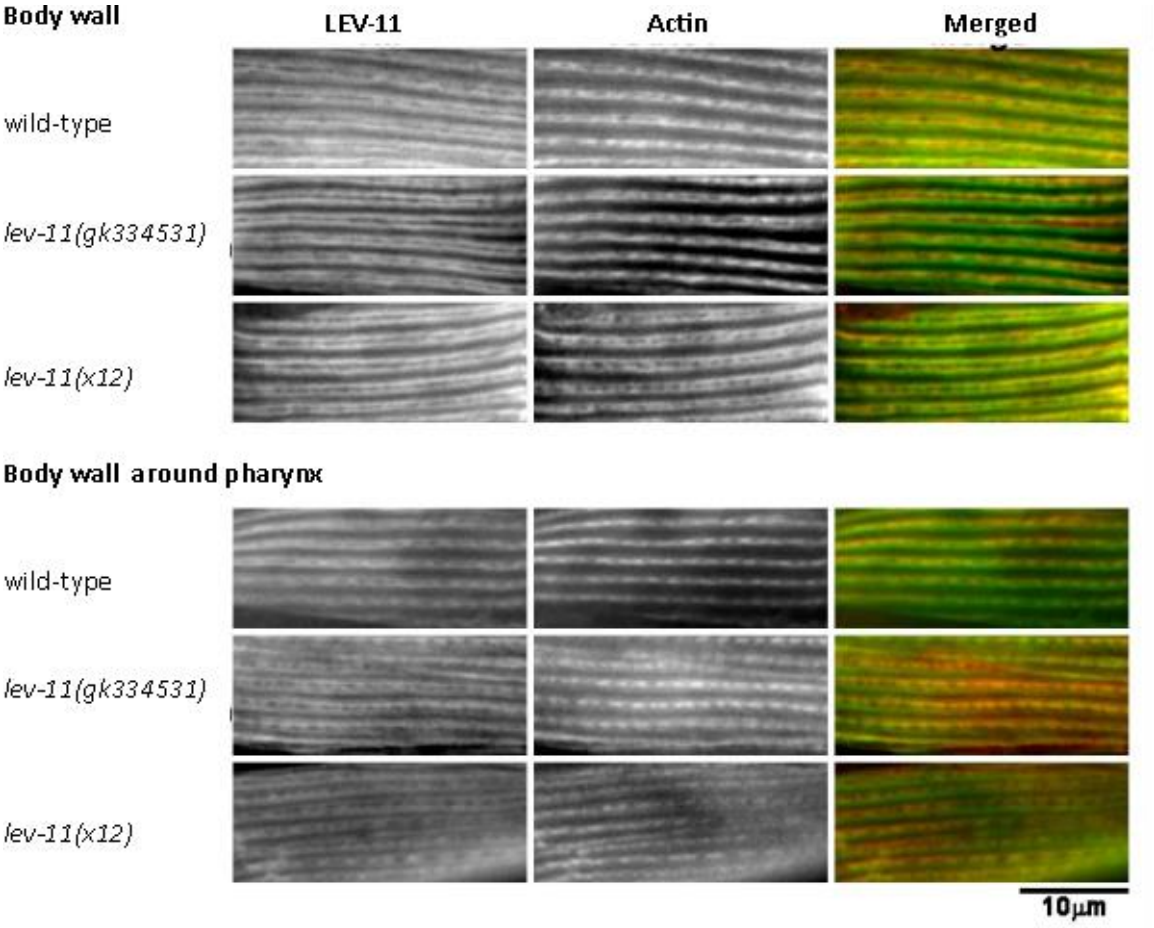

Figure 4.3. *lev-11* mutants exhibit normal LEV-11 protein localization and actin organization in both the *C. elegans* head and body. An antibody to multiple isoforms of tropomyosin isoforms showed that in wild-type nematodes, tropomyosin (LEV-11) localizes to sarcomeric actin filaments in both the mid-body and head. *lev-11 (gk334531)* and *lev-11 (x12)* mutant worms also exhibited similar tropomyosin and actin localization patterns.

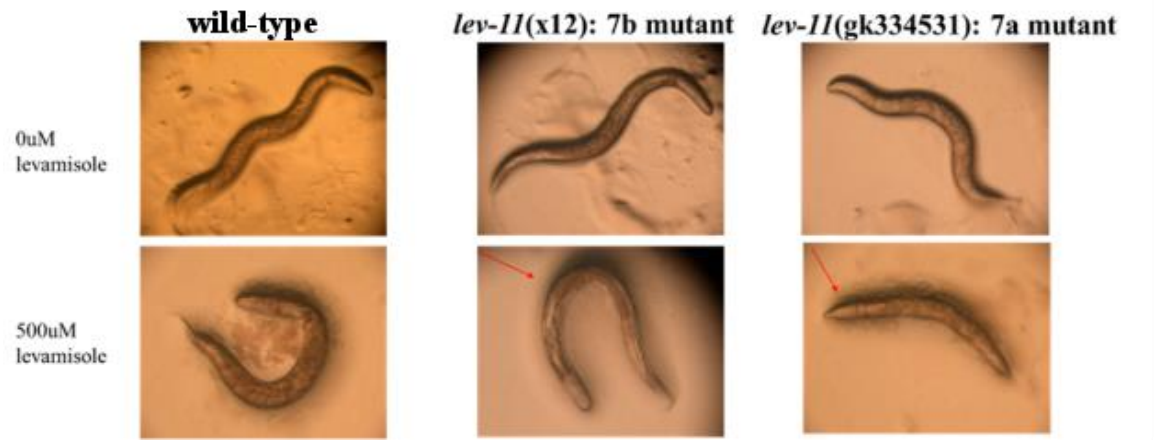

Figure 4.4: Levamisole resistance was restricted to regions where the mutated isoforms were expressed. On levamisole plates, wild-type worms exhibited both a contracted body and head. *lev-11(x12)* worms had a relaxed body (indicated by arrow) and contracted head. *lev-11(gk334531)* worms exhibited a contracted body and their head could still move (indicated with arrow). On 0µM levamisole plates all worms have their head at the top of the image. On 500µM levamisole plates the wild-type worm head is on the top, the *lev-11(x12)* worm head is on the bottom left, and the *lev-11(gk334531)* worm has its head on the left.

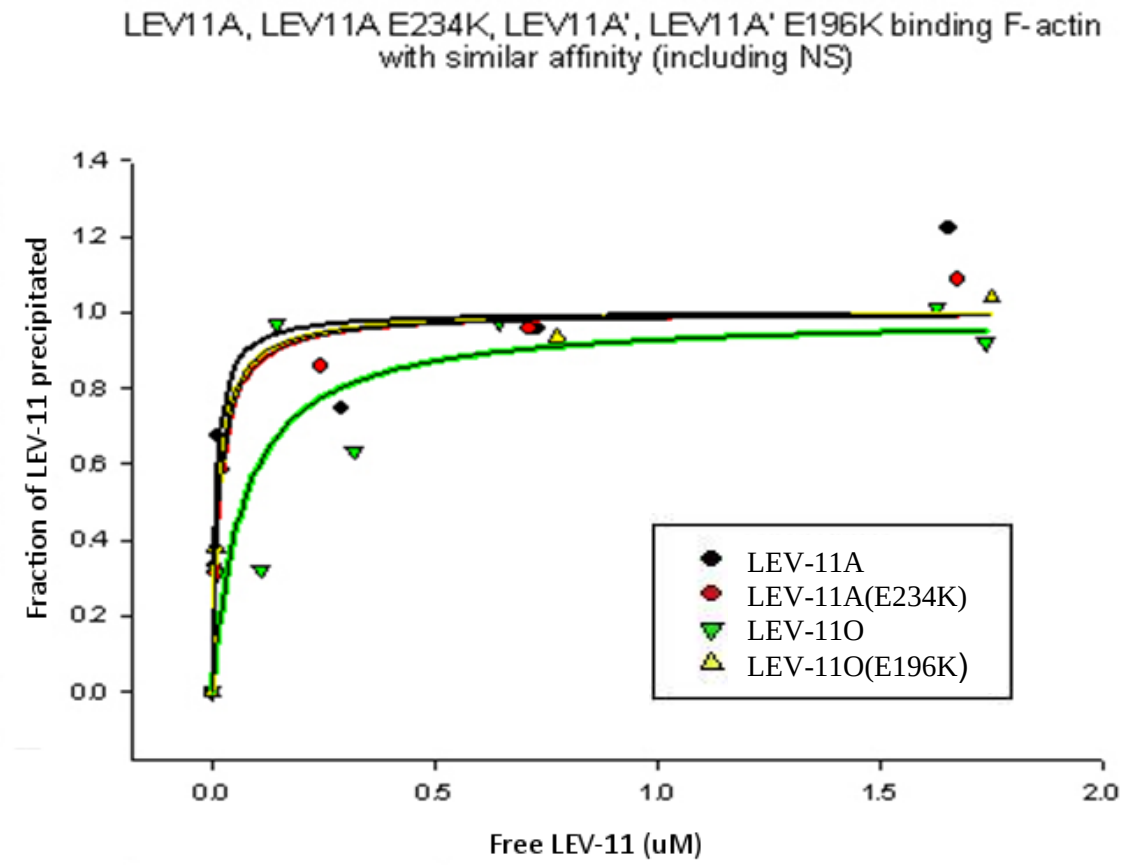

Figure 4.5. LEV-11A, LEV-11A (E234K), LEV-11O, and LEV-11O(E196K) variants bind F-actin with similar affinity. A co-sedimentation assay was utilized to test the binding affinity of LEV-11 proteins, of increasing concentrations, with a constant 5µM F-actin. The fraction of LEV-11 proteins precipitated (y-axis) was calculated as a fraction of its maximal binding. Unbound LEV-11 was graphed on the x-axis. LEV-11A K_d= 0.0085 µM; LEV-11A (E234K) K_d=0.0157 µM; LEV-11O K_d= 0.0687 µM; LEV-11O (E196K) K_d= 0.0136 µM.

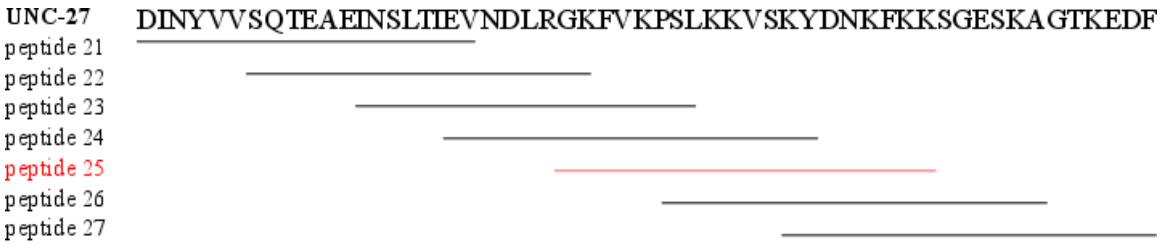

Figure 4.6 UNC-27 peptides spanning the suspected inhibitory region. By utilizing sequence alignment with human cardiac troponin I, the above sequence was hypothesized to contain the region within UNC-27 that is sufficient to stabilize tropomyosin in an inhibitory position. Peptides, 20 amino acids in length, were synthesized within this region, at six amino acid intervals. These peptides were utilized in myosin ATPase assays. Peptide 25 (red) had the greatest inhibitory activity.

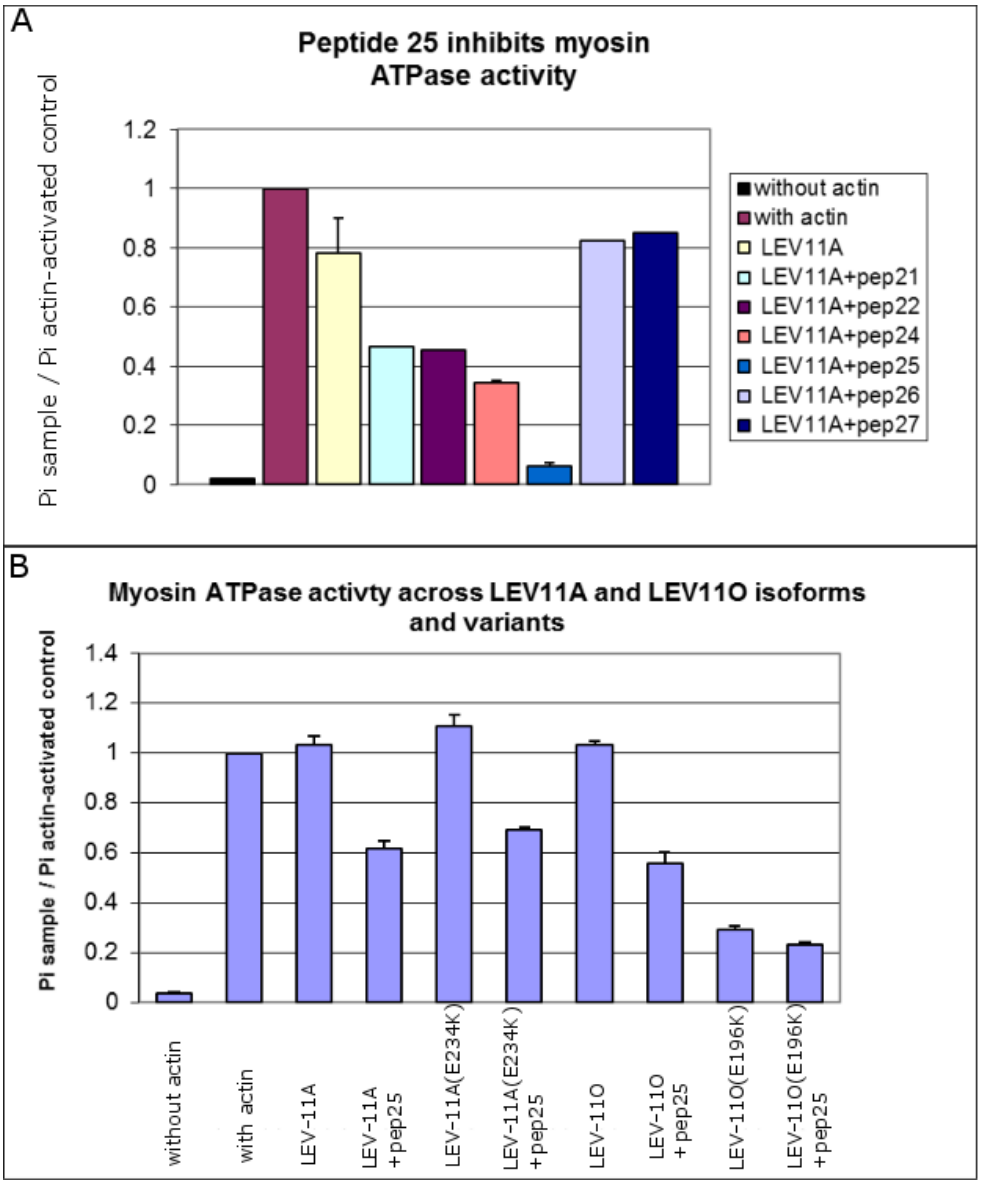

Figure 4.7. LEV-11 inhibits myosin ATPase activity in the presence of the UNC-27 (TNI) inhibitory peptide. A myosin ATPase assay was utilized to quantify the actomyosin interactions. The greater the actomyosin interactions, the greater the myosin ATP hydrolysis. We quantified the rate of free inorganic phosphate concentrations. A) To screen for the region of UNC-27 with the greatest inhibitory effects, overlapping peptides were incubated with actin, myosin, and LEV-11A. Myosin ATPase activity was activated by actin. LEV-11A did not decrease activity significantly. Overlapping peptides from the UNC-27 sequence (Figure 4.6) were tested. Peptide 25 is in the predicted inhibitory region of UNC-27 and it decreased ATPase activity the most, when paired with LEV-11A, $p<0.05$. B) LEV-11A, LEV-11A E234K, LEV-11O did not differ in their effect on ATPase activity or the ability of peptide 25 to inhibit ATPase activity; however, LEV-11O E196K decreased ATPase activity even in the absence of peptide 25, and this activity was further reduced in the presence of peptide 25, $n=3$, $p<0.05$.Error bars represent standard error.

4.4 DISCUSSION/CONCLUSIONS

We have demonstrated that *C. elegans* tropomyosin (*lev-11*) produces at least 5 isoforms from a single gene. We have identified a novel isoform, *lev-11o,* which contains the alternative Exon 7 (7a). This is the first isoform identified with Exon 7a. This alternative exon has important spatial expression differences: Exon 7b (LEV-11A) is expressed in *C. elegans* body and pharynx, while Exon 7a (LEV-11O) is expressed in *C. elegans* head muscles. From whole worm mRNA, Exon 7a was used in only five percent of the total Exon 7 (7a+ 7b)[160], however, this is the result of 7a-containing isoforms having a prominent role in the body wall muscles of the head and neck, a small subset of total worm muscle, rather than exhibiting low levels across all body wall muscles. Both LEV-11A and LEV-11O exhibit important functional roles in body wall muscles, as seen by levamisole resistance in the body regions with mutations in the predominant *lev-11* isoform.

Interestingly, these patterns correlate with differences in troponin I TNI-3 and UNC-27 isoform expression patterns, with TNI-3 concentrated in the head and UNC-27 in the body[46]. The variations in TNI expression are achieved from different genes, which is an independent mechanism from the splice variants for LEV-11. The body wall muscles are classified based on their source of neuronal innervation[163]. The four anterior muscles, in each of the four longitudinal quadrants, are innervated by nerve ring motor neurons[163]. The subsequent four muscles, in each of the four longitudinal quadrants, are innervated by both nerve ring and ventral chord motor neurons[163]. The remaining dorsal body wall muscles are innervated by ventral chord motor neurons[163]. This pattern of neuronal innervation correlates with the differences between Exon 7a and Exon 7b,

including the area of overlap around the pharynx. While the body is restricted to bending along the dorsoventral plane, muscle in the head also move laterally. Functional difference in LEV-11O may be important for this different muscle bending.

In our analysis of LEV-11A and LEV-11O biochemical differences, we found that LEV-11A and LEV-11O do not exhibit a significant difference in their affinity for actin. Additionally, their LEV-11A(E234) and LEV-11O(E196K) variants also did not change the affinity for actin. However, LEV-11O(E196K), present in the *lev-11(gk334531)* mutant strain, did inhibit myosin ATPase activity, even in the absence of UNC-27 peptide. We hypothesize that this is the result of destabilizing LEV-11 dimer formation because the mutation is in a predicted site for ionic dimer interactions. This destabilized dimer may favor the outer groove of F-actin and thus block binding of myosin heads to F-actin. *lev-11(x12)* worms exhibited spontaneous muscle twitching and resistance to levamisole, which correlated with the inability to maintain muscle contraction. However, LEV-11A(E234K) did not have significant effects on myosin ATPase activity. The conversion from an acidic to a basic residue in a position on the outside of the tropomyosin coiled-coil may disrupt interactions with other actin binding proteins. We are still working to identify the cause of *lev-11(x12)* levamisole resistance but speculate it is due to interactions with proteins within the troponin complex. We speculate that variations within Exon 7b and 7a are important in different functional regulations from troponin. The sarcomeric LEV-11A and LEV-11O variations may be important for difference within the movement of head and body muscles, whether due to differences in neuronal stimulation, calcium signaling, or muscle bending.

4.5 MATERIALS AND METHODS

4.5.1 *C. elegans* strains

Nematodes were grown at 20˚C as described previously[146]. N2 wild-type strain was obtained from the *Caenorhabditis* Genetics Center (St. Paul, MN). l*ev-11(x12)* and *lev-11(gk334531)* were obtained from *Caenorhabditis* Genetics Center (St. Paul, MN). *lev-11(gk334531)* worms were outcrossed five times, to remove other mutations. These mutants were used as homozygotes in this study.

4.5.2 *In vivo* fluorescence reporter analysis of splicing patterns of *lev-11* Exons

To detect localized splicing of Exon 7a and 7b, extra chromosomal arrays with symmetric fluorescence reporter minigenes were constructed as described previously[164] (Figure 4.2). We utilized EGFP and mCherry cassettes in pENTR-L5/L2 vectors that have a linker sequence GGS_6, six repeats of Gly-Gly-Ser and lack an initiation codon. With the ubiquitous *Peft-3* promotor, mCherry was expressed when Exons 6-7a-8 were expressed. GFP was expressed with Exons 6-7b-8 were expressed. The same system was used with the body-wall specific *Pmyo-3* promotor.

4.5.3 Levamisole sensitivity assay in *C. elegans*.

Levamisole induces hyper-contraction in nematodes as an agonist of acetylcholine receptors (cite). Wild-type (N2), *lev-11(x12),* and *lev-11(gk334531)* were exposed to 500uM levamisole in NGM agar plates and their bodies were qualitatively visualized for contracted or relaxed muscles using a Nikon SMZ1500 stereo microscope and a Nikon CoolPix 995 digital camera.

4.5.4 Preparation of actin and LEV-11 proteins

cDNA for LEV-11A was amplified by RT-PCR from N2 total RNA and cloned at the BamHI-NcoI sites of pET-3d. From the same RT-PCR product, cDNA for LEV-11O was enriched by digestion of LEV-11A cDNA by BstYI and cloned at the BamHI-NcoI sites for pET-3d. The cDNA inserts were sequenced to confirm the absence of PCR-induced error. For both LEV-11A and LEV-11O, an extra sequence Met-Ala-Ser was added to the N-terminus that is known to mimic the acetylation state of tropomyosin. LEV-11A(E234K) and LEV-11O(E196K) were generated by site-directed mutagenesis using the following primers, and their complements: for lev-11a the forward primer was CGTCTCATCCAGACTGAAGAAGGCTGAGACCCTGCCGAATTCG-3'; for lev-11o the forward primer was 5'-CAAGATCGTGGAGCTTGAAGAGAAGTTGCGCGTCGTTGGTAAT-3'.

LEV-11 proteins were expressed in *E. coli* BL21(DE3) in M9ZB media with 0.4mM ampicillin, while shaking at 37˚C. Expression was induced at O.D. 0.6 with IPTG. Proteins were purified, at 4˚C, in the following steps. Crude bacterial lysate was made by suspending pelleted E. coli in Sonication Buffer with PMSF and DTT and the solution was sonicated, on ice. The lysate was centrifuged (Beckman JA20 rotor) at 16000rpm, for 20 minutes, and the pellet discarded. Supernatant was incubated with ammonium sulfate at 35% saturation, for 30 minutes at 4˚C. The solution was centrifuged again at 18000rpm (Beckman JA20) for 30 minutes. The supernatant was subsequently dialyzed against 20mM TrisHCl pH6.8 & 0.1M NaCl, loaded on a DE53 anion exchange column and eluted with a gradient from 20mM TrisHCl pH6.8 & 0.1M NaCl to 20mM

TrisHCl pH6.8 & 0.6M NaCl. Fractions containing LEV-11 proteins were applied to a hydroxyapatide column and eluted with a gradient from 0.01M KPO4 & 0.05M KCl to 0.3M KPO4 & 0.05M KCl. The purified protein was dialyzed against F-buffer with glycerol (20mM HEPES-KOH pH7.5, 10mM KCl, 50% glycerol). Protein concentration was calculated against an F-actin concentration curve in 12% SDS-PAGE gel. Then Rabbit skeletal muscle actin was purified as described[165].

4.5.5 F-actin co-sedimentation of LEV-11 proteins

To determine affinity of LEV-11 proteins with actin, increasing concentrations of LEV-11 proteins were incubated for 1 hour at room temperature, in F-buffer (0.1M KCl, 2mM MgCl2, 20mM HEPES-KOH pH7.5, 0.2mM DTT), with 5µM F-actin as described previously[166]. Samples were centrifuged (Beckman 42.2Ti rotor) at 42,000rpm for 20 minutes, at 20˚C. Supernatant and precipitate fractions were separated and 50µL (equal to the initial volume) of 2x SDS PAGE loading buffer was added to each. Samples were added to 12% SDS PAGE gels and separated with electrophoresis. Gels were scanned with an Epson Perfection V700 Photo Scanner, at 300 dots per inch. Supernatant and precipitate proteins were quantified with densitometry, using ImageJ.

4.5.6 Myosin ATPase activity

Actin-activated myosin ATPase activity was determined by colormetric quantification of inorganic phosphate as previously described[167,168] in the presence of LEV-11A, LEV-11A(E234K), LEV-11O, or LEV-11O(E196K). In the presence of LEV-11 proteins, P_i was quantified in the presence or absence of the inhibitory region of UNC-27 (peptide

25) at a ratio of 5 actin: 1 LEV-11: 1 peptide 25. Previously, LEV-11A had been incubated with UNC-27 peptides 21 to 27, at 7actin: 1 LEV-11: 10 peptide ratio, to determine the most inhibitory peptide. The assays were performed at 20˚C, for 5 minutes. The myosin ATPase activity was calculated as pmoles of Pi liberated in a minute per milligram of protein (pmoles Pi mg-1 min-1) and all samples were normalized as a ratio of their actin-activated control. Myosin was purified from rabbit back muscle, as described previously[169].

4.5.7 Immunofluorescence microscopy

Whole worms were fixed, as described previously[26]. Anti-CeTM and anti-actin (AAN01) antibodies were used as primary antibodies, which were visualized by Alexa488-labeled goat anti-guinea pig IgG (Molecular Probes) and Cy3-labeled goat anti-rabbit IgG (Jackson ImmunoResearch Laboratories). Samples were mounted with ProLong Gold (Invitrogen) and observed by epifluorescence, as described previously[170].

4.5.8 Statistical analysis

Tropomyosin and troponin work together to regulate actomyosin interactions and activated myosin ATPase. To compare differences between LEV-11A alone and in combination with peptides 21-27, One-way ANOVA was used, with subsequent follow-up analyses. To compare differences between LEV-11 isoforms, alone or in combination with peptide 25, One-way ANOVA was also utilized.

Chapter 5

Discussion/Conclusions

5.1 Sarcomere proteins are important in muscle

Misregulation of muscle function can lead to diseases such as cardiomyopathies[55,171,172]. Muscle structure and muscle proteins are highly-conserved so the information gained from *C. elegans* research can be extrapolated to vertebrates[64]. In vertebrates, there are three principle types of muscle: skeletal, cardiac, and smooth. Each type of muscle has its own method of regulating contractility. Skeletal and cardiac muscles are both striated muscles, which regulate muscle contraction/ relaxation through changes within actin binding proteins. Within the nematode *Caenorhabditis elegans*, there are also differences in their striated muscles, in particular the body wall muscle of the anterior/ head region and those of the main body. Even though they are all striated muscles, variations within their actin binding proteins are important for their different roles within the body. Our work has analyzed differences between different actin binding protein isoforms, with the goal of understanding the role of their functional domains in that larger process of muscle contractility.

5.2 Optogentic analysis of muscle contractility in *C. elegans*

5.2.1 Development of the optogenetic application in analyzing muscle kinetics

C. elegans are an excellent model organism for the study of the function of the sarcomere in striated muscle[64]. *C. elegans* have obliquely-striated muscles and the genes for many of the sarcomeric proteins have been identified. Their localization within the sarcomere and molecular interactions have been partially identified. However, the phenotypical analysis of mutants in genes encoding these proteins has been limited by the qualitative and quantitative methods, such as bending amplitude and frequency, generally resulting in an overall uncoordinated ("unc") phenotype. To analyze the functions of sarcomeric proteins in muscle kinetics, we developed a method to utilize the optogenetically-controlled ZX460 worm strain in combination with worms with mutated alleles for sarcomeric proteins. We utilized the whole worm because isolation of individual muscles is currently not achievable. By studying intact animals we can characterize protein function under physiological conditions.

Through quantitative analysis of rate constants for contraction and relaxation, relative body area at steady state, predicted plateau after relaxation, and minimum radius of curvature, we found clustering of sarcomeric proteins with functional relationships. We were unable to achieve the same clustering capacity with traditional methods of bending amplitude, beat frequency, and crawling wavelength. This indicates our optogenetic muscle analysis is an ideal method to identify functional relationships.

5.2.2 Sarcomeric proteins can be involved in both contraction and/or relaxation

We compared the rate of contraction between wild-type worms and 16 muscle-affecting mutant strains. Only the *unc-54(s74)* mutant exhibited a decrease in its contraction rate. UNC-54 is a myosin heavy chain that includes the myosin motor[52] and thus it makes sense that mutations in this protein would result in a decrease in contraction, due to reduced motor velocity. We were surprised to observe that, of the seven mutants with differences in the rate of contraction, six exhibited a decrease in the rate of contraction. The slower locomotion observed in bending frequency experiments had previously suggested that these phenotypes were a product of slower contraction or relaxation kinetics, or the switch between the two phases. The increased contraction rate indicates these proteins typically inhibit muscle contraction. Neither *unc-27 (e155)* nor *lev-11(x12)* exhibited changes in muscle contraction.

We compared the rate of relaxation between wild-type and muscle-affecting mutant strains. It was interesting that none of the mutants exhibited a decrease in relaxation rate. We speculate this is due to relaxation being a passive process. However, nine of the mutants exhibited an increased relaxation rate. *unc-27(e155)* was one of the mutants that exhibited an increase in relaxation rate. This makes sense because UNC-27 is involved in inhibiting actomyosin interactions within the sarcomere. Additionally, *unc-27(e155)* worms exhibit disorganized sarcomeres and hyper-contracted muscles. The whole-body analyses are a ratio of the resting body size. Upon light-activated muscle contraction, *unc-27(e155)* worms contract further and upon light-extinction, the muscles relax beyond their resting state, as seen by the post-relaxation crest (Figure 2.7). The body size then returns to their initial resting state. This greater change in size over the

same period of time would cause an increased rate of relaxation. *lev-11(x12)* worms did not exhibit a difference in their rate of relaxation.

5.2.3 Levamisole resistance correlated with the inability to maintain contraction

lev-11(x12) worms were identified by their ability to resist the levamisole-induced hyper-contraction. LEV-11, the *C. elegans* homolog for tropomyosin[50], is responsible for regulating actomyosin interactions within sarcomeres[173]. It does this by sliding between the inner and outer actin grooves, the latter position sterically-hinders myosin binding sites[174]. *lev-11(x12)* worms are also characterized by a twitching phenotype, which is exacerbated in the presence of levamisole (data not pictured). The optogenetics curves showed *lev-11(x12)* worms did not maintain muscle contraction, even while continually stimulated by light (relative body area at steady state). These data suggests *lev-11(x12)* resistance to levamisole is the result of mutations that reduce LEV-11 affinity for the inner actin groove, whether through disrupting interactions with actin or troponin. Additionally, *lev-11(x12)* worms occasionally exhibited spontaneous contraction when light-induced contraction was extinguished. This data was not constant enough to be observable in the average of n>40 worms (data not pictured). The worms had already partially-relaxed, due to their inability to maintain contraction. These data suggest the twitching phenotype is the result of spontaneous contraction as calcium concentrations decrease within muscle cytoplasm. This may be the result of interactions with the calcium-sensing troponin complex. Our biochemical data support this hypothesis because the resistance to muscle contraction is not due to changes in actin affinity or myosin ATPase activity in the presence of troponin I inhibitory peptide (Chapter 4).

5.2.4 UNC-27 N-terminal extension did not affect contraction or relaxation rates in isolation

Optogenetics enabled us to induce maximal muscle contraction of the entire worm. While this may have helped elucidate functional roles of sarcomeric proteins that were unobservable by traditional analysis methods, the non-physiological levels of calcium may have also overwhelmed phenotypical differences that are the result of smaller changes in function. In our *unc-27* worms, transgenic expression of either GFP-UNC-27(WT) or GFP-UNC-27(ΔN) did not affect the rate of contraction and rescued the relaxation rate of *unc-27* worms to the wild-type rate. There were no differences between GFP-UNC-27(WT) and GFP-UNC-27(ΔN); however, there are differences in the bending frequency and amplitude between these transgenic worms. These data suggests the UNC-27 N-terminal extension is important in the coordinated contraction/relaxation necessary for the sinusoidal locomotion of worms.

5.2.5 Future applications of optogenetics to analyze sarcomeric protein function

The data for relaxation showed no mutant strains with decreased rates. We speculate this is due to relaxation being a passive process. To test the involvement of sarcomeric proteins in relaxation, we would like to utilize optogenetic strains with channelrhodopsin in GABAergic neurons. In this way we could initiate light-activated muscle relaxation. The ZX460 strain has light-inducible channelrhodopsin in its cholinergic motor neurons. This stimulation of motor neurons signals the muscles to contract. In the muscle-affecting mutant strains, some muscles are characterized by

hyper-contraction or other phenotypes that may affect the neuromuscular junction. Differences we observed in muscle kinetics may be the result of changes in the neuromuscular junction. To better-isolate the function of these sarcomeric proteins within muscle contractility, we would like to also utilize optogenetic strains with channelrhodopsin in the body wall muscles[175]. With this strain, we would be able to better confirm the role of sarcomeric proteins in muscle kinetics.

5.3 Molecular evolution of troponin I and its N-terminal extension in nematode locomotion

5.3.1 Evolutionary analysis: the troponin complex appears in Bilateria

Troponin is a complex of three proteins: troponin I (inhibitory), troponin C (calcium sensing), and troponin T (tropomyosin binding). Troponin is the calcium-sensing complex that translates increases in cytoplasmic calcium into muscle contraction. This complex is present across both vertebrate and invertebrate animals, however, little is known about the evolutionary development of this complex. We utilized data mining and sequence analysis to trace the evolutionary appearance and loss of troponin proteins and isoforms.

Troponin is not present in striated muscles of all organisms. Troponin is absent from cnidarians and ctenophores, despite the presence of striated muscles[19], which suggests troponin evolved in bilaterians. Troponin components in both protostomes and deuterostomes suggest that troponin evolved early in bilaterians. Within some phyla, all

three troponin proteins have been characterized both genetically and biochemically. However, within other phyla, troponin presence and homology has only been analyzed based on cDNA, genomic sequences, and/or immunoreactivity with troponin antibodies. Biochemical analyses of troponin proteins across species would help elucidate the function of these proteins within muscles. Analyses of the differences in domains would also help with understanding molecular interactions in the sarcomere.

5.3.2 TNI N-terminal extension appears to be lost in a subset of Deuterostomia isoforms

Alignment of TNI sequences agreed with the phylogenetic relationship of the organisms (Figure 2). This suggests TNI may provide a tool for determining phylogenetic positioning of organisms within Bilateria that are still under debate. Sequence alignment demonstrates that the central region of TNI (helices 1-4 and the inhibitory region) is highly-conserved. This suggests a conserved function of these regions within the troponin complex and thin filament.

TNI N- and C-terminal sequences do not maintain the same level of homology in either sequence or length. These regions vary both between species as well as between isoforms within the same organism. The presence of a C-terminal tail of variable homology between and within species suggests a common ancestor that was variably modified, retained, or truncated during evolution.

Troponin I NTEs are present in TNI in Protostomia Ecdysozoa, Lophotrochozoa, and Deuterostomia Chordata cardiac isoforms (Figure 2). However, TNI NTE is absent from non-cardiac TNI in Deuterostomia (Figure 2). This suggests that ancestral TNI had

an NTE that evolved sequence diversity or was lost in some organisms (flatworms) and isoforms. The length and sequence of the NTE is highly-variable, however, it is common to have a high percentage of charged amino acids. This suggests a functional role for molecular interactions of TNI NTEs. Isoform variability was achieved by gene duplication in mammals[116] and alternative splicing in sea squirts[117,118] and this suggests that isoform functional diversity is important in establishing diversity in filamentous actin function.

5.3.3 TNI NTE is important for *C. elegans* locomotor function

C. elegans have four TNI isoforms, achieved through gene duplication: *tni-1, tni-2 (unc-27), tni-3, tni-4*. UNC-27 is the major isoform expressed in body wall muscles. We utilized *unc-27(e155)* worms, as well as *unc-27(e155)* worms with GFP-UNC-27(WT) or GFP-UNC-27(ΔN) transgenically expressed to study the function of TNI NTE within invertebrate muscle. *unc-27* null worms exhibited disorganized sarcomeres and hyper-contracted muscles. Both GFP-UNC-27(WT) or GFP-UNC-27(ΔN) were able to localize to thin filaments and rescue actin organization. This data suggests the NTE is not essential for thin filament localization or regulating baseline actomyosin interactions (Figure 4).

On the other hand, absence of TNI NTE did reduce the amplitude of body bending in worms induced to move backwards. When compared to wild-type worms, this effect also correlated with a reduction in bending frequency within both *unc-27(e155)* and *unc-27*+GFP-UNC-27(ΔN) worms. This indicates the TNI NTE is involved in the coordinated locomotion in *C. elegans*. It would be interesting to study the function of the

NTE in an invertebrate organism that does not move through coordinated simultaneous initiation of contraction and relaxation.

5.4 *C. elegans lev-11* utilizes alternative Exon 7a in a head-muscle-specific isoform, LEV-11O

5.4.1 Tropomyosin isoforms give functional variability to F-actin

Actin is a highly-conserved protein with little isoform variability; however, actin is involved in numerous different processes within the cell. Functional variety is provided by numerous actin binding proteins, including tropomyosin (LEV-11 in *C. elegans*). High molecular weight isoforms of LEV-11 regulate actomyosin interactions within the sarcomere and consequently affect muscle contractility. We have cloned a novel high molecular weight isoform (*lev-11o*), which is homologous to *lev-11a*, with the exception of alternative Exon 7. *lev-11a* contains Exon 7b (previously believed to be a constitutive exon), while *lev-11o* contains Exon 7a. These two exons share 71.2% nucleotide sequence identity and 78.3% amino acid identity.

There appears to be a pattern of differences between the two exons: 7b translates to four amino acids that are polar neutral (glutamine or serine), which are either hydrophobic or acidic (glutamic acid) in Exon 7a. These amino acids may play a role in regulating tropomyosin binding within the actin major groove, or interactions with the troponin complex. If LEV-11 favorably-binds within even a slightly variable location in the actin major groove, it could differentially regulate the exposure of myosin binding

sites on actin. Considering troponin binds around Exon 7, differences in charge may regulate interactions with the troponin complex. The pattern of TNI isoforms TNI-3 and UNC-27 expression follows the head vs body patterns found in LEV-11O and LEV-11A, respectively.

Alternatively, phosphorylation of domains often play important roles for regulating interactions with other proteins, such as in the case of TNI NTE phosphorylation decreasing its affinity for TNC N-lobe. Functional differences between the two exons may be achieved through a reversible (LEV-11A) phosphorylation vs permanent (LEV-11O) phosphor-mimic. In the future, we would like to examine LEV-11A for phosphorylation. Additionally, tropomyosin isoforms in mammals have been studied and it will be helpful to examine these isoforms for variations in phosphorylation.

5.4.2 LEV-11O is the primary isoform in the body wall muscles of the head

Within the whole worm, *lev-11o* is only a small fraction, in comparison to *lev-11a*. This is because *lev-11a* is expressed in the main body and neck of the worm, while *lev-11o* is expressed in the head and neck. This suggests that LEV-11O has important functional properties in the muscles of the head. The head muscles are innervated by motor neurons from the nerve ring, body muscles are innervated by motor neurons from the ventral chord, and the neck is innervated by both sources. The two isoforms may form heterodimers in the neck region. This differential neuron stimulation may cause different splicing factors to be expressed and/or active. In the future, we would like to identify the splicing factors responsible for the inclusion of Exon 7a or 7b.

5.5 Model for the regulation of muscle relaxation

UNC-27 (troponin I) is sufficient to stabilize tropomyosin (LEV-11) in a position to sterically-hinder actomyosin interactions and facilitate muscle relaxation. *unc-27 null* worms relaxed faster than wild-type worms. This result was counter-intuitive to our understanding of the function of troponin I. We propose three potential options for why *unc-27 null* worms relaxed faster than wild-type worms:

5.5.1 There is a currently unidentified protein (Protein X) present in the sarcomere that can modify accessibility of myosin binding sites, in a calcium-dependent manner

We suspect this Protein X is calponin-like UNC-87. UNC-87 has been localized to the thin filaments, along with tropomyosin. UNC-87 lays along actin filaments and inhibits ADF-cofilin induced actin-severing and depolymerization. In the absence of UNC-27, calcium-induced changes in troponin C (and troponin T) may change UNC-87 position and/or interactions to block actomyosin binding or modify cross-linking. Alternatively, UNC-87 affects actin-myosin crosslinking and it may disrupt the crosslinking so that muscle relaxation rate is increased.

5.5.2a Troponin I, isoform TNI-1, may have stronger inhibitory activity than UNC-27

UNC-27 is the primary troponin I isoform in body wall muscles. TNI-1 is also expressed in body wall muscles at low levels. In the absence of UNC-27, TNI-1 acts as the principle inhibitory peptide within the thin filament troponin complex. If TNI-1 has stronger

inhibitory capabilities (through a higher affinity for tropomyosin or a lower affinity for troponin C), then its presence could induce a faster rate of relaxation. Additionally, TNI-1 may interact with troponin T, tropomyosin, or actin differently to facilitate a reduction in actomyosin interactions.

5.5.2b Fewer complete troponin complexes may permit greater flexibility in tropomyosin movement.

Tropomyosin proteins overlap at their N- and C-termini, to form an extended polymer. This overlap permits tropomyosin to move in a highly-cooperative manner where the sliding between outer and inner actin grooves can facilitate a similar movement in its neighboring tropomyosin dimers. Similarly, the inverse is also possible. In *unc-27 null* worms, there is less troponin I in the body wall muscles and thus fewer complete troponin complexes. The lower frequency of troponin along thin filaments may permit tropomyosin to move more freely and thus, when calcium is removed from the system, conformational changes within troponin may cooperatively stabilize tropomyosin along the outer actin grooves with greater speed. Alternatively, a greater flexibility in tropomyosin movement may dissociate myosin binding quicker.

5.6 Model: *lev-11* exon 7a and exon 7b may be important for regulating different thin filament qualities

We identified a novel tropomyosin isoform, LEV-11O, that contains Exon 7a. LEV-11A is a similar isoform that contains Exon 7b. Exon 7 is alternatively-spliced in a cell-type

specific pattern within *C. elegans* nematode, with Exon 7a in the head/neck and Exon 7b in the neck/body. Mutations within these alternative exons lead to disruptions in the ability to maintain muscle contraction, which are isolated to the region the exon is alternatively incorporated. We hypothesize that Exon 7a and Exon 7b are important for translating different functional qualities to their respective LEV-11O and LEV-11A protein isoforms. We propose potential models for how Exon 7a and 7b are important in regulating thin filament functions:

5.6.1 LEV-11 (tropomyosin) Exon 7a is important for specific interactions with amino acids of TNI-3 and LEV-11 Exon 7b is important for specific interactions with amino acids of UNC-27 (TNI-3)

Exon 7a was incorporated in the isoforms expressed in the *C. elegans* head and neck. This pattern of alternative splicing matched up with the head/neck-specific body wall expression of the troponin I isoform, TNI-3. Exon 7b was incorporated in the isoforms expressed in *C. elegans* neck and body. UNC-27 (TNI-2) is the principle troponin I isoform in body wall muscles. The cell-type specific expression pattern of these thin filaments isoforms are achieved through different methods: tropomyosin utilizes alternative splicing and troponin I uses expression of different genes. The amino acid differences between Exon 7a and 7b may be important for optimal interactions with TNI-3 and UNC-27, respectively.

5.6.2a Charge differences between *lev-11* Exon 7a and Exon 7b may alter interactions with troponin proteins

Exon 7a contains hydrophobic amino acids that had been polar neutral in 7b.

Additionally, 7a contains two negatively charged amino acids that had been polar neutral amino acids in 7b. These differences in charge may be important for altering interactions with troponin proteins. The negatively charged glutamic acid and aspartic acid of 7a are often used as phospho-mimics and phosphorylation is known to change protein binding. Additionally, one of those 7b amino acids is a serine, which has potential to be reversibly-phosphorylated.

5.6.2b Charge differences between *lev-11* Exon 7a and Exon 7b may alter binding with actin that can change LEV-11 positioning with the actin groove, to optimize favorable interactions

The binding affinity of tropomyosin for actin is very low and tropomyosin appears to float along the actin grooves. The different positioning of tropomyosin isoforms within the inner and outer actin grooves could change the exposure of myosin binding sites. Additionally, differences in tropomyosin position may also stabilize actin filaments differently, which could lead to differences in cooperative tropomyosin polymer sliding, as well as changes in myosin affinity for binding sites on actin.

5.7 Future directions

5.7.1 To test our models for differential muscle kinetics in *unc-27 null* worms

To test if UNC-87 is able to facilitate muscle relaxation faster than UNC-27-containing troponin, we will utilize an *unc-27; unc-87* double-mutant to examine differences in contraction or relaxation kinetics *in vivo*, through optogenetically-regulated muscle contractility. To test if the numbers of troponin complexes effect the rate of relaxation, or

if there is variability in isoform-regulated muscle relaxation kinetics, where TNI-1-containing troponin complexes induce relaxation at a faster rate than UNC-27-containing complexes, we will over-express TNI-1-GFP in *unc-27 null* worms. We will then conduct all of the same phenotypical analyses utilized to study the function of the UNC-27 N-terminal extension: beat frequency, bending radius, and optogenetically-regulated muscle kinetics.

5.7.2 To test our models for *lev-11* exon 7a and 7b function *in vivo*

We have identified different expression patterns for the alternatively-spliced exon 7a and exon 7b. We don't know if there are functional differences resultant from Exon 7a and 7b. To test this, we would like to conduct isoform/exon switching studies. For example, utilize CRISPR to mutate 7a or 7b to be the other.

Chapter 6

References

1. Moerman, D. G. & Williams, B. D. Sarcomere assembly in C. elegans muscle. *WormBook* 1–16 (2006). doi:10.1895/wormbook.1.81.1
2. Vyskočil, F., Malomouzh, A. I. & Nikolsky, E. E. Non-quantal acetylcholine release at the neuromuscular junction. *Physiological Research* **58,** 763–784 (2009).
3. Chandra, S., Henderson, J. E., Morrison, G. H. & Hess, G. H. Imaging acetylcholine-receptor-induced influx of inorganic ions at single-cell resolution with ion microscopy. *Anal. Biochem.* **197,** 284–289 (1991).
4. Pessah, I. N., Stambuk, R. a & Casida, J. E. Ca2+-activated ryanodine binding: mechanisms of sensitivity and intensity modulation by Mg2+, caffeine, and adenine nucleotides. *Mol. Pharmacol.* **31,** 232–238 (1987).
5. Fill, Copello, Fill, M. & Copello, J. a. Ryanodine Receptor Calcium Release Channels. *Physiol. Rev.* **82,** 893–922 (2002).
6. Rossi, A. E. & Dirksen, R. T. Sarcoplasmic reticulum: The dynamic calcium governor of muscle. *Muscle and Nerve* **33,** 715–731 (2006).
7. Takeda, S., Yamashita, A., Maeda, K. & Maéda, Y. Structure of the core domain of human cardiac troponin in the Ca(2+)-saturated form. *Nature* **424,** 35–41 (2003).
8. Potter, J. D., Sheng, Z., Pan, B. S. & Zhao, J. A direct regulatory role for troponin T and a dual role for troponin C in the Ca2+ regulation of muscle contraction. *J Biol Chem* **270,** 2557–2562 (1995).
9. Herzberg, O., Moult, J. & James, M. N. G. A model for the Ca2+-induced conformational transition of troponin C. A trigger for muscle contraction. *Journal of Biological Chemistry* **261,** 2638–2644 (1986).
10. Spyracopoulos, L. *et al.* Calcium-induced structural transition in the regulatory domain of human cardiac troponin C. *Biochemistry* **36,** 12138–46 (1997).
11. Putkey, J. A., Sweeney, H. L. & Campbell, S. T. Site-directed mutation of the trigger calcium-binding sites in cardiac troponin C. *J. Biol. Chem.* **264,** 12370–12378 (1989).
12. Sia, S. K. *et al.* Structure of cardiac muscle troponin C unexpectedly reveals a closed regulatory domain. *J. Biol. Chem.* **272,** 18216–18221 (1997).
13. Krudy, G. A. *et al.* NMR studies delineating spatial relationships within the cardiac troponin I-troponin C complex. *J. Biol. Chem.* **269,** 23731–23735 (1994).
14. Zhang, Z., Akhter, S., Mottl, S. & Jin, J. P. Calcium-regulated conformational change in the C-terminal end segment of troponin i and its binding to tropomyosin. *FEBS J.* **278,** 3348–3359 (2011).
15. Ward, D. G. *et al.* Characterization of the Interaction between the N-Terminal Extension of Human Cardiac Troponin I and Troponin C. *Biochemistry* **43,** 4020–4027 (2004).
16. Towbin, J. a & Bowles, N. E. The failing heart. *Nature* **415,** 227–233 (2002).

17. Gomes, A. V. & Potter, J. D. Cellular and molecular aspects of familial hypertrophic cardiomyopathy caused by mutations in the cardiac troponin I gene. *Mol. Cell. Biochem.* **263,** 99–114 (2004).
18. Sadayappan, S. *et al.* Role of the acidic N' region of cardiac troponin I in regulating myocardial function. *FASEB J.* **22,** 1246–57 (2008).
19. Steinmetz, P. R. H. *et al.* Independent evolution of striated muscles in cnidarians and bilaterians. *Nature* **487,** 231–4 (2012).
20. Lehman, W. & Craig, R. Tropomyosin and the steric mechanism of muscle regulation. *Adv. Exp. Med. Biol.* **644,** 95–109 (2008).
21. Galinska, A. *et al.* The C terminus of cardiac troponin I stabilizes the Ca2+-activated state of tropomyosin on actin filaments. *Circ Res* **106,** 705–711 (2010).
22. Gordon, a M. *et al.* Regulation of Contraction in Striated Muscle. **80,** 853–924 (2009).
23. Jung, H. S. & Craig, R. Ca2+-Induced Tropomyosin Movement in Scallop Striated Muscle Thin Filaments. *J. Mol. Biol.* **383,** 512–519 (2008).
24. What, P., The, N. & Cawston, R. Biochemistry 1989, 28, 8501-8506. 8501–8506 (1989).
25. Weigt, C., Schoepper, B. & Wegner, A. Tropomyosin-troponin complex stabilizes the pointed ends of actin filaments against polymerization and depolymerization. *FEBS Lett.* **260,** 269–272 (1990).
26. Ono, S. & Ono, K. Tropomyosin inhibits ADF/cofilin-dependent actin filament dynamics. *J. Cell Biol.* **156,** 1065–1076 (2002).
27. Yu, R., Ono, S. Dual Roles of Tropomyosin as an F-Actin Stabilizer and a Regulator of Muscle Contraction in Caenorhabditis Elegans Body Wall Muscle. *November* **63,** 659–672 (2006).
28. Ishikawa, R., Yamashiro, S. & Matsumura, F. Differential modulation of actin-severing activity of gelsolin by multiple isoforms of cultured rat cell tropomyosin. Potentiation of protective ability of tropomyosins by 83-kDa nonmuscle caldesmon. *J. Biol. Chem.* **264,** 7490–7497 (1989).
29. DesMarais, V., Ichetovkin, I., Condeelis, J., Hitchcock-DeGregori, S. E. Spatial regulation of actin dynamics: a tropomyosin-free, actin-rich compartment at the leading edge. *J. Cell Sci.* **115,** 4649–4660 (2002).
30. Creed, S. J., Desouza, M., Bamburg, J. R., Gunning, P. & Stehn, J. Tropomyosin isoform 3 promotes the formation of filopodia by regulating the recruitment of actin-binding proteins to actin filaments. *Exp. Cell Res.* **317,** 249–261 (2011).
31. Fasken, M. B. & Corbett, A. H. Mechanisms of nuclear mRNA quality control. *RNA Biol.* **6,** 237–241 (2009).
32. van der Veen, R. *et al.* Excised group II introns in yeast mitochondria are lariats and can be formed by self-splicing in vitro. *Cell* **44,** 225–234 (1986).
33. Delmas, V. *et al.* Alternative usage of initiation codons in mRNA encoding the cAMP-responsive-element modulator generates regulators with opposite functions. *Proc. Natl. Acad. Sci.* **89,** 4226–4230 (1992).
34. Hershberger, R. P. & Culp, L. a. Cell-type-specific expression of alternatively spliced human fibronectin IIICS mRNAs. *Mol. Cell. Biol.* **10,** 662–71 (1990).
35. Krainer, A. R., Conway, G. C. & Kozak, D. The essential pre-mRNA splicing factor SF2 influences 5′ splice site selection by activating proximal sites. *Cell* **62,**

35–42 (1990).
36. Ge, H. & Manley, J. L. A protein factor, ASF, controls cell-specific alternative splicing of SV40 early pre-mRNA in vitro. *Cell* **62,** 25–34 (1990).
37. Francis, G. R. & Waterston, R. H. Muscle organization in Caenorhabditis elegans: Localization of proteins implicated in thin filament attachment and I-band organization. *J. Cell Biol.* **101,** 1532–1549 (1985).
38. Ono, S. Purification and biochemical characterization of actin from Caenorhabditis elegans: Its difference from rabbit muscle actin in the interaction with nematode ADF/cofilin. *Cell Motil. Cytoskeleton* **43,** 128–136 (1999).
39. Yamashiro, S., Mohri, K. & Ono, S. The two Caenorhabditis elegans actin-depolymerizing factor/cofilin proteins differently enhance actin filament severing and depolymerization. *Biochemistry* **44,** 14238–14247 (2005).
40. Ono, S. & Pruyne, D. Biochemical and cell biological analysis of actin in the nematode Caenorhabditis elegans. *Methods* **56,** 11–17 (2012).
41. Waterston, R. H., Hirsh, D. & Lane, T. R. Dominant mutations affecting muscle structure in Caenorhabditis elegans that map near the actin gene cluster. *J. Mol. Biol.* **180,** 473–496 (1984).
42. Terami, H. *et al.* Genomic organization, expression, and analysis of the troponin C gene pat-10 of Caenorhabditis elegans. *J Cell Biol* **146,** 193–202 (1999).
43. Williams, B. D. & Waterston, R. H. Genes critical for muscle development and function in Caenorhabditis elegans identified through lethal mutations. *J. Cell Biol.* **124,** 475–490 (1994).
44. Warner, A. *et al.* CPNA-1, a copine domain protein, is located at integrin adhesion sites and is required for myofilament stability in Caenorhabditis elegans. *Mol. Biol. Cell* **24,** 601–16 (2013).
45. Mcardle, K., Allen, T. S. & Bucher, E. A. Ca2+-dependent Muscle Dysfunction Caused by Mutation of the Caenorhabditis elegans Troponin T-1 Gene. **143,** 1201–1213 (1998).
46. Ruksana, R. *et al.* Tissue expression of four troponin I genes and their molecular interactions with two troponin C isoforms in Caenorhabditis elegans. *Genes Cells* **10,** 261–276 (2005).
47. Obinata, T., Ono, K. & Ono, S. Troponin I controls ovulatory contraction of non-striated actomyosin networks in the C. elegans somatic gonad. *J. Cell Sci.* **123,** 1557–66 (2010).
48. Dawn E. Barnes, Hyundoo Hwang, Kanako Ono, Hang Lu, S. O. Molecular evolution of troponin I and a role of its N-terminal extension in nematode locomotion. *Cytoskeleton* **130,** 117–130 (2016).
49. Anyanful, a, Sakube, Y., Takuwa, K. & Kagawa, H. The third and fourth tropomyosin isoforms of Caenorhabditis elegans are expressed in the pharynx and intestines and are essential for development and morphology. *J. Mol. Biol.* **313,** 525–37 (2001).
50. Kagawa, H. *et al.* Genome structure, mapping and expression of the tropomyosin gene tmy-1 of Caenorhabditis elegans. *J. Mol. Biol.* **251,** 603–13 (1995).
51. Epstein, H. F., Waterston, R. H. & Brenner, S. A mutant affecting the heavy chain of myosin in Caenorhabditis elegans. *J. Mol. Biol.* **90,** (1974).
52. Moerman, D. G., Plurad, S., Waterston, R. H. & Baillie, D. L. Mutations in the

unc-54 myosin heavy chain gene of caenorhabditis elegans that alter contractility but not muscle structure. *Cell* **29,** 773–781 (1982).

53. Bejsovec, A. & Anderson, P. Myosin heavy-chain mutations that disrupt Caenorhabditis elegans thick filament assembly. *Genes Dev.* **2,** 1307–1317 (1988).
54. Moerman, D. G., Benian, G. M., Barstead, R. J., Schriefer, L. A. & Waterston, R. H. Identification and intracellular localization of the unc-22 gene product of Caenorhabditis elegans. *Genes Dev.* **2,** 93–105 (1988).
55. Benian, G. M., Kiff, J. E., Neckelmann, N., Moerman, D. G. & Waterston, R. H. Sequence of an unusually large protein implicated in regulation of myosin activity in C. elegans. *Nature* **342,** 45–50 (1989).
56. Benian, G. M., Tinley, T. L., Tang, X. & Borodovsky, M. The Caenorhabditis elegans gene unc-89, required for muscle M-line assembly, encodes a giant modular protein composed of Ig and signal transduction domains. *J. Cell Biol.* **132,** 835–848 (1996).
57. JM, Z. & HF, E. Identification of genetic elements associated with muscle structure in the nematode C. elegans. *Cell Motil.* **1,** 73–97 (1980).
58. Mercer, K. B. *et al.* Caenorhabditis elegans UNC-96 is a new component of M-lines that interacts with UNC-98 and paramyosin and is required in adult muscle for assembly and/or maintenance of thick filaments. *Mol. Biol. Cell* **17,** 3832–47 (2006).
59. Mercer, K. B. *et al.* Caenorhabditis elegans UNC-98, a C2H2 Zn finger protein, is a novel partner of UNC-97/PINCH in muscle adhesion complexes. *Mol Biol Cell* **14,** 2492–2507 (2003).
60. Kagawa, H., Takuwa, K. & Sakube, Y. Mutations and Expressions of the Tropomyosin Gene and the Troponin C Gene of Caenorhabditis elegans. *Cell Struct. Funct.* **22,** 213–218 (1997).
61. Burkeen, a K. *et al.* Disruption of Caenorhabditis elegans muscle structure and function caused by mutation of troponin I. *Biophys. J.* **86,** 991–1001 (2004).
62. Ono, S., Baillie, D. L. & Benian, G. M. UNC-60B, an ADF cofilin family protein, is required for proper assembly of actin into myofibrils in Caenorhabditis elgans body wall muscle. *J. Cell Biol.* **145,** 491–502 (1999).
63. Ono, S. The Caenorhabditis elegans unc-78 gene encodes a homologue of actin-interacting protein 1 required for organized assembly of muscle actin filaments. *J Cell Biol* **152,** 889– (2001).
64. Benian, G. M. & Epstein, H. F. Caenorhabditis elegans muscle: A genetic and molecular model for protein interactions in the heart. *Circulation Research* **109,** 1082–1095 (2011).
65. Epstein, H. F. & Thomson, J. N. Temperature sensitive mutation affecting myofilament assembly in C. elegans. *Nature* **250,** 579–580 (1974).
66. Nahabedian, J. F., Qadota, H., Stirman, J. N., Lu, H. & Benian, G. M. Bending amplitude - A new quantitative assay of C. elegans locomotion: Identification of phenotypes for mutants in genes encoding muscle focal adhesion components. *Methods* **56,** 95–102 (2012).
67. Krajacic, P., Shen, X., Purohit, P. K., Arratia, P. & Lamitina, T. Biomechanical profiling of Caenorhabditis elegans motility. *Genetics* **191,** 1015–1021 (2012).
68. Edman, K. A. P. Contractile performance of striated muscle. *Adv. Exp. Med. Biol.*

682, 7–40 (2010).
69. Swank, D. M. Mechanical analysis of Drosophila indirect flight and jump muscles. *Methods* **56,** 69–77 (2012).
70. Liewald, J. F. *et al.* Optogenetic analysis of synaptic function. *Nat Methods* **5,** 895–902 (2008).
71. Stirman, J. N. *et al.* Real-time multimodal optical control of neurons and muscles in freely behaving Caenorhabditis elegans. *Nat. Methods* **8,** 153–158 (2011).
72. Stirman, J. N., Brauner, M., Gottschalk, A. & Lu, H. High-throughput study of synaptic transmission at the neuromuscular junction enabled by optogenetics and microfluidics. *J. Neurosci. Methods* **191,** 90–93 (2010).
73. Ono, S. Regulation of structure and function of sarcomeric actin filaments in striated muscle of the nematode caenorhabditis elegans. *Anat. Rec.* **297,** 1548–1559 (2014).
74. Matsunaga, Y., Qadota, H., Furukawa, M., Choe, H. H. & Benian, G. M. Twitchin kinase interacts with MAPKAP kinase 2 in Caenorhabditis elegans striated muscle. *Mol. Biol. Cell* **26,** 2096–111 (2015).
75. Dibb, N. J. *et al.* Sequence analysis of mutations that affect the synthesis, assembly and enzymatic activity of the unc-54 myosin heavy chain of Caenorhabditis elegans. *J Mol Biol* **183,** 543–551 (1985).
76. Forbes, J. G. *et al.* Extensive and modular intrinsically disordered segments in C. elegans TTN-1 and implications in filament binding, elasticity and oblique striation. *J. Mol. Biol.* **398,** 672–689 (2010).
77. Perry, S. V. Troponin I: inhibitor or facilitator. *Mol Cell Biochem* **190,** 9–32 (1999).
78. Probst, W. C. *et al.* cAMP-dependent phosphorylation of Aplysia twitchin may mediate modulation of muscle contractions by neuropeptide cotransmitters. *Proc. Natl. Acad. Sci. U. S. A.* **91,** 8487–8491 (1994).
79. Siegman, M. J. *et al.* Phosphorylation of a twitchin-related protein controls catch and calcium sensitivity of force production in invertebrate smooth muscle. *Proc. Natl. Acad. Sci. U. S. A.* **95,** 5383–5388 (1998).
80. Funabara, D. *et al.* Unphosphorylated twitchin forms a complex with actin and myosin that may contribute to tension maintenance in catch. *J.exp.Biol.* **210,** 4399–4410 (2007).
81. Hole, W., Lehman, W., Szent-Gyorgyi, A. G. & Szent-Györgyi, a G. Regulation of muscular contraction. Distribution of actin control and myosin control in the animal kingdom. *J.Gen.Physiol* **66,** 1–30 (1975).
82. Squire, J. M. & Morris, E. P. A new look at thin filament regulation in vertebrate skeletal muscle. *FASEB J.* **12,** 761–771 (1998).
83. Somlyo, A. P. & Somlyo, A. V. Signal transduction and regulation in smooth muscle. *Nature* **372,** 231–236 (1994).
84. Wang, C. L. Caldesmon and smooth-muscle regulation. *Cell Biochem Biophys* **35,** 275–288 (2001).
85. Winder, S. J., Allen, B. G., Clément-Chomienne, O. & Walsh, M. P. Regulation of smooth muscle actin-myosin interaction and force by calponin. *Acta Physiol. Scand.* **164,** 415–426 (1998).
86. Hooper, S. L., Hobbs, K. H. & Thuma, J. B. Invertebrate muscles: Thin and thick

filament structure; molecular basis of contraction and its regulation, catch and asynchronous muscle. *Progress in Neurobiology* **86,** 72–127 (2008).
87. Goldberg, A. & Lehman, W. Troponin-like proteins from muscles of the scallop, Aequipecten irradians. *Biochem. J.* **171,** 413–418 (1978).
88. Ojima, T. & NISHITA, K. Isolation of troponins from striated and smooth adductor muscles of Akazara scallop. *J.Biochem.* **100,** 821–824 (1986).
89. Tanaka, H. *et al.* Comparative studies on the functional roles of N- and C-terminal regions of molluskan and vertebrate troponin-I. *FEBS J.* **272,** 4475–4486 (2005).
90. Szent-Györgyi, a G., Kalabokis, V. N. & Perreault-Micale, C. L. Regulation by molluscan myosins. *Mol. Cell. Biochem.* **190,** 55–62 (1999).
91. Myers, C. D., Goh, P. Y., Allen, T. S., Bucher, E. A. & Bogaert, T. Developmental genetic analysis of troponin T mutations in striated and nonstriated muscle cells of Caenorhabditis elegans. *J. Cell Biol.* **132,** 1061–1077 (1996).
92. Ono, K. & Ono, S. Tropomyosin and troponin are required for ovarian contraction in the Caenorhabditis elegans reproductive system. *Mol. Biol. Cell* **15,** 2782–93 (2004).
93. Ebashi, S. Ca2+ and the Contractile Proteins. **16,** 129–136 (1984).
94. Galińska-Rakoczy, A. *et al.* Structural Basis for the Regulation of Muscle Contraction by Troponin and Tropomyosin. *J. Mol. Biol.* **379,** 929–935 (2008).
95. Vinogradova, M. V *et al.* Ca(2+)-regulated structural changes in troponin. *Proc. Natl. Acad. Sci. U. S. A.* **102,** 5038–5043 (2005).
96. Kowlessur, D. & Tobacman, L. S. Significance of troponin dynamics for Ca2+-mediated regulation of contraction and inherited cardiomyopathy. *J. Biol. Chem.* **287,** 42299–42311 (2012).
97. Lehman, W., Galińska-Rakoczy, A., Hatch, V., Tobacman, L. S. & Craig, R. Structural Basis for the Activation of Muscle Contraction by Troponin and Tropomyosin. *J. Mol. Biol.* **388,** 673–681 (2009).
98. Dennisson, J. G. *et al.* Functional characteristics of amphioxus troponin in regulation of muscle contraction. *Zoolog. Sci.* **27,** 461–469 (2010).
99. Bullard, B. & Pastore, A. Regulating the contraction of insect flight muscle. *J. Muscle Res. Cell Motil.* **32,** 303–313 (2011).
100. Donahue, M. J., Michnoff, C. A. & Masaracchia, R. A. Calcium-dependent muscle contraction in obliquely striated Ascaris suum muscle. *Comp. Biochem. Physiol. -- Part B Biochem.* **82,** 395–403 (1985).
101. Obinata, T., Ono, K. & Ono, S. Detection of a troponin I-like protein in non-striated muscle of the tardigrades (water bears). **1,** 96–102 (2011).
102. Prasath, T., Greven, H. & D'Haese, J. EF-Hand Proteins and the Regulation of Actin-Myosin Interaction in the Eutardigrade Hypsibius klebelsbergi (Tardigrada). *J. Exp. Zool. Part A Ecol. Genet. Physiol.* **317,** 311–320 (2012).
103. Philippe, H. *et al.* Acoelomorph flatworms are deuterostomes related to Xenoturbella. *Nature* **470,** 255–258 (2011).
104. Chiodin, M., Achatz, J. G., Wanninger, A. & Martinez, P. Molecular architecture of muscles in an acoel and its evolutionary implications. *J. Exp. Zool. Part B Mol. Dev. Evol.* **316 B,** 427–439 (2011).
105. Urchin, S. The Genome of the Sea Urchin. *Science (80-.).* **314,** 941–952 (2006).
106. Obinata, T., Ikeda, M. & Hayashi, T. The native actin filaments from sea urchin

muscle. *Int. J. Biochem.* **5,** (1974).
107. Obinata, T. *et al.* Sea lily muscle lacks a troponin-regulatory system, while it contains paramyosin. *Zoolog. Sci.* **31,** 122–8 (2014).
108. Blair, J. E. & Hedges, S. B. Molecular phylogeny and divergence times of deuterostome animals. *Mol. Biol. Evol.* **22,** 2275–2284 (2005).
109. Halanych, K. M. The phylogenetic position of the pterobranch hemichordates based on 18S rDNA sequence data. *Molecular phylogenetics and evolution* **4,** 72–76 (1995).
110. Sievers, F. *et al.* Fast, scalable generation of high-quality protein multiple sequence alignments using Clustal Omega. *Mol. Syst. Biol.* **7,** 539 (2011).
111. Egger, B. *et al.* To be or not to be a flatworm: The Acoel controversy. *PLoS One* **4,** (2009).
112. Lowe, C. J. & Pani, A. M. Animal evolution: A soap opera of unremarkable worms. *Current Biology* **21,** (2011).
113. Luo, Y. *et al.* Photocrosslinking of benzophenone-labeled single cysteine troponin I mutants to other thin filament proteins. *J. Mol. Biol.* **296,** 899–910 (2000).
114. Syska, H., Wilkinson, J. M., Grand, R. J. & Perry, S. V. The relationship between biological activity and primary structure of troponin I from white skeletal muscle of the rabbit. *Biochem J* **153,** 375–387 (1976).
115. Talbot, J. A. & Hodges, R. S. Synthetic studies on the inhibitory region of rabbit skeletal troponin I. Relationship of amino acid sequence to biological activity. *J. Biol. Chem.* **256,** 2798–2802 (1981).
116. Hastings, K. E. M. Molecular evolution of the vertebrate troponin I gene family. *Cell Struct. Funct.* **22,** 205–211 (1997).
117. MacLean, D. W., Meedel, T. H. & Hastings, K. E. M. Tissue-specific alternative splicing of ascidian troponin I isoforms: Redesign of a protein isoform-generating mechanism during chordate evolution. *J. Biol. Chem.* **272,** 32115–32120 (1997).
118. Yuasa, H. J., Kawamura, K., Yamamoto, H. & Takagi, T. The structural organization of ascidian Halocynthia roretzi troponin I genes. *J.Biochem.* **132,** 135–141 (2002).
119. Solaro, R. J. The special structure and function of troponin I in regulation of cardiac contraction and relaxation. *Adv. Exp. Med. Biol.* **538,** 382–389 (2003).
120. Solaro, R. J., Rosevear, P. & Kobayashi, T. The unique functions of cardiac troponin I in the control of cardiac muscle contraction and relaxation. *Biochem. Biophys. Res. Commun.* **369,** 82–87 (2008).
121. Cohen, N. & Sanders, T. Nematode locomotion: Dissecting the neuronal-environmental loop. *Current Opinion in Neurobiology* **25,** 99–106 (2014).
122. Mello, C. C., Kramer, J. M., Stinchcomb, D. & Ambros, V. Efficient gene transfer in C.elegans: extrachromosomal maintenance and integration of transforming sequences. *EMBO J.* **10,** 3959–70 (1991).
123. Moulder, G. L. *et al.* ??-Actinin Is Required for the Proper Assembly of Z-Disk/Focal-Adhesion-Like Structures and for Efficient Locomotion in Caenorhabditis elegans. *J. Mol. Biol.* **403,** 516–528 (2010).
124. Stirman, J. N., Crane, M. M., Husson, S. J., Gottschalk, A. & Lu, H. A multispectral optical illumination system with precise spatiotemporal control for the manipulation of optogenetic reagents. *Nat. Protoc.* **7,** 207–20 (2012).

125. Nagel, G. *et al.* Light activation of Channelrhodopsin-2 in excitable cells of caenorhabditis elegans triggers rapid behavioral responses. *Curr. Biol.* **15,** 2279–2284 (2005).
126. Hwang, H. *et al.* Muscle contraction phenotypic analysis enabled by optogenetics reveals functional relationships of sarcomere components in Caenorhabditis elegans. *Sci. Rep.* **6,** 19900 (2016).
127. Endo, T. & Obinata, T. Troponin and its components from ascidian smooth muscle. *J. Biochem.* **89,** 1599–1608 (1981).
128. Ohshiro, K., Obinata, T., Dennisson, J. G., Ogasawara, M. & Sato, N. Troponin in both smooth and striated muscles of ascidian ciona intestinalis functions as a Ca2+-dependent accelerator of actin-myosin interaction. *Biochemistry* **49,** 9563–9571 (2010).
129. Zhang, F. *et al.* Multimodal fast optical interrogation of neural circuitry. *Nature* **446,** 633–9 (2007).
130. Howarth, J. W., Meller, J., Solaro, R. J., Trewhella, J. & Rosevear, P. R. Phosphorylation-dependent Conformational Transition of the Cardiac Specific N-Extension of Troponin I in Cardiac Troponin. *J. Mol. Biol.* **373,** 706–722 (2007).
131. Ward, D. G., Brewer, S. M., Cornes, M. P. & Trayer, I. P. A cross-linking study of the N-terminal extension of human cardiac troponin I. *Biochemistry* **42,** 10324–10332 (2003).
132. Warren, C. M., Kobayashi, T. & Solaro, R. J. Sites of intra- and intermolecular cross-linking of the N-terminal extension of troponin I in human cardiac wholetroponin complex. *J. Biol. Chem.* **284,** 14258–14266 (2009).
133. Gaponenko, V. *et al.* Effects of troponin I phosphorylation on conformational exchange in the regulatory domain of cardiac troponin C. *J. Biol. Chem.* **274,** 16681–16684 (1999).
134. Kentish, J. C. *et al.* Phosphorylation of troponin I by protein kinase A accelerates relaxation and crossbridge cycle kinetics in mouse ventricular muscle. *Circ. Res.* **88,** 1059–1065 (2001).
135. Zhang, R., Zhao, J., Mandveno, A. & Potter, J. D. Cardiac troponin I phosphorylation increases the rate of cardiac muscle relaxation. *Circ Res* **76,** 1028–1035 (1995).
136. Zhang, R., Zhao, J. & Potter, J. D. Phosphorylation of both serine residues in cardiac troponin I is required to decrease the Ca2+ affinity of cardiac troponin C. *J. Biol. Chem.* **270,** 30773–30780 (1995).
137. Murphy, R. T. *et al.* Novel mutation in cardiac troponin I in recessive idiopathic dilated cardiomyopathy. *Lancet* **363,** 371–372 (2004).
138. Arad, M. *et al.* Gene mutations in apical hypertrophic cardiomyopathy. *Circulation* **112,** 2805–2811 (2005).
139. Yu, Z. Bin, Zhang, L. F. & Jin, J. P. A Proteolytic NH2-terminal Truncation of Cardiac Troponin I that is Up-regulated in Simulated Microgravity. *J. Biol. Chem.* **276,** 15753–15760 (2001).
140. Barbato, J. C., Huang, Q. Q., Hossain, M. M., Bond, M. & Jin, J. P. Proteolytic N-terminal truncation of cardiac troponin I enhances ventricular diastolic function. *J. Biol. Chem.* **280,** 6602–6609 (2005).
141. Biesiadecki, B. J. *et al.* Removal of the cardiac troponin I N-terminal extension

improves cardiac function in aged mice. *J. Biol. Chem.* **285,** 19688–19698 (2010).
142. Feng, H. Z., Chen, M., Weinstein, L. S. & Jin, J. P. Removal of the N-terminal extension of cardiac troponin I as a functional compensation for impaired myocardial ??-adrenergic signaling. *J. Biol. Chem.* **283,** 33384–33393 (2008).
143. Pethica, R., Barker, G., Kovacs, T. & Gough, J. TreeVector: Scalable, interactive, phylogenetic trees for the web. *PLoS One* **5,** (2010).
144. Riutort, M., ??lvarez-Presas, M., L??zaro, E., Sol??, E. & Paps, J. Evolutionary history of the Tricladida and the platyhelminthes: An up-to-date phylogenetic and systematic account. *Int. J. Dev. Biol.* **56,** 5–17 (2012).
145. Flot, J. *et al.* Genomic evidence for ameiotic evolution in the bdelloid rotifer Adineta vaga. *Nature* **500,** 453–457 (2014).
146. Brenner, S. The genetics of Caenorhabditis elegans. *Genetics* **77,** 71–94 (1974).
147. Stiernagle, T. Maintenance of C. elegans. *WormBook* 1–11 (2006). doi:10.1895/wormbook.1.101.1
148. Okkema, P. G., Harrison, S. W., Plunger, V., Aryana, A. & Fire, A. Sequence requirements for myosin gene expression and regulation in Caenorhabditis elegans. *Genetics* **135,** 385–404 (1993).
149. Mohri, K., Ono, K., Yu, R., Yamashiro, S. & Ono, S. Enhancement of actin-depolymerizing factor/cofilin-dependent actin disassembly by actin-interacting protein 1 is required for organized actin filament assembly in the Caenorhabditis elegans body wall muscle. *Mol. Biol. Cell* **17,** 2190–9 (2006).
150. Otey, C. a, Kalnoski, M. H. & Bulinski, J. C. Identification and quantification of actin isoforms in vertebrate cells and tissues. *J. Cell. Biochem.* **34,** 113–24 (1987).
151. Firtel, R. A. Multigene families encoding actin and tubulin. *Cell* **24,** 6–7 (1981).
152. Gunning, P. W., Schevzov, G., Kee, A. J. & Hardeman, E. C. Tropomyosin isoforms: Divining rods for actin cytoskeleton function. *Trends Cell Biol.* **15,** 333–341 (2005).
153. Gunning, P. W., Hardeman, E. C., Lappalainen, P. & Mulvihill, D. P. Tropomyosin - master regulator of actin filament function in the cytoskeleton. *J. Cell Sci.* 1–10 (2015). doi:10.1242/jcs.172502
154. Brown, J. H. *et al.* Deciphering the design of the tropomyosin molecule. *Proc. Natl. Acad. Sci. U. S. A.* **98,** 8496–8501 (2001).
155. Hitchcock, S. E. & Carlsson, L. Depolymerization of F-actin by deoxyribonuclease I. **7,** 531–542 (1976).
156. Mckillop, D. F. A. & Geeves, M. A. Regulation of the interaction between actin and myosin subfragment 1: evidence for three states of the thin filament. **65,** 693–701 (1993).
157. Eyk, J. E. Van *et al.* Distinct Regions of Troponin I Regulate Ca 2 ⁄. -dependent Activation and Ca 2 ⁄. Sensitivity of the Acto-S1-TM ATPase Activity of the Thin Filament *. **272,** 10529–10537 (1997).
158. Lewis, J. A., Wu, C. H., Berg, H. & Levine, J. H. The genetics of levamisole resistance in the nematode Caenorhabditis elegans. *Genetics* **95,** 905–928 (1980).
159. Rayes, D., De Rosa, M. J., Bartos, M. & Bouzat, C. Molecular basis of the differential sensitivity of nematode and mammalian muscle to the anthelmintic agent levamisole. *J. Biol. Chem.* **279,** 36372–36381 (2004).
160. Kuroyanagi, H., Takei, S. & Suzuki, Y. Comprehensive analysis of mutually

exclusive alternative splicing in C. elegans. *Worm* **3,** e28459 (2014).
161. Thompson, O. *et al.* The million mutation project: a new approach to genetics in *Caenorhabditis elegans*. *Genome Res.* **23,** 1749–1762 (2013).
162. Milligan, R. a & Flicker, P. F. Structural relationship of actin, myosin and tropomyosin revealed by cryo-electron microscopy. *J. Cell Biol.* **105,** 29–39 (1987).
163. White, J. G., Southgate, E., Thomson, J. N. & Brenner, S. The Structure of the Nervous System of the Nematode *Caenorhabditis elegans*. *Philos. Trans. R. Soc. B Biol. Sci.* **314,** 1–340 (1986).
164. Kuroyanagi, H., Ohno, G., Sakane, H., Maruoka, H. & Hagiwara, M. Visualization and genetic analysis of alternative splicing regulation in vivo using fluorescence reporters in transgenic Caenorhabditis elegans. *Nat. Protoc.* **5,** 1495–1517 (2010).
165. Pardee, J. D. & Spudich, J. A. Purification of Muscle Actin. **24,** (1982).
166. Klaavuniemi, T., Yamashiro, S. & Ono, S. Caenorhabditis elegans gelsolin-like protein 1 is a novel actin filament-severing protein with four gelsolin-like repeats. *J. Biol. Chem.* **283,** 26071–26080 (2008).
167. Obinata, T. The Myosin of Developing Chick Embryo. 184–197 (1969).
168. Tausskey, H.H., Shorr, E. A Microcolormetric Method for the Determination of Inorganic Phosphorous. *J. Biol. Chem.* 675–686 (1952). doi:10.1017/CBO9781107415324.004
169. Perry, S. V. [94] Myosin adenosinetriphosphatase. ATP H2 O???ADP+H3 PO4. *Methods Enzymol.* **2,** 582–588 (1955).
170. Nomura, K., Ono, K. & Ono, S. CAS-1, a C. elegans cyclase-associated protein, is required for sarcomeric actin assembly in striated muscle. *J. Cell Sci.* **125,** 4077–89 (2012).
171. Sehnert, A. J. *et al.* Cardiac troponin T is essential in sarcomere assembly and cardiac contractility. *Nat. Genet.* **31,** 106–110 (2002).
172. Gomes, A. V., Harada, K. & Potter, J. D. A mutation in the N-terminus of Troponin I that is associated with hypertrophic cardiomyopathy affects the Ca2+-sensitivity, phosphorylation kinetics and proteolytic susceptibility of troponin. *Journal of Molecular and Cellular Cardiology* **39,** 754–765 (2005).
173. Wnuk, W., Schoechlin, M. & Stein, E. A. Regulation of actomyosin ATPase by a single calcium-binding site on troponin C from crayfish. *J. Biol. Chem.* **259,** 9017–9023 (1984).
174. Maytum, R., Lehrer, S. S. & Geeves, M. A. Cooperativity and switching within the three-state model of muscle regulation. *Biochemistry* **38,** 1102–1110 (1999).
175. Kawazoe, Y., Yawo, H. & Kimura, K. D. A simple optogenetic system for behavioral analysis of freely moving small animals. *Neuroscience Research* **75,** 65–68 (2013).